Master's thesis

NTNU
Norwegian University of Science and Technology
Faculty of Engineering
Department of Mechanical and Industrial Engineering

Håvard Holm Bjørnebekk

# Modeling Degradation for Prognosis in a Complex Environment - From a Physics-Based Perspective

Master's thesis in Mechanical and Industrial Engineering
Supervisor: Jørn Vatn
Co-supervisor: Tom Ivar Pedersen
June 2021

NTNU
Norwegian University of Science and Technology

Håvard Holm Bjørnebekk

# Modeling Degradation for Prognosis in a Complex Environment - From a Physics-Based Perspective

Master's thesis in Mechanical and Industrial Engineering
Supervisor: Jørn Vatn
Co-supervisor: Tom Ivar Pedersen
June 2021

Norwegian University of Science and Technology
Faculty of Engineering
Department of Mechanical and Industrial Engineering

NTNU
Norwegian University of
Science and Technology

RAMS
Reliability, Availability,
Maintainability, and Safety

# Modeling Degradation for Prognosis in a Complex Environment - From a Physics-Based Perspective

Håvard Holm Bjørnebekk

June 2021

MASTER THESIS

Department of Mechanical and Industrial Engineering
Norwegian University of Science and Technology

Supervisor 1: Professor Jørn Vatn
Supervisor 2: PhD Candidate Tom Ivar Pedersen

# Preface

This thesis concludes the Master thesis in RAMS for Håvard Holm Bjørnebekk at the Norwegian University of Science and Technology (NTNU) as a part of the study program Mechanical and Industrial Engineering. The master thesis was written in the spring semester of 2021. The thesis seeks to find ways of developing physics-based models for prognosis and explore its possibilities with Predictive Maintenance. The work is based on a case study originating from work conducted by Tom Ivar Pedersen for Elkem. The cooperation with Elkem included several digital meetings and a visit to the production plant at Thamshavn. The reader of the report is expected to have the same knowledge of RAMS engineering and risk management accordingly to what a student at the RAMS program at NTNU has, and a grasp of what Industry 4.0 entails.

Trondheim, 2021-06-10

Håvard Holm Bjørnebekk

# Acknowledgment

I would like to thank the following persons for their great help during the spring of 2021: Professor Jørn Vatn for guidance and insight in statistics, PhD Candidate Tom Ivar Pedersen for valuable insight and great discussions. In addition, Elkem Thamshavn employees, especially Bjørnar Hynne for great insight into the production process of silicon and Jan Erik Evjen for guidance connected to the electric operation. Lastly, Håkon Grøtt Størdal for tips and valuable code that aid in conducting this thesis.

H.H.B.

# Executive Summary

With the current trend of automation and data exchange in manufacturing technologies, known as *Industry 4.0*, maintenance has developed to become an important business function. Degradation modeling and consequently the prognosis of an asset's lifetime is seen as an important part of new sophisticated maintenance policies that become available to companies. However, the industry is seen to meet challenges when trying to implement such maintenance policies based on the prognosis of an asset's lifetime in practice.

In this thesis, the main goal is to highlight ways of modeling degradation for prognosis from a physics-based approach. It seeks to develop a physics-based model and discuss the connected challenges to such an approach. The overarching research question for this project thesis is:

*How is the degradation of physical equipment best modeled?*

To answer this question, a case study from Elkem with real data is used as an example. It revolves around flexsibles, a type of equipment that regularly causes unplanned shutdown of silicon production at Elkem Thamshavn. A literature review on physics-based models for degradation modeling was performed, where it was found that a good system understanding was a prerequisite to developing accurate physics-based models. Hence, following this review, system functions and the equipment's failure mechanisms were analyzed to be used in a physics-based model for prognosis of the flexsibles. However, as a physics-based model was found difficult to obtain, a stochastic modeling approach was used to better model the uncertainty that was present.

It has been concluded that physics-based models can provide a good starting point for any prognosis and degradation modeling process. A framework on how to approach a degradation modeling and prognosis process is suggested. In addition, the work in this thesis show how it is possible to use the physical understanding one obtains through a physics-based modeling approach to improve a stochastic prognosis model.

# Kortfattet Sammendrag

Med den pågående trenden av automatisering og datautveksling i produksjonsteknologier, kjent som *Industry 4.0*, har vedlikehold utviklet seg til å bli en viktig funksjon i industrien. Modellering av degradering og prognose av en ressurs' livstid blir sett på som en viktig del av nye sofistikerte vedlikeholdsprogrammer som blir tilgjengelig for selskaper. I tillegg ser industrien ut til å møte på utfordringer i praksis, når de prøver å implementere vedlikeholdsprogrammer basert på ressursers livstidsprognose.

I denne masteroppgaven er hovedmålet å fremheve måter å modellere degradering for prognose fra en fysikkbasert tilnærming. Masteroppgaven søker å utvikle en fysikkbasert modell og diskutere de tilknyttede utfordringene til en slik tilnærming. Det overordnede forskningsspørsmålet for denne prosjektoppgaven er:

*Hvordan modelleres degradering av fysisk utstyr best?*

For å svare på dette spørsmålet brukes en case-studie fra Elkem med reelle data som et eksempel. Case-studien dreier seg om fleksibler, en type utstyr som regelmessig forårsaker uplanlagt stans av silisiumsproduksjon ved Elkem Thamshavn. En litteraturgjennomgang av fysikkbaserte modeller for degraderingsmodellering ble utført, der det ble funnet at god systemforståelse var en forutsetning for å utvikle nøyaktige fysikkbaserte modeller. Derfor, etter denne gjennomgangen, ble systemfunksjoner og utstyrets sviktmekanismer analysert for å kunne bli brukt i en fysikkbasert modell for prognose av fleksiblene. Ettersom en fysikkbasert modell ble funnet vanskelig å oppnå, ble det brukt en stokastisk modelleringsmetode for bedre å modellere usikkerheten som var til stede.

Det er konkludert med at fysikkbaserte modeller kan gi et godt utgangspunkt for enhver prognose og prosess for å lage degraderingsmodeller. Det foreslås et rammeverk for hvordan man kan tilnærme seg en degraderingsmodellering- og prognoseprosess. I tillegg viser arbeidet i denne oppgaven hvordan det er mulig å bruke den fysiske forståelsen man oppnår gjennom en fysikkbasert modelleringstilnærming for å forbedre en stokastisk prognosemodell.

# Contents

# Chapter 1

# Introduction

Emerging digital technological advancements has lead to a digitization transformation in the manufacturing industry, known as Industry 4.0. The fourth in the series of technological leaps: Mechanization, intensive use of electrical energy, widespread digitization, and now, advanced digitization (Lasi et al. [2014];Fuller et al. [2020]). Industry 4.0 is unique because it is predicted before it has happened, while it seems to bring with it the same as its predecessors - huge economic opportunities (Hermann et al. [2016]). Manufacturing companies worldwide seem to recognize this huge potential but face challenges when implementing theories into real systems and processes (Zeller et al. [2018]).

In conjunction with the development of the Industry 4.0 concept, maintenance has developed to become widely recognized as an essential business function and a critical element of asset management (de Jonge and Scarf [2020]). As new developing technologies such as cheap sensors, computational hardware, and Machine Learning (ML) are more readily available, more sophisticated maintenance policies become available for companies. Currently, there is a shift from conventional preventive maintenance policies based on time and age, to predictive maintenance policies based on condition monitoring (CM). Multiple studies have empirically found that Condition-Based Maintenance (CBM) results in a substantial reduction of the equipment's downtime and total maintenance costs compared to other maintenance strategies (Jardine et al. [2006]; Veldman et al. [2011]). For instance, GE [2020] saved $1.5BN for its customers through real-time condition monitoring of their assets.

Although considerable research effort has been expended on developing the technical aspects of CBM programs, a pilot study by Van de Kerkhof et al. [2016] indicates that many firms in the process industry struggle with systematically employing CBM activities in general, and prognostic CBM approaches in particular. Werner et al. [2019] states that despite the great importance of predictive maintenance as stated by companies, corrective and preventive maintenance is still the most commonly used maintenance strategies. Van de Kerkhof et al. [2016] further explains the technical barriers as mainly the collection and analysis of large amounts of

data. de Jonge and Scarf [2020] finds that only a limited number of studies report on applying maintenance models to a case study with real-life data and that the availability of relevant data is a prerequisite for maintenance optimization within CBM. Moreover, Lei et al. [2018] claims that most of the existing data used for prognosis in the scientific literature are generated through simulation or in a laboratory environment. Therefore, prognostics based on real data are still needed in future research. Van de Kerkhof et al. [2016] uncovers that a lot of data is gathered and stored already, though for different purposes than maintenance. Hence, this implies a large potential for better maintenance policies across the industry if the available data are used in practice.

## Problem Formulation

Elkem, a company in the process industry, is currently using simple and conventional maintenance practices in its production of silicon. The water-cooled, flexible high current cables, called *flexsibles*, supply the silicon furnace with the electrical current used to heat up and drive the reaction. These are prone to fail unexpectedly, which will stop production and incur high costs. In addition, failure of water-carrying equipment can lead to explosions, which impose a substantial safety risk. Therefore, a better prognosis of the failure (degradation model) of flexsibles is believed to reduce cost and increase safety.

There are many ways to construct degradation models. In this Master Thesis, the focus will be on physics-based approaches. At Elkem Thamshavn, there are data on equipment available, which are normally used for other purposes like process control. Hence, this thesis will revolve around how to develop a prognosis of flexsibles by applying physic-based approaches on the data collected from the Elkem data source.

Physics-based models are preferable when a physical model is available, and this model is believed to explain the real physical equipment to a sufficient degree. While there is no such model available in this case and most of the research on physics-based models is on equipment that is much simpler than the flexsibles (Jardine et al. [2006];Lei et al. [2018]), a large part of the work in this thesis revolves around finding and developing such a model. In general, this thesis seeks the least complex, most accurate physics-based model that can model the degradation of flexsibles to a sufficient degree. Another benefit to physics-based models is inference, as it is easier to understand how the models work compared to e.g., data-driven models based on Machine-Learning. Hence, this thesis will also create a logical foundation and will work as a cornerstone for further work for CBM on flexsibles.

While physics-based models are effective for prognosis in equipment experiencing certain types of failure modes (e.g., crack growth) it is commonly criticized for lacking generalization and adaptiveness to other problems (An et al. [2015]). Hence, this thesis also seeks to evaluate effective ways to generally develop physics-based models when they are not available. Finally,

this thesis will uncover the hurdles of implementing physics-based solutions, and the advantages and disadvantages a lifetime prognosis of flexsibles can have in an operational setting.

As the industry is struggling with implementing the cost-efficient and safety-enhancing algorithms proposed by the literature, this work will contribute to closing this gap, using the promising techniques for prognosis found in the literature on real-world systems and data. Most importantly, bring value to the scientific literature, the industry, and Elkem specifically. Parallel to this work, Håkon Grøtt Størdal works on the same case study, focusing on a data-driven approach for prognosis. It is believed that better knowledge on the system's physical properties will aid in developing a more precise data-driven model. On the other hand, proper data handling and code can help increase efficiency in pursuing physics-based models. This work will also be valuable for Ph.D. candidate Tom Ivar Pedersen, as it can serve as input for predictive maintenance policies.

This thesis aims at answering the following question: How is the degradation of physical equipment best modeled ? Moreover, the practical barriers of developing physics-based models with industrial data must be thoroughly discussed. What are the main challenges tied to data processing, developing prognosis models for industrial equipment in the process industry, and what are the advantages and disadvantages of physics-based models in this context?

## 1.1 Objectives

The following objectives are defined to address the aforementioned challenges:

1. Review related work regarding diagnostics and prognostics of similar equipment to the flexsibles.

2. Develop a physics-based model on the degradation of flexsibles.

3. If a physics-based model is not available, propose ways of developing a stochastic degradation model based on the physical knowledge obtained through the process.

4. Implement a prognosis model based on the physics of the failure of flexsibles and evaluate its performance.

5. Evaluate and discuss the quality of the prognosis method and whether physics-based models are suitable for modeling degradation of physical equipment in the process industry.

6. Discuss the hurdles of implementing physics-based models in such a complex operational context.

By completing these objectives, this thesis research how prognosis can be applied for real, operating equipment in the process industry using relevant sensory data. It explores how to develop a physics-based model and what is to be done when such a model is not available. In addition, it seeks to generalize the findings to make it easier to develop degradation models in general, and physics-based models specifically for future researchers. Lastly, it aims at finding the best way of modeling the flexsibles to improve the prognosis results.

## 1.2 Approach

To the author's knowledge, the scientific literature on the specific equipment (flexsibles) is limited. Hence, most of the work in this thesis will revolve around connecting well-established theories to solve the problem described in the case study. A large amount of work is concentrated on understanding system functions, as this is a prerequisite for developing physics-based models. Data obtained from Elkem concerning the production process will be studied regarding the system's physical properties. Different statistical techniques will be used to elaborate on these properties. To be able to handle this large amount of data, coding is required. For this reason, the coding language of Python is going to be used, with different applicable libraries. As the coding is only an aid in this work, it will not be focused on generalizing the code into e.g., functions. From the code, different graphs and figures will be made for a visual representation of the data which are shown throughout this thesis.

## 1.3 Contributions

This thesis mainly investigates how to best use available data and knowledge to improve maintenance decision-making. The following things are the contributions of this thesis:

1. A literature review on physics-based modeling for prognosis and diagnosis.
2. A literature review on degradation mechanisms concerning the flexsibles.
3. Prognosis of flexsibles based on their physics of failure.
4. Suggestions on how this prognosis can be used for better maintenance decision-making.
5. A proposed framework on how to practically develop degradation models for prognosis.

## 1.4 Limitations

There is limited literature on flexsibles specifically, which might affect the degradation model accuracy. A literature review concerning similar components such as corrosion in copper pipes

and erosion in oil pipes is provided for better system understanding. These are used to elaborate on the physics of different failure mechanisms, but might not be directly transferable to this case as flexsibles are more complex components in a more complex environment. The silicon production process is complex and the knowledge obtained about the system only comes from discussion with Elkem and more general information found in Schei et al. [1998].

There are not used statistical methods on all the data, especially on all the CM data. This is done mainly for simplicity because of the large amount of data that was available. The author have then tried to do as much statistical analysis on the data that seemed most important. Hence, bias in choosing what to focus the efforts on, might have altered the outcome of the end results.

## 1.5 Outline

Chapter 2 will include a literature review on related work mainly concerning physics-based machinery modeling authored the last 25 years. Chapter 3 introduces the theoretical framework used in this thesis. Chapter 4 gives an extensive overview of the system to be studied, which forms the basis for the Chapter 5 - focusing on an FMSA and FMECA. Chapter 6 contain a literature review on the most important failure mechanisms found in the previous chapter. Chapter 7 is focused on developing a HI and HSs for a prognosis approach based on the linear Wiener process. After the prognosis is performed, all knowledge from the previous chapters are integrated to form a discussion in Chapter 8, discussing how this can be used in a larger context and propose further work. At last, in Chapter 9 a conclusion is presented.

# Chapter 2

# Related Work

As there is little research dedicated to the failure of flexsibles in the literature, it is not straightforward to classify which type of physics-based models are best suited for this case. Initially, the silicon furnace, controlled (regulated) and supplied with current, might look like a good case for diagnosis and fault-tolerant techniques outlined by (Gao et al. [2015]). These approaches usually do a type of frequency or signal analysis based on block diagrams. Using block diagrams builds on a fundamental understanding of the system. Block diagrams are usually available in industrial electronics as they are used in the design phase of the product. There are several problems with trying to use these types of physics-based models on the flexsible case: (1) A block-diagram, or a well-established model of the furnace operation is not available to the author; (2) the nature of the electric operation and measurements (presented in 4.5) results in a great amount of uncertainty in these measurements; (3) the data available does not have the appropriate amount of resolution for this kind of analysis (Gao et al. [2015]).

In the literature on machinery diagnostics and prognostics, there are mainly two different approaches to physics-based models: (1) Degradation models based on *causal-based* first-principles and (2), degradation models based on *rules-based* first principles (ISO [2012]). Causal-based first principles are considered to be models based on well-known first principle relationships or mathematical equations. Rules-based first principle models are considered to be models based on the same principles. Still, for some reason (e.g., lack of data or lack of confidence in the model), rules are made instead of directly incorporating the principles for diagnosis and prognosis.

The flexsibles are relatively simple systems with few failure modes, making them a good candidate for a causal-based or rules-based first-principle model. Hence, related work to the flexsibles is considered to be in machinery diagnostics and prognostics.

## 2.1 Machinery Diagnostics and Prognostics

Prognostics build on diagnostics, which make diagnostics a prerequisite for a reliable prognosis (Sikorska et al. [2011]). In the earlier work on machinery diagnostics, the emphasis is mainly on diagnosing by dynamic models (e.g., block diagrams) based on vibration signals (Choi and Choi [1996];Howard et al. [2001];Wang [2002];Vania and Pennacchi [2004];Bartelmus [2003]). Simply put, the dynamic models are obtained, and the diagnosis is based on the nature of signals deemed unhealthy.

In later works, the trend has shifted more towards prognosis. When there are CM data available, which can serve as a Health Indicator (HI) of an item, the diagnosis can be made by looking at a starting degradation trend. This is probably due to the increase in available sensor equipment and computational power to companies, which have seen an increase in the last 20 years. In addition, there are also some other clear trends in the literature. A large part considers well-known laws for crack propagation (usually the Paris-Erdogan law) (Qian et al. [2017];Oppenheimer and Loparo [2002];Lei et al. [2016];Cadini et al. [2009];Zio and Peloni [2011]; Haile et al. [2016];Xu et al. [2012]). The concept of RUL seems to be preferred by most when performing prognosis (Liao [2014];Lei et al. [2016];Cadini et al. [2009];Zio and Peloni [2011];Orchard and Vachtsevanos [2009];Zhao et al. [2013];Chiachío et al. [2015];El-Tawil and Jaoude [2013];Baraldi et al. [2012]). Parameter estimation based on Bayesian Inference (e.g., Kalman- and Particle-Filter) generates more accurate RUL estimates (Lei et al. [2016];Cadini et al. [2009];Zio and Peloni [2011];Orchard and Vachtsevanos [2009];Zhao et al. [2013];Chiachío et al. [2015];Haile et al. [2016];Baraldi et al. [2013];Baraldi et al. [2012]). Almost every article considers only one failure mode (either implicit or explicit), which fits well with reviews considering physics-based models to be failure mode-specific (Jardine et al. [2006];Sikorska et al. [2011];Lei et al. [2018]).

Jin et al. [2013] concerns a physical degradation mechanism, but as the physical model is deemed uncertain, a Wiener process (presented in 3.8.4) is used instead for RUL estimation. Liao [2014] perform a hybrid approach, where the selection of features to be used in the physical model are extracted by a data-driven method (genetic programming). The selection of features simplifies the development of prognosis. There are only a few articles that consider real-life data ((Orchard and Vachtsevanos [2009]);Jin et al. [2013]).

In the literature on machinery diagnostics and prognostics, physics-based models only represent 10% of the research. The most researched topics are statistical models (56%) and AI (data-driven) approaches (26%) (Lei et al. [2018]). This is mainly since physics-based models require lots of knowledge on the system at hand are almost always failure mode-specific. Hence, there are problems when trying to generalize the findings done in diagnostics and prognostics performed by physics-based models. This is reflected in the literature as a large part of the literature on physics-based models in machinery diagnostics and prognostics concern laws on crack propagation.

# Chapter 3

# Theoretical background

This chapter is aimed at clarifying subjects and establishing common ground for concepts that further used in this study. The tools presented here, are used in the rest of this thesis.

## 3.1 Statistical Learning

Statistical Learning is mainly a set of approaches for estimating a function $f$, based on $p$ specific input variables, denoted $X = (X_1, X_2, ..., X_p)$, and some output, denoted $Y$. It is assumed that there is a relationship between the inputs and outputs, which can be written generally:

$$Y = f(X) + \epsilon \tag{3.1}$$

Here $f$ is some fixed but unknown function of $X = (X_1, X_2, ..., X_p)$ and $\epsilon$ is a random error term, which is independent of X and has mean zero. Input has several synonyms, such as predictors, features, independent variables (or just variables). Output is usually called the response or dependent variable.

### 3.1.1 Unsupervised and Supervised Statistical Learning

Statistical Learning deals with a vast set of tools for understanding data, finding relationships between them (Casella et al. [2013]). These tools are generally classified into *supervised* and *unsupervised*. Supervised statistical learning involves predicting and estimating an output based on one or more inputs. Unsupervised deals with inputs, but no supervised outputs. The user does not supervise the model, which means that there is not necessarily any known or understandable logic behind the model. However, with supervised statistical learning, it is possible to follow a path of deductive arguments.

There are several different kinds of problems that will determine what types of outputs will be obtained in statistical learning models. Casella et al. [2013] operates with mainly three types

of problems: *regression* problems, *classification* problems, and *clustering* problems. Regression problems involve predicting continuous or quantitative output values, which can be the RUL of the flexsible. Classification problems involve predicting categorical or qualitative outputs, such as determining a healthy or unhealthy state of the flexsible. Clustering problems involve situations in which there are only input variables, but no corresponding output. It revolves around grouping inputs according to their observed characteristics, such as developing a Principal Component Analysis (PCA) of all the measurements available for the flexsibles.

#### Semi-Supervised Learning

Sometimes it is not clear-cut if an analysis should be considered supervised or unsupervised. For instance, suppose that we have a set of $n$ observations. For $m$ of the observations, where $m < n$, we have both predictor measurements and response measurement. For the remaining observations, we have predictor measurements but no response measurements. This is the case when there is flow measurement on the flexsibles, but no corresponding logged replacement when the flow hits the replacement threshold. This is referred to as a *semi-supervised learning* problem.

## 3.2 Inference and Prediction

As the goal in Statistical Learning is to estimate $f$ in 3.1, there are mainly two reasons for this: *inference* and *prediction*. In short, the inference is when we are concerned with understanding how the input $X = (X_1, X_2, ..., X_p)$ affect the output $Y$ (i.e. understanding $f$), while prediction is concerned with obtaining the most accurate predictions of $Y$ (i.e. no understanding of $f$ is necessary).

Casella et al. [2013] states that, when focusing on **inference**, there are some typical questions one might want to answer:

**Which predictors are associated with the response?**
If several predictors are available, it is usually the case that only a small portion of the predictors actually is associated with the response $Y$. Therefore, identifying the important predictors can be very useful.

**What is the relationship between the response and each predictor?**
Predictors can have a positive or negative relationship with $Y$, or for complex situations - one input/output relationship can depend on the values of other predictors.

**Is $f$ adequately summarized using a linear equation or not?**
Most real-world applications tend to have a more complicated relationship, thus it is important to understand if a linear model provides accurate representations of the relationship between

the input and output variables.

When focusing on **prediction**, the goal is to minimize the error term $\epsilon$, to increase the accuracy of the prediction. When there are lots of predictors available, the error term $\epsilon$ averages to zero, and the equation become

$$\hat{Y} = \hat{f}(X) \tag{3.2}$$

where $\hat{f}$ is the estimate for $f$, and $\hat{Y}$ is the resulting prediction of $Y$. However, the accuracy of $\hat{Y}$ will be affected by two types of errors, called the *reducible* error and the *irreducible* error. The reducible error is connected to the imperfect estimate $\hat{f}$ of the ideal function $f$. It is called *reducible* because we can potentially improve the accuracy of $\hat{f}$ by using the most appropriate statistical learning technique to estimate $f$. However, if we found the best estimate $\hat{f}$ based on the predictors available, there could exist unmeasured variables that are useful in predicting $Y$. The error induced by these unknown variables is called the *irreducible* error because it cannot be reduced as long as it is unknown. The irreducible error will always provide an upper bound on the accuracy of our prediction for $Y$. This bound is almost always unknown in practice Casella et al. [2013].

$$\begin{aligned} E(Y - \hat{Y})^2 &= E[f(X) + \epsilon - \hat{f}(X)]^2 \\ &= [f(X) - \hat{f}(X)]^2 + Var(\epsilon) \end{aligned} \tag{3.3}$$

Equation 3.3 shows that the expected value of the difference between the ideal output and the estimated output is equal to the reducible error (first term) and the irreducible error (second term).

#### Trade-off between Inference and Prediction

When modeling $f$ there are several types of methods to use. These can be classified into how flexsible they are i.e. how large the range of shapes to estimate $f$ are. Linear regression is for instance a relatively inflexible method as it can only generate linear functions (or lines). In general, when modeling for inference there are clear advantages to using simple and relatively inflexible statistical learning methods Casella et al. [2013]. This is because it is rather intuitive to understand the relationships between $Y$ and $X_1, X_2, ..., X_p$, while more complex and flexsible methods can lead to complicated estimates of $f$ where it is difficult to understand how any individual predictor is associated with the response. When prediction is the goal, flexible approaches are not always the best. This comes from the fact that one might overfit the model, which means that it works very well on the trained data, but cannot be generalized for other similar data. The

model is in essence following the errors, or noise, too closely. Therefore, inflexible methods are generally better than flexible ones, because of a higher degree of *generalization* and *inference*.

## 3.3 Modeling $f$

When modeling $f$, there are usually two methods: *parametric* and *non-parametric*. **Parametric** methods involve a two-step approach: (1) assume the functional form of $f$, (2) use the data available to train or fit the model (estimate parameters). The potential disadvantage of a parametric approach is that it might not match the true unknown function $f$. **Non-parametric** methods, however, do not make any explicit assumptions about the functional form of $f$. This mitigates the problem of choosing the wrong $f$, but it usually results in a large number of parameters to estimate. Thus, a large number of observations is needed to obtain an accurate estimate for $f$. Non-parametric methods are usually also more prone to overfitting the model.

## 3.4 Modeling Accuracy

When evaluating the performance of a statistical model on a specific data set, it is important to quantify to which extent the predicted response value for a given observation is close to the true response value for that observation. When dealing with regression, the most common measure is the mean squared error (MSE):

$$MSE = \frac{1}{n}\sum_{i=1}^{n}(y_i - \hat{f}(x_i))^2 \tag{3.4}$$

where $\hat{f}(x_i)$ is the prediction that $\hat{f}$ gives for the $i$th observation. The MSE will be small if the predicted responses are very close to the true responses, and will be large if, for some of the observations, the predicted and true responses differ substantially.

### Training and Test Sets

The MSE in Equation 3.4 is computed using training data, which is used to fit the model. The MSE obtained there is usually called the *training MSE*. However, it is not very interesting to know how the model works on already obtained data (where the events connected to it are probably already known). Rather, it is interesting to know the accuracy of the predictions that we obtain when applying the method to previously unseen test data. This is because the method then can be used to predict similar future data sets accurately. In other words, an external test set with predictors $x_0$ and corresponding response $y_0$ should be combined to see if $\hat{f}(x_0)$ is approximately equal to $y_0$. The test set, $(x_0, y_0)$ is previously unseen and not used to train the statistical

learning method. Therefore, one should choose the model that minimizes the test MSE ($MSE_t$) rather than the training $MSE$. The computation would be

$$MSE_t = Ave(y_0 - \hat{f}(x_0))^2 \tag{3.5}$$

the average squared prediction error for the test observations $(x_0, y_0)$. There are several ways of choosing how the training and test data set is split up. One such way is called the validation set approach (Casella et al. [2013]).

#### Validation Set Approach

The validation set approach is one of the simplest validation approaches. It involves randomly dividing the available set of observations into a training set and a validation set (or hold-out set). The model is fit on the training set, and the fitted model is used to predict the responses for the observations in the validation set. The resulting validation set error rate—typically assessed using MSE in the case of a quantitative response—provides an estimate of the test error rate. There are mainly two drawbacks to this type of validation: (1) the test error can be variable as it depends on which observations are used in the test and validation sets and (2) as the validation set is held out, the training data are trained on fewer observations (which will increase the test error).

## 3.5 Overfitting and Underfitting of Models

Casella et al. [2013] goes on to show that the *expected test MSE* can always be decomposed into the sum three fundamental quantities:

$$E(y_0 - \hat{f}(x_0))^2 = Var(\hat{f}(x_0)) + [Bias[\hat{f}(x_0)]]^2 + Var(\epsilon) \tag{3.6}$$

The variance of $\hat{f}(x_0)$ the squared bias of $\hat{f}(x_0)$ and the variance of the error terms $\epsilon$.

*Variance* refers to the amount by which $\hat{f}$ would change if it was estimated using a different training data set. This is also called overfitting (Barros [2019]). On the other hand, *bias* refers to the error that is introduced by approximating a real-life problem, which may be extremely complicated, by a much simpler model. This is also called underfitting (Barros [2019]). To minimize the expected test error, the statistical learning method that simultaneously achieves low variance and low bias needs to be chosen. Notice that the variance of the error terms are not dependent on $x_0$ and are the irreducible error introduced in 3.3.

As a general rule, as we use more flexible methods, the variance (overfitting) will increase and the bias (underfitting) will decrease (Casella et al. [2013]). For inflexible models, such as

linear regression, the opposite is true.

## 3.6 Linear Regression

In the context of the flexsibles, and consequently this master thesis, the main goal is to develop a prognosis of the flexsibles, to improve maintenance decision-making. In addition, the focus is on physics-based models, which are a good choice when modeling for inference. Linear regression also has a low probability of overfitting, as it is a rather inflexible approach. Hence, the focus will be on linear regression as a basis for the prognosis. First, *simple* linear regression is presented. Mathematically there is assumed a linear relationship between the response $Y$ and the predictor $X$

$$Y \approx \beta_0 + \beta_1 X + \epsilon \tag{3.7}$$

Where $\beta_0$ (intercept) and $\beta_1$ (slope) are model parameters. To be able to develop a regression model, the parameters need to be estimated. In the linear regression case, this is usually done by minimizing the *least-squares* criterion, which is a special case of the more general *maximum likelihood estimator* (MLE). The error term $\epsilon$ is typically assumed to be independent of X.

### 3.6.1 Assessing Model Fit

The $R^2$ statistic quantifies to which extent the model fits the data in form of a proportion. The proportion of variance explains the measure of fit independently from the scale of Y. This makes the $R^2$ statistic more usable in cases where fits are compared across different data sets. To calculate $R^2$, the following equations are used:

$$RSS = \sum_{i=1}^{n} (y_i - \hat{y}_i)^2 \tag{3.8}$$

$$TSS = \sum_{i=1}^{n} (y_i - \bar{y})^2 \tag{3.9}$$

$$R^2 = \frac{TSS - RSS}{TSS} = 1 - \frac{RSS}{TSS} \tag{3.10}$$

Where $RSS$ is the residual sum of squares, which measures the amount of variability that is left unexplained after the regression is performed. $TSS$ is the total sum of squares, which can be thought of as the variability that is inherent in the response $Y$ before the regression is performed. Thus, $R^2$ measures the proportion of variability in $Y$ that can be explained using $X$. Notice that $R^2$ can be negative, which would indicate that a horizontal line would do a better job at explaining the variance in $Y$ because of $X$. The $R^2$ statistic is found to be a good tool regardless of the type of regressional fit that is used (Casella et al. [2013]).

## 3.7 Diagnosis, Health Indicator and Health States

Diagnostics characterizes the status of damage through detection, isolation, and identification using collected data from structural health monitoring (An et al. [2015];Sikorska et al. [2011]). Detection concerns detecting when something is wrong. Isolation is to specify which component is faulty, while identification is to identify which type(s) of failure mode(s) that the item is suffering from and how severe it is. When diagnosing it is useful to distinguish between two different types of fault (Martin [1994]). Types of fault are divided into **hard** and **soft** failures. The soft fault experiences a trend and develops gradually over time. The hard fault happens instantaneously, without any previous warning. Soft faults are typically seen in mechanical elements, while hard faults are typically seen in electrical circuit elements.

For a soft failure, which is recognized if the system exhibits an unsatisfactory performance, the lifetime is regarded as the first hitting time (FHT) that the degradation process exceeds a pre-set failure threshold. Most degradation-data analysis methods focus on soft failures.

Thus, to do a proper diagnosis, and consequently, prognosis based on CM data, a Health Indicator is needed. A Health Indicator (HI) is a sensor measurement (or several combined) that indicates the health of the item and its chosen failure mode in question (Lei et al. [2018]). Thus, the HI predicts the soft fault to a sufficient degree.

### 3.7.1 Health Indicator

A suitable HI is expected to simplify the prognostic modeling and produce accurate prediction results (Lei et al. [2018]). There are mainly two things to consider when constructing a HI: (1) How to construct HIs from the available monitoring signals and (2) how to evaluate the suitability of the constructed HIs for RUL prediction. When it comes to (1) there are mainly two approaches: Physical HI (PHI) and Virtual HI (VHI). PHIs are usually extracted directly from sensor measurements that are related to the physics of failure. VHIs are usually several fused PHIs (multi-sensor signals) and loose physics meaning but still relate to the degradation of the item. When it comes to (2) Lei et al. [2018] goes on to list 5 criteria to assess the suitability of the HI:

1. Monotonicity: to what degree the trend of the HI is monotonically increasing or decreasing. In machinery prognostics, there is assumed monotonicity, as equipment can not suddenly improve performance.

2. Robustness: how much variance there is in the data compared to the drift. If the HI is robust is presents a smooth degradation trend. (signal-to-noise ratio).

3. Trendability: how the HI is related to time (age). Higher trendability means that the HI degrades more as time goes on. A Health Indicator that has a consistent trend over time

4. Identifiability: How good the HI is to identify different HSs. There are usually several Health States during the lifetime of an item, consequently a good HI should be able to identify these.

5. Consistency: when there are multiple HIs. Different HIs on the same unit usually present some sort of correlation between each other – because they contain information on the same degradation process. In addition, the same HI on different units should induce minimal variance in their time to failure.

When using these criteria, there are sometimes important to consider which of them that are more important and optimize these to select the best HI. Hence, Lei et al. [2018] propose *hybrid metrics* approaches to select the right HI.

### 3.7.2 Health States

While fault diagnosis is to identify fault pattern and its severity at one point in time, health states concerns with dividing the HI into two or more states according to the different trends the HI experiences. When conducting a two-stage division, the simplest strategy for the division of health states is by determining a constant alarm level (Lei et al. [2018]. However, when random fluctuations can occur in the HI, the constant alarm threshold can yield false alarms. A two-stage division is applicable in cases where the degradation trends in the unhealthy state are consistent and can be expressed by a single degradation model. When this is not the case a multi-stage division might be more appropriate. This is usually applicable when the degradation trends change due to variations in the fault patterns or operational conditions (Lei et al. [2018]). When there two health states are considered a simple and effective way of dividing the health states is the Neyman-Pearson's test (Barros [2019]).

### 3.7.3 Neyman-Pearson's test

The Neyman-Pearson test considers two states, an unhealthy and a healthy. The observation $X$ are stochastic and can fall in the unhealthy distribution ($p_1(x)$) and the healthy distribution ($p_0(x)$). A hypothesis test can then be obtained, where the null hypothesis ($H_0$) is considered to be when the observation $X$ is healthy ($X \sim p_0(x)$), while the alternative hypothesis ($H_1$) is when $X \sim p_1(x)$. Then a decision structure can be defined as:

$$\delta(x) = \begin{cases} 0, & D_0 : H_0 \text{is accepted} \\ 1, & D_1 : H_1 \text{is accepted} \end{cases} \tag{3.11}$$

By introducing the likelihood ratio $\Lambda(x) = \frac{p_1(x)}{p_0(x)}$, the following decision structure can be obtained: $\Lambda(x) < \lambda_n = D_0$ and $\Lambda(x) > \lambda_n = D_1$. Where the $\lambda_n$ is defined as the Neyman-Pearson threshold. From this it is easy to obtain the probabilities of false alarm ($\alpha$) and non-detection ($\beta$):

$$\alpha = P(\Lambda(x) > \lambda_n \mid H_0) \tag{3.12}$$

$$\beta = P(\Lambda(x) < \lambda_n \mid H_1) \tag{3.13}$$

## 3.8 Prognosis

Sikorska et al. [2011] states that prognostics is related to and highly reliant upon, diagnostics. This is because diagnostics involves identifying and quantifying the damage that has occurred, while prognostics is concerned with trying to predict the damage that is yet to occur. When doing maintenance decisions in real-time, information about both of these aspects proves valuable. Diagnostics may provide useful business outputs on its own and decision-making linked to prognostics can be rather complex. Prognosis is usually called *degradation modeling* in the maintenance literature as the goal of the prognosis is to obtain a remaining useful life (RUL) of the item under analysis. Degradation modeling is one of the most important aspects of Prognostics and Health Management (PHM) as well as the foundation for decision-making for maintenance (Zhang et al. [2018]). Hence, PHM is discussed next together with the concept of RUL.

### 3.8.1 Prognostics and Health Management

In the last decade, several international scientific societies (Center for Advanced Life Cycle Engineering, phmsociety, ESRA) and conferences (PHM Conference, IEEE Conference on Prognostics and Health Management, Prognostics and System Health Management Conference) have promoted research on Prognostics (**?**). Within the fields of PHM, a range of different definitions of prognostics have been proposed, as pointed out in Sikorska et al. [2011]. Byington et al. [2002] states: *"Prognostic is the ability to predict the future condition of a machine based on the current diagnostic state of the machinery and its available operating and failure history data"*. Sikorska et al. [2011] argues that the most all-encompassing description of prognostics is made by the french standard ISO13381-1, as it defines prognostics as *"an estimation of time to failure and risk for one or more existing and future failure modes"*. Baruah and Chinnam [2005] says that: *"Prognostics builds upon the diagnostic assessment and are defined as the capability to predict the progression of this fault condition to component failure and estimate the remaining useful life (RUL)"*. From these definitions, it can be deduced that prognostics is based upon diagnostics of current health states which is based upon both past and present history of the item, and the prediction of future health states and failure modes. Hence, to provide an accurate failure

prediction of an item; history, age, current state, and future usage need to be considered.

### 3.8.2 Remaining Useful Lifetime (RUL)

Estimation of the RUL is essential within both CBM and Prognostics and Health Management (Si et al. [2011]). RUL is typically a random variable, and as such needs to be estimated from available condition and health monitoring information (Si et al. [2011]). A general definition of RUL can be formulated by letting $RUL(t_j)$ denote a random variable that corresponds to the remaining useful life at time $t_j$, such that:

$$RUL(t_j) = inf\{h : Y(t_j + h) \in S_L | Y(t_j) < L, Y(s)_0 \leq s \leq t_j\} \tag{3.14}$$

$Y(t_j)$ denotes the condition (health indicator) of the item at time $t_j$. The notation is changed from the last chapter, where the state of an item was denoted $X(t_j)$. This is because the health indicator can be much more complex considering several factors e.g. environmental factors and several sensors. $Y(t_j)$ is considered to be the health indicator built from $X(t_j)$. The future health state is denoted $Y(t_j + h)$ - related to prognosis. $S_L$ is a set of unacceptable states representing failure and $L$ represents a fixed threshold limit which defines unit or system failure if exceeded. As the limit $L$ is what defines when the system fails, it is possible to adjust it in context with the system you are looking at. This is the line that indicates if the system/item is useful or not.

Following this, $RUL$ of an asset/item is a random variable that depends on the current age and condition of the asset, the operational environment, and the available condition monitoring (CM) and health information (Barros [2019];Si et al. [2011]). There are different ways of estimating the RUL, which are frequently referred to as degradation modeling.

### 3.8.3 Degradation Modeling

Degradation modeling is an integral part of any predictive maintenance policy. Degradation modeling can be divided into four categories: physics model-based approaches, statistical (or stochastic) model-based approaches, AI approaches, and hybrid approaches (Lei et al. [2018];Jardine et al. [2006];Barros [2019]).

**Physics-based models** are preferable when a physical model is available and the data available makes it easy to estimate the model parameters (An et al. [2015]). However, these models can be hard to obtain as real-life systems tend to be rather complex and a deep understanding of the system's physics is required (Zhang et al. [2018]). The prognosis accuracy is heavily reliant upon the type of physical model used.

**AI models** or data-driven approaches are preferable when there are large amounts of data available and the system's physics are poorly understood. By using large amounts of data they

are capable of dealing with prognostic issues of complex mechanical systems whose degradation processes are difficult to be interrelated by physics-based models or statistical models (Lei et al. [2018]). They can find relationships and physics that are unavailable to humans at the present moment (Rasheed et al. [2020]).

**Stochastic** and statistical models fall in between the aforementioned types of models. While the AI models and physics-based models try to decrease the uncertainty of the system's physics in their own way, stochastic models can capture these stochastic dynamics within the degradation processes (Zhang et al. [2018]). They can handle the unexplained randomness and incorporate it into the stochastic models. The stochastic models are by Alaswad and Xiang [2017] classified into three different classes: discrete-state degradation, proportional hazard models, and continuous degradation. In situations where the degradation is continuous, the condition can be measured through sensor measurements, the continuous degradation models are most relevant (Alaswad and Xiang [2017]). Stochastic continuous degradation models are further classified into Gamma, Inverse Gaussian (IG), and Wiener processes (Zhang et al. [2018];Alaswad and Xiang [2017]). These processes are considered to be independent increment processes (Barros [2019];Zhang et al. [2018]). The Gamma and IG processes are only suitable to model monotonically increasing degradation (Zhang et al. [2018]). On the other hand, Wiener processes are applicable for non-monotonous degradation processes resulting from minor repair, self-healing, or reduced intensity of use, which are frequently encountered in practice.

### 3.8.4 The Wiener Process with Linear Drift

The Wiener process can be used in cases where the increments are normally distributed and independent (Barros [2019]). The Wiener process with linear drift can be formulated as (Zhang et al. [2018]):

$$X(t) = x_0 + \mu(t) + \sigma_B B(t) \tag{3.15}$$

Where $x_0$ is the initial state of the degradation (i.e. when prognosis start), $\mu$ is the drift coefficient which translates to the general rate of degradation, $\sigma_B$ is the diffusion coefficient and $B(t)$ represents the Brownian Motion, with mean zero and variance $t$ (Barros [2019];Elwany and Gebraeel [2009]). The Brownian Motion considers the stochastic properties of the degradation process. A great advantage to the Wiener process is that the first passage time to a fixed threshold L (RUL) follows an IG distribution (Zhang et al. [2018]). Based on this RUL can be modeled as (Rausand and Høyland [2004]):

$$RUL(t_j) \sim IG(\mu_t, \lambda_t) \tag{3.16}$$

Where the parameters can be estimated by the following equations (Zhang et al. [2018];Elwany and Gebraeel [2009]):

$$\mu_t = \frac{(L - x_0)}{\mu} \tag{3.17}$$

$$\lambda_t = \frac{(L - x_0)^2}{\sigma_B^2} \tag{3.18}$$

Where the $\mu_t$ is the mean and $\lambda_t$ is the shape parameter of the IG distribution. This is in the case of deterministic model parameters ($\mu$ and $\sigma_B$), while under a Bayesian Framework, updating the parameters, the calculation is found to be rather similar (Fabrice et al. [2010]). Estimating the parameters $\mu$ and $\sigma_B$ to be used at the start of prognosis are further discussed.

### Parameter Estimation

Zhang et al. [2018] states that the problem of parameters estimation is an essential part of degradation modeling and the RUL prediction. The most common way of identifying parameters in the Wiener process with linear drift is by using the degradation data in an MLE method. For the linear regression, the MLE reduces to minimizing the Least Square Errors (LSE). In this case, it is assumed that the parameters are deterministic based on historically obtained data. When the model parameters are deemed to be stochastic, a Bayesian Analysis (Inference Framework) can be used to continuously update the parameters based on combining historical and new data (Casella et al. [2006]). Bayes' rule combines the prior probabilities with the likelihood to compute the posterior probabilities. The *prior* probabilities typically denote the model obtained before any data are obtained (e.g. a probability density function). The *likelihood* is the probability of observing the data under the prior model. The *posterior* probabilities are available after the data are observed and are proportional to the product of the prior probability and the likelihood. This relationship can be expressed as follows (Casella et al. [2006]):

$$P(Model|Data) \propto P(Model) \times P(Data|Model) \tag{3.19}$$

A Bayesian analysis in which accumulating information is incorporated over time (e.g. time series), with the posterior probabilities from one step becoming the prior probabilities for the next step, is called a Bayesian sequential analysis (Casella et al. [2006]).

### Bayesian Sequential Analysis

When looking at the problem with the Bayesian Inference perspective, the parameters are now assumed to be able to change with new degradation paths. In this section, the special case of assuming the $\mu$ unknown and the $\sigma_B$ known is considered. This is a somewhat unrealistic assumption, but simplify the problem and make it possible to find analytical solutions (Casella

et al. [2006]). This is in the case where both PDFs for $\mu$ (prior and posterior) are assumed to be normally distributed. The posterior distribution for the drift $\mu$ at time $t$ ($\mu_t$) can be found by the expression:

$$\mu_t|\mathbf{y} \sim N\left(\frac{n\delta\overline{y_t}\tau^2 + \tau_0^2\mu_0}{n\tau^2 + \tau_0^2}, \frac{1}{n\tau^2 + \tau_0^2}\right) \tag{3.20}$$

Where **y** is the new data, n is the sample size of data observations, $\delta\overline{y_t}$ is a sufficient statistic of the new data **y**, (e.g. the sample mean in this case).$\tau^2$ is the precision of the posterior distribution and $\tau_0^2$ is the precision of the prior distribution. The precision is simply the inverse of the variance and simplifies the calculation of the posterior density of $\mu$ (Casella et al. [2006]). To be clear, the precision is the inverse variance of the $\mu_t$. The precision is formulated as follows: $\tau = \frac{1}{\sigma^2}$, where $\sigma^2$ is some arbitrary variance. $\tau^2$ is the precision of $\delta\overline{y_t}$ based on the sample size $n$, while $\tau_0^2$ is the precision of the prior distribution.

### 3.8.5 Estimating RUL by Monte-Carlo Simulations

When estimating the RUL of a Wiener process with linear drift, it is showed that this is rather straightforward. One simply estimates the parameters for the IG distribution and then obtains a PDF of the RUL distribution. However, when adding additional constraints or increasing the complexity of the model analytical solutions are in general hard to obtain (Zhang et al. [2018]). In these situations, Monte-Carlo simulations can be more effective. Simply put, a Monte-Carlo simulation simulates the degradation path of a Wiener process increment by increment. Every increment is stochastic and normally distributed with parameters $\mu$ and $\sigma_B$. The distribution of the RUL for a Monte-Carlo simulated Wiener process with linear drift would be equal to the analytical solution if enough degradation paths are simulated.

However, when adding new constraints and additional complexity to the model, such as age or the state of the degradation, this can simply be incorporated into the simulation. In the analytical approach, this will result in integration for each extra constraint one adds to the model.

#### Validation of RUL Prediction

When calculating RUL distribution by analytical methods, Monte-Carlo simulations are usually being compared to the analytical solution to validate the model. Analytical models are computationally favorable as they use substantially less amount of computing power compared to simulations. Hence, an analytical solution would not be a good way to validate a simulation, as a simulation model is done to omit to make the more complex analytical model. Validation tests such as the ones described in earlier about regressions are also not suitable in the case of the RUL. This is because RUL gives a stochastic estimate rather than a deterministic one, which

means that there are uncertainties tied to the estimate.

For these reasons, the RUL predictions will be performed by a Validation set approach approach. In this case, the training data are thirteen degradation paths, while the test data are one degradation path. The RUL predictions are first cross-validated on the thirteen training sets, optimizing the model parameters. Then, the model is tried on the test set, looking to see if the model holds for unknown degradation paths. The requirements of the prognosis should have a good prediction accuracy over all of the data sets, a sufficiently low uncertainty, and the estimation should be conservative, as the goal of the prognosis is to mitigate unplanned production stops.

## 3.9 Failure Mechanisms

In this thesis, the failure mechanisms of the failure mode *loss of cooling* are reviewed, which is found by an FMSA in Chapter 5. Hence, some theories on the failure mechanisms are presented here. The main failure mechanisms are considered to be corrosion, solid particle erosion, and overheating caused by current in the conductive copper - a type of electrical degradation. At the moment there is not found any specific scientific literature on "high current water-cooled flexible cables", thus the theory is based on similar components. For corrosion, the theory is be based on the corrosion of copper in aqueous solutions. Solid particle erosion is typically found in oil pipes, thus the theory is gathered from this research area. The overheating is linked to current and conductivity, where more general theories from textbooks are presented.

### 3.9.1 Corrosion of Copper in aqueous solutions

Corrosion is by Heusler [1990] defined as: *"Corrosion is an irreversible interfacial reaction of a material (metal, ceramic, polymer) with its environment which results in consumption of the material or dissolution of the material of a component of the environment"*.

Leidheiser jr. [1971] states that the resistance of a metal to corrosion is generally a consequence of three factors: (1) its thermodynamical stability, (2) the presence of insoluble corrosion products that insulate the metal from the environment (also called passive film), and (3) the absence of effective cathodes or cathodic depolarizing agents in the medium.

In aqueous solutions, the corrosion of copper generally occurs through an electrochemical mechanism in which areas remote from one another on an atomic scale serve as anodes and cathodes (Leidheiser jr. [1971]). When the anodic and cathodic areas can be separated, e.g. two dissimilar metals, the current flowing between the two electrodes quantitatively accounts for the amount of corrosion. The development of potential differences between areas on metal, and consequently the development of anodic and cathodic areas, can originate from many sources.

Because the anodic and cathodic reactions are important for the corrosion mechanism, these reactions are presented next.

### The Anodic Reaction

Pareek et al. [2019] states that the detailed electrochemical behavior leading to the **anodic** dissolution of copper remains uncertain. However, the chloride ion is known to have a strong influence on the copper corrosion mechanism (Leidheiser jr. [1971];Boulay and Edwards [2001];Kear et al. [2004]). The anodic reaction is regarded to be somewhat complex, which will be affected by a broad range of factors heavily dependent on the environment (Kear et al. [2004]). For instance, oxygen concentration, chloride concentration as well as temperature are some factors that will determine what types of passive films can be created at the anode. The anodic reaction will typically create a positive potential. This is due to the dissolution of the material happening at the anode, creating positive copper ions. When this happens the ions can either dissolve into the electrolyte or form a film at the surface of the material (Heusler [1990]).

### The Cathodic Reaction

The **cathodic** reaction is concerned to be more known and is considered to be dominated by oxygen reduction (Kear et al. [2004]; Pareek et al. [2019]). It is presented to be:

$$O_2 + 2H_2O + 4e^- \rightleftharpoons 4OH^- \tag{3.21}$$

In the current maintenance operation they are adding highly alkaline solutions to drive the cathodic reaction over to the left: mitigating the high oxygen concentration which will reduce the negative potential created by this reaction. The increase in $OH^-$ ions will reduce the solubility of oxygen in the water, thus creating less negative potential.

In corrosion of copper in aqueous solutions, it is typically because of the presence of oxygen. However, the rate of corrosion does not usually increase linearly with the rate of the oxygen supply because the anodic reaction (copper ion formation) may be inhibited by the formation of a protective (passive) film (Leidheiser jr. [1971]).

### Thermodynamical Stability

Copper has a low tendency to become passive in aqueous solutions, thus the chemical stability of copper is determined to a major degree by its thermodynamical stability (Leidheiser jr. [1971]). Thermodynamical stability is the degree to which the metal reacts to temperature differences. Thus, the corrosion of copper may be highly influenced by the temperature it experiences.

### 3.9.2 Solid Particle Erosion

Predicting solid particle erosion in gases and liquids is considered a challenging task. Despite all the resources that have been spent to investigate and study erosion, the solid particle erosion mechanism is still not fully understood (Parsi et al. [2014]). Erosion can happen in both brittle and ductile materials, and the mechanisms are different between the two. Researchers generally agree that the mechanism of erosion changes based on the ductility of the surface (Parsi et al. [2014]).

Parsi et al. [2014] goes on to explain the most important parameters that can predict solid particle erosion:

**Particle properties** - like shape, size, density, and hardness are properties of the particles that are deemed to have a significant influence on solid particle erosion. Harder particles tend to cause more corrosion, and the erosion rate increases in relation to increased particle size.

**Fluid properties** - carrier fluid probably has the largest influence on erosion ratio because carrier fluid can affect the impact velocity of particles. In geometries like a straight pipe, there are turbulent fluctuations that are changing the particles' paths and move them toward the wall, which causes erosion. Fluid properties can also alter the local concentration of particles. This means that even if the overall particle concentration is low, the local particle concentration can be high due to the flow pattern and can affect the erosion magnitude and erosion pattern.

**Target wall properties** - the correlation between the target material and solid particle erosion is not clear. As there are different mechanisms based on the ductility of the material, how much erosion occurs is reliant on the target wall's toughness. Increasing toughness indicates the increasing hardness of material without reduction of ductility.

**Particle impact speed** - erosion rate has a direct relation with particle impact velocity and the relation is believed to be as in the following equation:

$$E_r = (V_L)^n \tag{3.22}$$

Where $V_L$ is the particle impact velocity, $E_r$ is the erosion rate and $n$ is a constant. Recent research suggests that $n$ depends on the hardness of the eroded material. A higher hardness indicates a lower $n$, as the material can tolerate more before it erodes.

**Particle impact angle** - the effect of the impact angle on erosion is based on the surface material. This is because ductile materials experience higher erosion rates at lower impact angles. While maximum erosion for brittle material occurs at a near-normal impact angle because the dominant cause of erosion in brittle materials is cracking.

**Temperature effect** - the temperature effect on erosion are not certain. However, the erosion rate is in some studies find to be decreasing by increasing temperature. This is believed to be because metal ductility increases by temperature, thus more of the kinetic energy is absorbed

by plastic deformation.
**Particle-particle interaction** - when there are high concentrations of particles, particles that rebound off the wall can hit particles moving towards the wall and slow them down, leading to less erosion.

### 3.9.3 Current and Conductivity

In general the current follows the path of least resistance. However, when a current goes through a material it usually experiences some resistance, which will cause energy loss from the conductor to the environment. In the following sections, relationships explaining how heat are transferred from conductors to the environment are explained.

#### Heat Dissipation Law

Heat and heat fluctuation are found to be one of the most important indicators for failure in large electrical equipment and are usually modelled by arrhenius law (based an exponential degradaiton) FIND source!!!.

The amount of power (and thus heat) that is dissipated from a conductive material can be deduced by combining Ohm's Law with Joule's Law (Young and Freedman [2016];Schei et al. [1998]):

$$P = I^2 R \tag{3.23}$$

Where $I$ is the current (unit ampere ($A$)), $R$ is the resistance (unit ohm ($\Omega$)) and P is the power (unit watts ($W$)). The mechanism of the heat dissipation due to current in a resistor is twofold. Either the temperature of the resistor increase or there is a flow of heat out of it or both. The energy is considered dissipated in the resistor at a rate of $I^2R$. The heat dissipation comes from the moving charges (currents) colliding with the atoms in the resistor (e.g. a copper wire) and transfers some of their energy to these atoms, increasing the internal energy of the material Young and Freedman [2016]. Furthermore, the resistance of a material is reliant on several properties, which can be formulated as (Young and Freedman [2016]):

$$R = \frac{\rho L}{A} \tag{3.24}$$

Where $\rho$ is resistivity (unit $\Omega/m$), the length of conductor $L$ is in meter ($m$), and the cross-section of the conductor A is in $m^2$. The resistivity, $\rho$, depend on temperature. Young and Freedman [2016] presents a formula which work in the temperature range up to 100 °C:

$$\rho(T) = \rho_0[1 + \alpha(T - T_0)] \tag{3.25}$$

Where $\rho_0$ is the resistivity at reference temperature $T_0$. The $\alpha$ constant is the temperature coefficient of resistance and symbolizes the change in resistance per degree of temperature change.

#### The Skin Effect

When a conductor is experiencing an alternating current (AC), the current is not distributed uniformly across the copper wire cross-section. This is due to the *skin effect*, which is when AC penetrates the surface of a conductor only to a limited depth (Harold [1942]). In the most central part, it is believed to transfer a minimal amount of currents. If the thickness of a conductor is much greater than the depth of penetration, its behavior toward high-frequency alternating currents becomes a surface phenomenon rather than a volume phenomenon (Harold [1942]). It is a surface phenomenon if the thickness and the radius of curvature of exposed metal surfaces are much greater than the depth of penetration. Harold [1942] recommends that the depth is at least twice as great as its radius. The formula for the depth of the skin effect is:

$$d = \frac{1}{\sqrt{(\pi f \mu \sigma)}} \tag{3.26}$$

Where $f$ is the frequency (cycles per second, Hz), $\sigma$ is the conductivity (mhos/siemens per meter) and $\mu$ is the permeability (henrys per meter). Notice that the depth is not dependent on the radius of the conducting material used.

## 3.10 FMECA

An FMECA aims to identify the dominant failure modes and their causes and effects. An FMECA analysis is also good at finding dependent failures and gives a better overview of how the system's components interrelate Rausand and Høyland [2004]. It is used mostly in the design phase, but is also a great tool in data collection and maintenance management. The FMECA done on the flexsibles are shown in figure 5.1.

When it comes to the consequence classes, it is divided based on the criticality of the consequence(s). The criticality is judged on the plant level, and is ranked in these four consequence classes:

S: Safety of personnel
E: Environmental Impact
A: Product availability
M: Material loss

Most of the other theories are rather intuitive and the reader is referred to Rausand and Høyland [2004] for further clarifications on FMECA.

## 3.11 FMSA

Failure Mode Symptoms Analysis aims to select monitoring technologies and strategies that maximize the confidence level in the diagnosis and prognosis of any given failure mode ISO [2012]. The FMSA process is essentially a modification of an FMECA process with a focus on the symptoms produced by each failure mode identified and the subsequent selection of the most appropriate detection and monitoring techniques and strategies. FMSA should also be used in conjunction with an existing FMECA analysis that has identified and ranked possible failure modes. In the scientific literature concerning both FMSA and FMECA (i.e. Rausand and Høyland [2004];ISO [2012]), it is deemed difficult to distinguish failure modes and their causes and effects.

A failure mode is by definition how a failure would be observed or in other words a manner in which a component might fail (to us). There are usually overlaps between the terms used for failure modes, effects, and causes. An item may appear a cause of failure in one line when considering a component and as a failure mode in another. A term can be an effect in one line when dealing with a component and like a failure mode when dealing with an assembly. For example, leakage in flexsibles is an effect of either clogging or sudden hose break but would be a failure mode of the whole silicon furnace. To help with distinguishing these terms, the following form is applied to this case:

A **failure mode** could result in an effect, due to a cause.

To the FMSA sheet, some descriptions are needed. Correlation techniques are other measurements that can be used in conjunction with the primary monitoring technique and thus increase the confidence in diagnosis and prognosis.

**Rating detection (DET)**: denotes the likelihood of detection and is not dependent on the following accuracy of diagnosis and prognosis. Is designed to reflect the overall detectability of a failure mode. It is designed to highlight failure modes which: produce symptoms that are detectable but unrepeatable, produce undetectable symptoms, produce symptoms that are not measurable in practice, or produce symptoms that may be masked by other failure mode symptoms.

**Severity of failure (SEV)**: This is directly tied to the previous FMECA analysis and is designed to rank individual failure modes by risk. It focuses on the consequences of a failure.

**Diagnosis confidence (DGN)**: denotes the predicted accuracy of the diagnosis. This rating is designed to identify failure modes with: detectable, but unrepeatable symptoms, unknown symptoms, or symptoms that are not distinguishable from other failure mode symptoms.

**Prognosis confidence (PGN)**: denotes the predicted accuracy of the prognosis. This rating is designed to identify the same as for diagnosis, but also unknown failure rates and symptoms that are not sensitive to changes in degradation.

**Monitoring priority number (MPN)**: This ranking is the multiplication of the four preceding

rankings. A high MPN value indicates that the nominated technique is the most suitable for the detection, diagnosis, and prognosis of the associated failure mode.

*Measurements* are the raw measurement data obtained from CM of the process e.g. temperature, flow, and current. *Descriptors* are measurements that can describe a symptom or some attribute of the operation and can be used for diagnosis. A *Symptom* for a fault is something that indicates that a fault is looming.

The first four terms are combined into the MPN, which relatively gives an indication of which failure mode should be prioritized and to what degree. All four terms are rated from 1 to 5 - where 1 is low and 5 is high. SEV is an exception as it only is rated between 1 and 4. Notice the difference between DET and DGN: the DGN considers the diagnosis' accuracy, while DET considers the likelihood of detection.

# Chapter 4

# System overview

This Chapter will focus on the system of the silicon furnaces that are producing Silicon at Elkem Thamshavn. Initially, it is organized with the most high-level system functions, followed by incrementally moving down to the low-level system functions such as the flexsibles. It ends with some sections about operations that affect the flexsibles, such as the electric operation, water-cooling operation, maintenance operation, and how the production process affects the maintenance operation. Finally, the data available from sensors at Elkem are presented and discussed. Information not cited here explicitly is taken from discussions with Elkem about the process.

## 4.1 About Elkem

Elkem is a large company with around 6700 employees worldwide, with a total income of 22.7 billion NOK (Elkem [2020]). It divides its business mainly into three areas: Silicones, Silicon products, and carbon solutions. Silicon products, the second-largest business area with 42% of group sales, houses the production of silicon (Elkem [2020]). Silicon is used in a broad range of products; from aluminum and steel alloys to pharmaceuticals, rubbers, and all kinds of electrical equipment e.g. computers (Hanneson [2016]). Hence, it is a product in high demand, and Elkem produces approximately 120 000 metric tons of ferrosilicon and micro-silica each year at their production plant in Iceland (Hanneson [2016]).

Elkem has several production plants around the world, which have their own different characteristics. This master thesis will mainly revolve around data and information coming from the production plant at Thamshavn in Norway. At Thamshavn, there are two different furnaces with different characteristics. Through this chapter, there will be clearly stated when differences between the two furnaces are important to bring up. This is because they have more in common than what separates them.

## 4.2 The Production Process

The production of silicon takes place in large electrical furnaces, where quartz ($SiO_2$) and carbon materials ($C$) react to form silicon ($Si$) and carbon-monoxide ($CO$), illustrated in Figure 4.1. The reaction requires high temperatures of up to 2000 °C. To trigger this reaction, Elkem uses

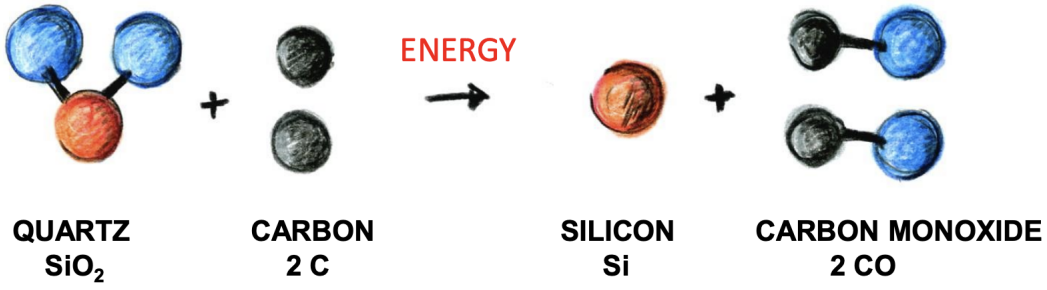


*Figure 4.1: The main compounds in the reaction bath of a conventional silicon production (Hanneson [2016]).*

large furnaces with self-baking electrodes which need continuous filling of a paste made of carbon. The paste hardens as it is heated up (the closer it gets to the reaction bath) and because of this, the electrode will have a continuous change in its length as well as the geometry inside the reaction bath. Because of the random nature of the electrode's physical parameters the electrode's length into the reaction bath needs to be adjusted regularly to optimize the electrical current flowing through the reaction bath. Thus, controlling the temperature of the reaction. There are three electrodes and they are adjusted independently of each other. Because of the way the temperature is regulated, the current supply needs to come through flexsibles. Flexsibles are flexible, water-cooled, high current cables, described in further detail in the next section. The flexsibles position in the furnace operation is shown in Figure 4.2. Each electrode got its own set of flexsibles supplying current to them. At Furnace 1 there are 12 flexsibles for each electrode (36 in total) while Furnace 2 uses 16 flexsibles for each electrode (48 in total).

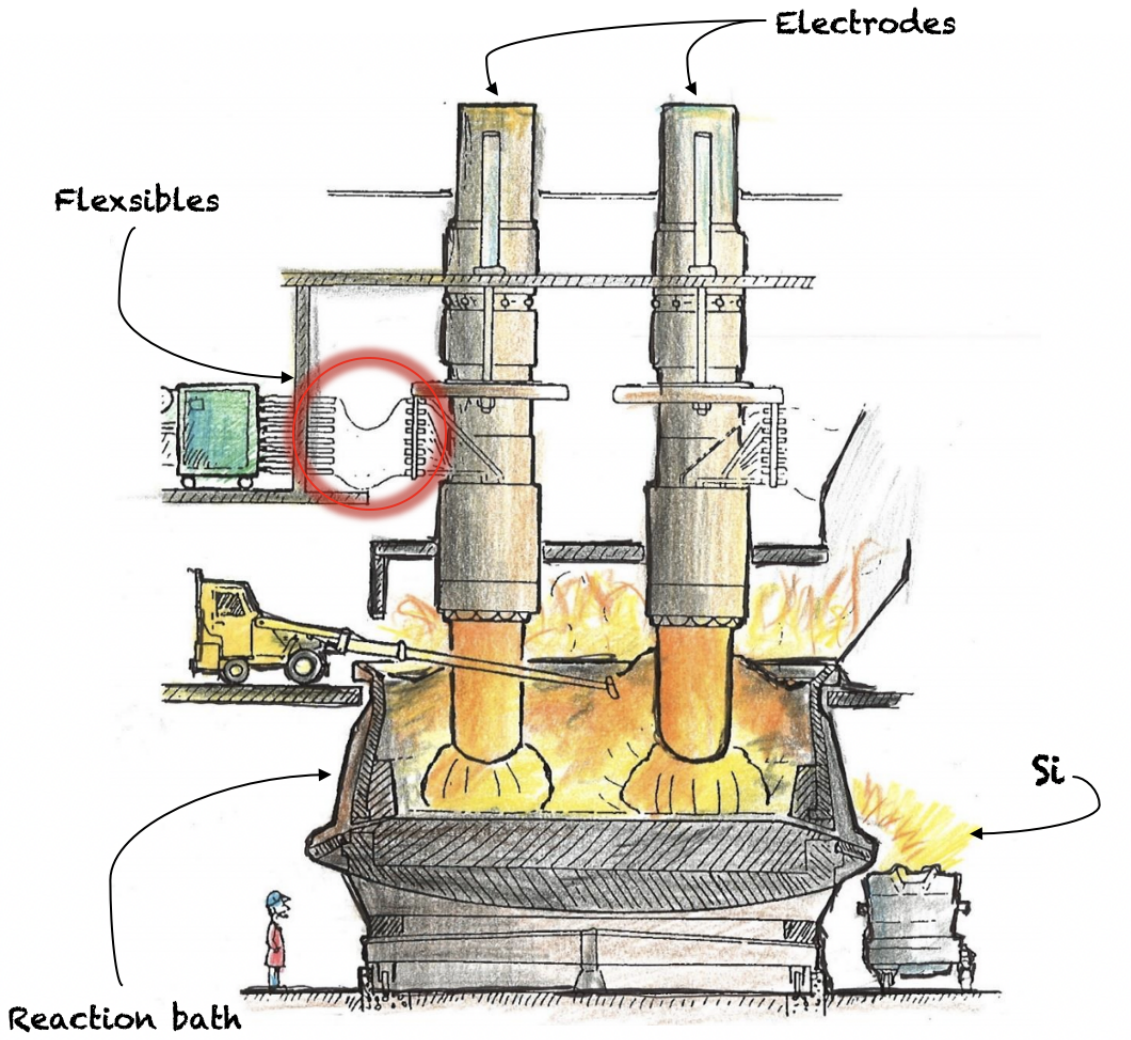


*Figure 4.2: The furnace as drawn by Hanneson [2016]. Additional descriptions are added by the author of this report.*

## 4.3 Flexsibles

The flexsibles' main function is to carry current to the electrodes. The flexsibles can be divided into three parts; live wires in the middle, an outer layer of rubber hose that keeps the water flowing in between, as illustrated in Figure 4.3. The copper *cable* is composed by thin copper *wires* that are intertwined. Each flexsible also have a label e.g. 104T or 104R. T and R denote the way water flows within each flexsible: T is short for *TUR* meaning towards the electrode, while R is short for *RETUR* meaning it is coming out from the electrode.

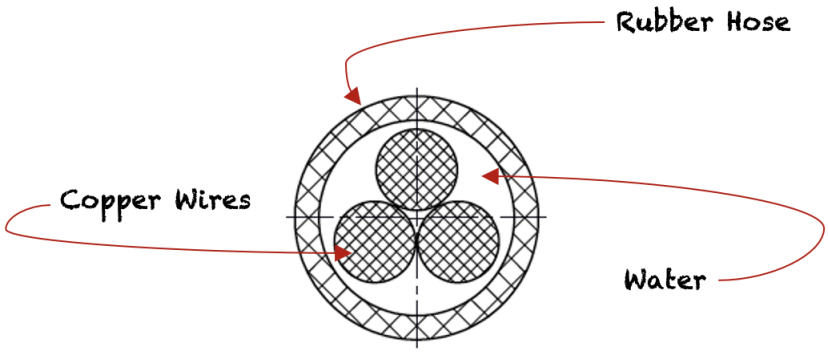


*Figure 4.3: Cross-section of flexsible used for both Furnace one and two.*

The flexsibles transfer a low voltage, but a high current. Because of this characteristic, they are prone to overheat, and the flexsibles are therefore water-cooled by transferring water through each cable. The flexibles must therefore be investigated both in terms of water operations and electric operations, see Section 4.4 and Section 4.5, before the system as a whole can be investigated.

When a flexsible fails it can result in water leakage which is inconvenient for production, requiring it to stop. The unforeseen stops lead to corrective maintenance actions, which may impose high costs. It is also a substantial safety risk that can lead to large accidents like explosions. This type of explosion happened in 2006 when one of the furnaces exploded due to the failure of some water-cooled equipment, where water found its way into the reaction bath (Aftenposten [2006]). The consequences of these types of explosions can be dire as there are working people in close proximity to the furnaces, and in this case, one person passed away (BJØRU [2007]). For this reason, there are water-flow measurements both ways on every flexsible, at every plant, to be able to detect potential water leaks.

### 4.3.1 Flexsible types

The furnace operation and production of silicon is a continuous process, which continuously changes over time. It is always subject to tweaks and changes to optimize and increase production efficiency and safety. Hence, the type of flexsibles ordered from the manufacturer Flohe are naturally changed historically to try and optimize the process. This is also the case for the manufacturer Flohe, where the type of flexsibles they produce have changed over time. Figure 4.4 illustrate the cross-section of an old type of flexible. As a result, there have been several different types of flexsibles in use at the furnaces at Thamshavn during the years of logged replacements. In general, there are different types of flexsibles in use between the furnaces which are directly tied to the power requirements for each furnace. The difference in cross-section is presented in Table 4.1. FHER 1000 is used at Furnace 1 and FHER 1500 is used at Furnace 2. In addition, the flexsibles at Furnace 2 are longer (3259 $mm$) than the flexsibles at Furnace 1 (2994 $mm$).

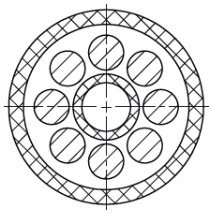

*Figure 4.4: Cross-section of the older type of flexsible with central cooling.*

While the length and cross-section of the flexsibles at both furnaces have been constant over time, their geometric properties have changed. Approximately 10 years ago they went from flexsibles with central cooling as shown in Figure 4.4, to the types depicted in Figure 4.3. However, at Furnace 2 some of these older flexsibles are still in operation. In addition, in later years they have implemented *tinned* flexsibles into their operation as they are believed to mitigate corrosion of the copper wires.

*Table 4.1: Manufacturer's recommendation extracted from FLOHE [2021].*

| **Oven** | **Flexsible Type** | **Cross-Section**[$mm^2$] | **Current at 50Hz** [$A$] | **Bending Radius** [$mm$] |
|---|---|---|---|---|
| **1** | FHER 1000 | 1000 | 8000 | 360 |
| **2** | FHER 1500 | 1500 | 9000 | 400 |

## 4.4 Water-Cooling Operation

Figure 4.5 shows how the flexsible pairs are connected to the electrodes. The flexsibles are labeled with numbers (e.g. 204), where the first number indicates the electrode, the second number indicates the furnace (0 means Furnace 1) and the last digit represents the flexsibles' position on the electrode (to which contact clamp). There are also used letters (e.g. 204T or 204R) indicating if it transfers the water to (T) or from (R) the electrode. A full overview of flexsible labels is given in Table 4.2 for Furnace 1 and in Table 4.3 for Furnace 2. Notice that Figure 4.5 only shows how **one** flexsible pair works.

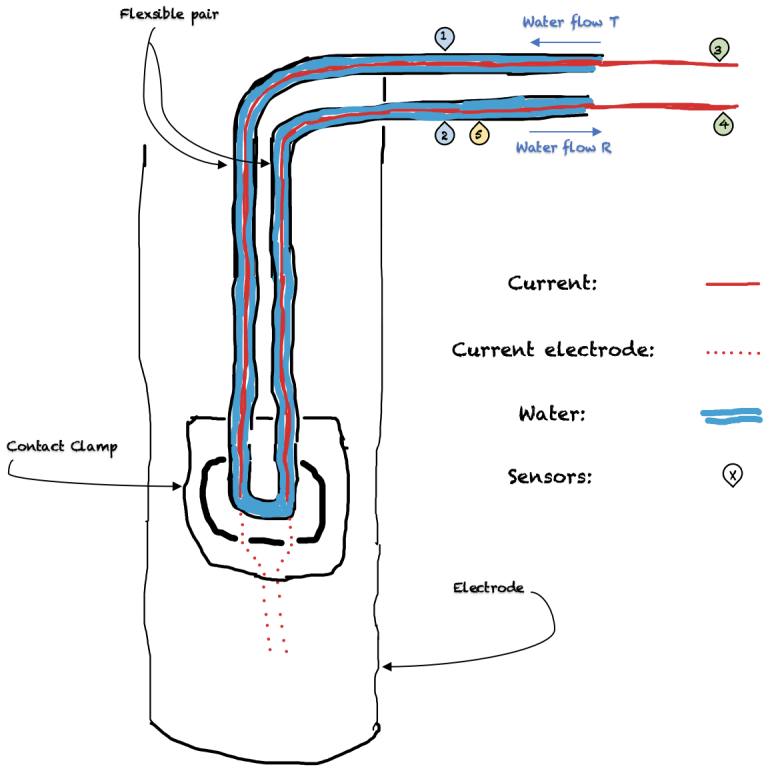


*Figure 4.5: Illustration of the water flow between the manifolds and the electrodes drawn by the author.*

There are two different types of water-cooling operations, one with low temperature (LT) water (around 50 °C) and one with high temperature (HT) water (around 75 °C). The flexsibles use the water coming from the LT-circuit. At Thamshavn the water circuit is closed, which means that the water circulating normally does not mix with water from other sources. However, if there are pressure drops, water from the municipality (normal tap water) is automatically added to mitigate this. If for some reason, the system is unable to maintain the pressure, water is added from the emergency water tank as a last resort. The water from the emergency water pool is placed outside and contains different debris, and is assumed to be more polluted than the

water used in the "closed" circuit within the system.

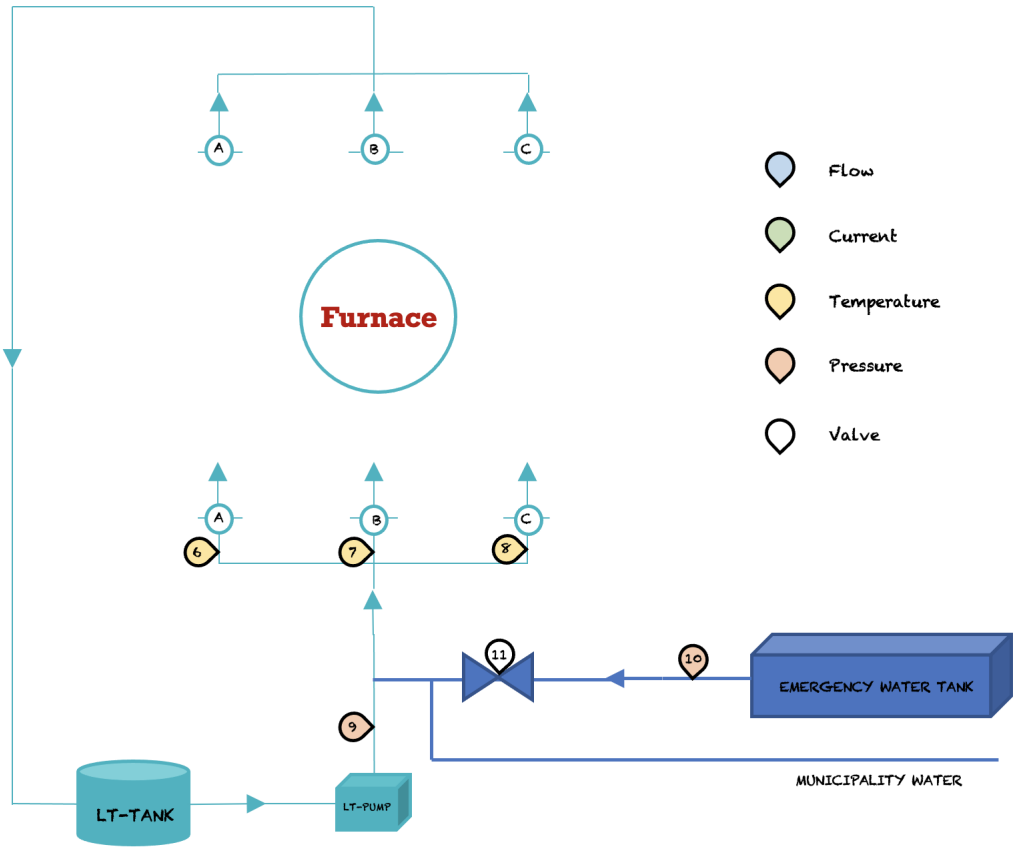


*Figure 4.6: Illustration of the water operation outside the furnace drawn by the author.*

Figure 4.6 shows the water operation as it is outside the furnace. The turquoise colored circuit indicates the "closed" LT-circuit, while the blue indicates the emergency water circuit. A, B, and C denote the manifolds that supply each electrode with water through flexsibles. The manifolds split the water into each flexsible and the flow is believed to follow the path of least resistance. Therefore, a flexsible operating at a slighter lower flow than others is believed to be performing worse. Notice that Figure 4.6 shows that the water goes "through" the furnace, while in practice what happens is depicted in Figure 4.5. Figure 4.6 also show what sensors are used in operation, where the colors indicate what type of information the sensor is obtaining and the numbers are used for location. A more thorough view of what information is available from which sensors are shown in Table 4.5.

### How the water flows

Figure 4.6 depicts how the water flows through the system. The water is supplied from the LT-tank, which keeps the water at the right temperature. After the tank, there is a LT-pump that

provides pressure for further water distribution as seen in Figure 4.6. Then there is an inlet from an emergency water tank and water from the municipality. After the inlet, the water flow is split into three, one for each manifold (denoted A, B, and C). In the manifolds, the water flow is split into each flexsible, where it travels to the contact clamps on the electrodes, and back as seen in figure 4.5. The water then comes back (heated) to the LT-tank, where it is cooled down again.

#### Differences across Furnaces

Each manifold at Furnace 1 supplies water to one corresponding electrode, where manifold A is for electrode 1 and so on. At Furnace 2 the water is supplied in accordance with how the current is distributed. This is more thoroughly discussed in Section 4.5, illustrated in Figure 4.7.

## 4.5 Electric Operation

The silicon furnaces operate with alternate current (AC) at 50 Hz, with three phases. Because the furnaces use AC, the flexibles need to distribute it in pairs, creating closed circuits. This is to obtain current symmetry through the reaction bath. From the transformers, the current is split in busbars and then transported through the aforementioned flexsibles before it goes through a contact clamp and into the electrode as shown in Figure 4.5. The electrode supplies current flowing through the reaction bath, heating and driving the reaction.

The electric operation slightly deviates from how the water-cooling operation concerns the flexsibles. As seen in Figure 4.7 the current from one transformer is split among two electrodes. As a result, there is a closed electric circuit going through the flexsible pair and the contact clamps at each electrode and then through the reaction bath.

The current follows the path of least resistance. The carbon and quartz distribution in the Furnace, the amount of electrical arc (current through gas), resistance in electrode, resistance in contact clamps, and the resistance in the copper wires inside the flexsibles change over time. As all these variables continuously change the resistance in the electric circuit, they will affect how the current distributes over each flexsible.

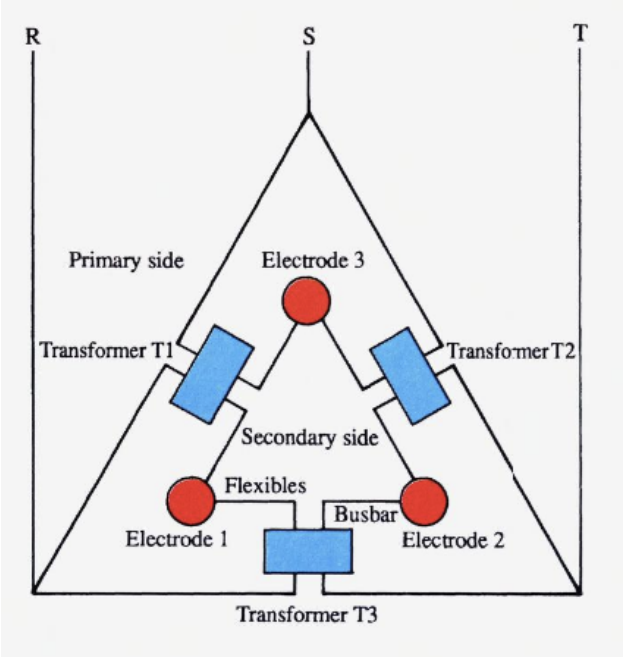


*Figure 4.7: Electrical operation, showing the elctrodes from above and how the AC pairs are split up differently from the water operation Schei et al. [1998].*

*Table 4.2: Table of Furnace 1, showing which flexsible pair that belong to each other. As one might notice, all pairs adds up to 13 and that TUR (T) and RETUR (R) are coupled.*

| **Furnace 1** | | |
|---|---|---|
| Electrode 1 and 2 | Electrode 2 and 3 | Electrode 1 and 3 |
| 104R & 209T | 204R & 309T | 304R & 109T |
| 104T & 209R | 204T & 309R | 304T & 109R |
| 105R & 208T | 205R & 308T | 305R & 108T |
| 105T & 208R | 205T & 308R | 305T & 108R |
| 106R & 207T | 206R & 307T | 306R & 107T |
| 106T & 207R | 206T & 307R | 306T & 107R |

**Differences across furnaces**

At Furnace 1, the current is connected in parallel on each transformer before they are split into their respective flexsible. In addition, the contact clamps on each electrode are also connected in parallel. As the current follows the path of least resistance, this can result in the current being distributed over other flexsibles and contact clamps if one electric circuit experiences larger resistance than the others.

At Furnace 2, the electric circuits are not connected in parallel - which results in a more stable operation. An electric circuit at Furnace 2 which have relatively more resistance than the others will not lead to more load on the others, such as is the case at Furnace 1. The increased resistance will probably lead to higher temperatures on the surface of the copper wire instead.

Because of these differences, the way the flexsibles' current is monitored is also different between furnaces. At Furnace 1, each flexsibles are monitored after the current is split into their respective flexsible. However, this measurement might not be too accurate, as the contact clamps are also connected in parallel. This will lead to the current that goes through one flexsible being able to go through each of the other contact clamps on the same electrode. To be clear, a smaller increase in resistance of one electric circuit will create marginally larger loads at the other circuits. The larger increase in resistance in one circuit will be able to detect with the current measurements because only a proportion of it will be distributed elsewhere.

At Furnace 2, only each electric circuit for one "electric flexsible pair" is monitored. This is due to the electric circuits at Furnace 2 are independent and not connected in parallel. Hence, the monitored current through each circuit at Furnace 2, is more accurate than at Furnace 1. If there is an increase in resistance in one circuit, this will directly lead to less current going through the flexsible. Consequently, there is energy loss from the conducting copper cable to its environment and there would be an increase in the temperature of the cooling water. How the electric circuits are connected in the terms of their flexsible position indication (e.g. 204T) is not intuitive. Hence, the current pairing for Furnace 1 is shown in Table 4.2 and for Furnace 2 in Table 4.3.

*Table 4.3: Table of Furnace 2, showing which flexsible pair that belong to each other. Notice that the pairs always add up to 9 and that TUR (T) and RETUR (R) are coupled.*

| **Furnace 2** | | |
|---|---|---|
| Electrode 1 and 2 | Electrode 2 and 3 | Electrode 1 and 3 |
| 115R & 214T | 215R & 314T | 315R & 114T |
| 115T & 214R | 215T & 314R | 315T & 114R |
| 116R & 213T | 216R & 313T | 316R & 113T |
| 116T & 213R | 216R & 313R | 316T & 113R |
| 117R & 212T | 217R & 312T | 317R & 112T |
| 117T & 212R | 217R & 312T | 317T & 112R |
| 118R & 211T | 218R & 311T | 318R & 111T |
| 118T & 211R | 218T & 311R | 318T & 111R |

**Process Operation**

The heat, which generates the reaction, is produced by dissipation of electrical energy when current passes through the furnace Schei et al. [1998]. The current has two possible paths through the reaction bath: Through the charge bed or through the electrical arc. The charge bed is considered to be the solids in the reaction bath, while the electric arc is a particular type of current through a gas Schei et al. [1998]. To maintain current symmetry and thus a stable and effective production of silicon, the electrodes are adjusted independently up and down into the reaction bath. The further down the electrodes are, the more current passes through the reaction bath. This is due to the fact that the further down you come into the reaction bath, the more of the materials are in liquid form. Molten quartz and silicon transfer current better than the same materials in a solid form that lie on top. However, great care must be taken when adjusting the electrodes as they can break if they touch the bottom of the reaction bath - creating longer unplanned stops. Thus, the electrodes are constantly adjusted automatically between some thresholds to obtain the optimal current symmetry. The resistance (and thus the current flowing through the reaction bath) in the reaction can also be adjusted by either adding more carbon (less resistance) or quartz (more resistance).

## 4.6 Maintenance Operation

To mitigate the unplanned shutdown of the production and substantial safety risk due to failure of a flexsible, Elkem has implemented a preventive maintenance policy based on CM data at Thamshavn. When the difference in flow between a flexsible pair is too high (above $0.5 m^3/h$) it would indicate a leak. When this happens, the flexsible in question is immediately replaced and it incurs an unplanned stop.

When the flow in a flexsible pair is below $4.5 m^3/h$ it indicates a *loss of cooling* that is so

substantial that some action is required. When the flow is below the threshold, two things can happen: flushing or an As-Good-As-New (AGAN) replacement.

**Flushing** is when the flow of the water is reversed. Then the water and its particulates are drained out of the flexsible. Flushing can be done at all times, also during operation. Usually, this gives better flow measurements afterward. This indicates that most of the particulates are accumulated within each flexsible and only small parts of what accumulates inside one flexsible are distributed to the larger water operation. However, there is nothing that stops the particulates to spread to the larger water operation (e.g. filters). After longer stops, there is sometimes experienced a build-up of particles in the flexsibles. For this reason, after stops with a duration of more than a couple of days, they would need to be flushed before start-ups.

If a trend can be seen on the flow measurements (decreasing flow), the concerned flexsibles are replaced at a planned production stop which is once a week. If not, the concerned flexsible is replaced correctively the moment it hits the threshold. Flexsibles are also visually inspected at the planned production stop and are replaced if there is observed outer damage to the rubber hose.

#### Differences across Furnaces

Flushing can only be done at Furnace 1 because the loss of cooling by a degrading flow very rarely happens at Furnace 2. Hence, there are only AGAN replacements at Furnace 2. More about how the flexsibles fail and the differences between the furnaces can be read about in Chapter 5. Since the flexsibles differ in size between the furnaces, how easy they are to **replace** also differ.

There are two different types of planned stops done at Thamshavn. The most regular are stops each week, lasting for 30-40 minutes (sometimes up to an hour). Longer stops happen every fifth week, lasting 3-4 hours. At both furnaces, it is possible to replace one flexsible in the window of 30-40 minutes. The replacements are deemed to be more difficult at Furnace 2 because the flexsibles are larger and heavier. Sometimes, it is possible to change two flexsibles at Furnace 1, if the right mechanics are at work. This is not deemed possible at Furnace 2 and sometimes one replacement at Furnace 2 can take longer than the planned stop of one hour (which happens once a week).

## 4.7 Data Acquisition

Data acquisition is the first step of any CBM-program (Jardine et al. [2006];Lei et al. [2018]). The data obtained from Elkem comes in different forms. The collected data that are important for both diagnostics and prognostics can be classified into two types; (1) event data or run-to-failure data and (2) condition monitoring (CM) data (An et al. [2015]). The event data is events that are

logged manually like stops in production and replacements of flexsibles. As this data is manually collected it requires motivated personnel to do it properly so that the data are reliable enough for use in the analysis. CM data is time series with continuous data obtained automatically from sensors. It is usually associated with a large volume of noise created by the continuous flow of data which eventually might lead to inaccurate analysis Alaswad and Xiang [2017] The sensors shown in Figure 4.6 and 4.5 are the CM data that is going to be used in this thesis. In CBM practice, event and CM data are equally important Jardine et al. [2006]. CM data can give indicators of the condition (features), while event data can be helpful in assessing the performance of these condition indicators.

### 4.7.1 Event Data

*Table 4.4: Table of Event data available from Elkem.*

| **Event Data** | |
|---|---|
| Type | Time Period |
| Stops of Furnace 1 and 2 | 2013-2020 |
| Replacements of Flexsibles | 2013-2020 |

The event data are discrete and gives the date and the location of flexsibles that are replaced. The stops are noted with both date and duration. There are some things that have changed during the period the event data is gathered. At the end of 2019, tinned flexsibles were introduced, as a way of mitigating corrosion. All new flexsibles replaced after this are tinned.

### 4.7.2 CM Data

*Table 4.5: Table of CM data available from Elkem. The color column is referring to Figure 4.6.*

| **CM Data** | | | |
|---|---|---|---|
| Type | Time Period | Location | Color |
| Flow $[m^3/h]$ | 2018-2020 | 1, 2 | Blue |
| Current $[kA]$ | 2018-2020 | 3, 4 | Green |
| Temperature [°C] | 2018-2020 | 5, 6, 7, 8 | Yellow |
| Pressure [bar] | 2018-2020 | 9, 10 | Red |
| Valve open/closed | 2018-2020 | 11 | White |

The CM data are obtained from Excel sheets, where three different sheets were obtained for all the CM data. The sheets were divided into minimum, average, and maximum value readings. The data points were averaged over one hour, making 24 data points per day. Hence, the data are pre-processed as the data used at Thamshavn are obtained in five-second intervals. The

resolution of the data is then rather coarse, but it is traded for easier and faster computation. Some information is of course lost, but it should still be useful for the purposes of this master thesis.

# Chapter 5

# Failure Mode Symptoms Analysis

This chapter is dedicated mainly to an FMSA of the flexsibles. The FMECA works as a prerequisite for the FMSA, which maps out how one should most effectively use CM data for diagnosis and prognosis purposes. The FMECA is carried out as outlined in Rausand and Høyland [2004], while the FMSA is done as described in ISO [2012]. This Chapter will first introduce the functions of the flexsibles before it goes into their failure modes. Then a section presenting an FMECA of the flexsibles follows. Lastly, a section about FMSA of the flexsibles is presented. It ends with a section about the results from the FMSA, which bind things together, and reflects on how the results in this chapter should be used for the rest of this thesis.

## 5.1 Functions and Failure Modes

The flexsibles have one main function and one support function. Its main function is transferring current to the electrode and through the furnace, driving the reaction that creates silicon. To do this without overheating, they are water-cooled, with an outside rubber hose keeping the water close to the copper wire. Therefore, there are these two functions that might be affected when a flexsible fails. For the main function, there is only one failure mode. The flexsible might fail in conducting current if the copper wire breaks. The failure mode is considered to be *no current*. Losing its ability to conduct current can be found by looking at current measurements on the flexsibles. At the moment, this is considered a hard fail that happens without any further warning. The support-function: cooling the flexsible with water, is reliant on the rubber hose qualities, the water qualities and the material in contact with the water. This function has mainly two failure modes: *no cooling* and *loss of cooling*. The hose breaking causes no cooling, and it can fail in several ways, by friction between the rubber hoses, by a large total thermal load, and by contact with high-temperature equipment. This can result in leakage, which can give large explosions mentioned in Chapter 4. Leakage is found by the difference in flow between TUR/RETUR. Darkening and friction can be found by visual inspection. When the flexsibles ex-

periences less cooling, it is because of clogging. This is believed to either come from corrosion of the copper (copper particulates) or debris from the water (e.g., from the emergency tank) or an erosion process. Clogging is found by decreasing flow measurements. Too much clogging can also lead to leakage, leading to higher internal temperatures in the flexsibles. Higher temperatures internally are believed to increase the rubber hose's and the copper wire's degradation. In the most extreme circumstances, the water can turn into vapor generating high pressure, which might burst the rubber hose. This can lead to large explosions in the furnace if water finds its way into the reaction bath.

## 5.2 FMECA

The FMECA of the flexsibles can be found in Table 5.1. The operational modes connected to the silicon furnace can be divided into four: Full stop, warm-up, normal operation, and cool-down. Since it is only during normal operation, the flexsibles are believed to be under substantial stress; all the failure modes are connected to this operational mode.

The failure cause for *no current* is that the copper wire breaks, with no known warning signs. There is not any knowledge on the mechanism of how this happens as of now, and it is assumed that the failure characteristic is a random process. However, this can be an aging process by, e.g., time, thermal load, or current load. The failure characteristic measure could then be time [$hours$], temperature [C], and current[$kA$]. Further investigations of the CM data should be done regarding this. If there is found that no current goes through a flexsible, it is immediately replaced, leading to an unforeseen stop and a corrective maintenance action. Thus, the consequence class is considered product availability (A), and the parenthesis H denotes a high criticality. The recommended interval for replacement is not known at the moment. Still, flexsibles are monitored with lots of sensors and are generally replaced if there are deviations from what the operators deem normal operation.

The failure cause for *no cooling* is that the rubber hose breaks, usually with no previous warning sign. The mechanisms leading to this type of failure are believed to be twofold. It is mainly because of abrasion caused by the flexsibles rubbing together, contact with high-temperature equipment, and total thermal load from the outside and inside. By age, the total thermal load and the probability that the flexsibles come in contact with high-temperature equipment increases. Also, the amount of abrasion caused by flexsibles rubbing together is likely to increase by age. The failure characteristic is deemed random and measured by the difference in flow between the TUR and RETUR in each flexsible pair. If the flow difference passes a certain threshold (0.5 $m^3/h$), the flexsibles are replaced. The consequence class is considered to concern both safety of personnel (S) and product availability (A), where both rankings are considered to have high criticality. This is because no cooling can lead to explosions in most

extreme cases and will always stop production.

The failure cause for *loss of cooling* is either clogging or leakage. The failure mechanism that causes clogging is either erosion, corrosion, or heat load because of high current. The failure characteristic is believed to be gradual, as a degrading flow measurement indicates less cooling capacity of the flexsible. If the flow measurement passes a predetermined threshold (at Thamshavn, they use 4.5 $m^3/h$), the flexsibles are replaced or flushed. The degrading flow usually happens over such a long period of time that it is possible to replace the flexsibles at either the planned stop each week (up to 1 hour stop) and the planned stop every five weeks (3-4 hour stop). The flexsibles are usually flushed before they are replaced. This is usually an effective way of resetting the flexsibles, incurring a larger flow, but the flow measurement still degrades. If it is believed that flushing won't help, the flexsibles are replaced. The consequence class is considered to be the same as for no cooling but with lower-ranked criticality. This is because the loss of cooling can lead to no cooling, hence the same consequences. In addition, less cooling will cause additional problems if several flexsibles cross the flow threshold at the same time due to the constraints of flexsible replacements.

All failure modes are critical and warrant further investigation as they demand a stop in production. Worst case probability, MTTF, MTTF percentage, and recommended intervals are not included in the FMECA. These are quantities that are either not interesting to look at in this context or are hard to find with the data available.

### Differences between Furnace 1 and 2

There are some differences when it comes to the aforementioned failure modes. Loss of cooling is believed to almost exclusively happen at Furnace 1, while the same is the case for no current at Furnace 2. Furnace 1 will usually experience loss of cooling before the flexsibles get the chance to experience wire break (failure mode - no current). Rubber hose breaks, leading to no cooling, are believed to be experienced equally at both furnaces. However, it is more evident in Furnace 2 as less cooling is the dominant failure mode in Furnace 1.

At Elkem, there is a belief that the failure mode *loss of cooling* mainly comes from a corrosion process caused by poor water quality. However, both furnaces use the same cooling water. The furnaces differ in the types of flexsibles and total current load. Hence, further investigations should be performed on the other failure mechanisms such as erosion and heat load from high current.

*Table 5.1: FMECA of the flexsibles*

| FMECA | | | | | | | | | |
|---|---|---|---|---|---|---|---|---|---|
| Operational mode | Function | Failure mode | Consequence class | Criticality | Failure cause | Failure mechanism | Failure characteristic | Maintenance action | Failure characteristic measure |
| Normal operation | Current | No current | A(H) | YES | Wire break | Current load | Random(aging) | Replacement | Current [$kA$] |
| Normal operation | Cooling | No cooling | S(H), A(H) | YES | Hose break (leakage) | Thermal load | Random(aging?) | Replacement | Difference in Flow [$m^3/h$] |
| Normal operation | Cooling | Loss of cooling | S(M), A(L) | YES | Clogging, leak | Corrosion, Erosion and Heat (current) | Gradual | Flushing/replacement | Degrading Flow [$m^3/h$] |

## 5.3 FMSA

The causes, effects connected to each failure mode are considered in the last section about FMECA, thus not mentioned here. The FMSA focuses on connecting these failure modes, causes, and effects with the right sensor measurements. The failure mode *no current* is considered to have no current as a symptom, which can be seen through the current measurement on each flexsible. The monitoring is done each 5 seconds, but the data available in this thesis are averaged over 1 hour. This failure mode is considered to be easily diagnosed, but there is no evidence for a gradual degradation (soft failure), making it hard to use for prognosis. Further work is needed to find such a health indicator.

*Table 5.2: Table of FMSA done on the flexsibles.*

| FMSA | | | | | | | |
|---|---|---|---|---|---|---|---|
| Function | Failure mode | Effect | Cause | Symptoms | Primary technique | Frequency of monitoring | Primary MPN |
| Current | No current | Stop | Wire break | No current | Current meas. | 5 seconds | DET: 5 , SEV: 2, DGN: 4 , PGN: 1 , MPN: 40 |
| Cooling | No cooling | Explosion/Stop | Hose break | Flow meas. (diff.) | Flow meas. (diff.) | 5 seconds | DET: 5 , SEV: 4, DGN: 4, PGN: 1 , MPN: 80 |
| Cooling | Loss of cooling | Explosion/Stop | Clogging | Flow meas. (degrading) | Flow meas. (degrading) | 5 seconds | DET: 5 , SEV: 2, DGN: 4 , PGN: 4 , MPN: 160 |

The failure mode *no cooling* is considered to have the difference in flow measurement between the TUR and RETUR flexsible as a symptom. If the difference is above a certain level, it indicates that somewhere along the way, water pressure is lost due to a leak. This failure mode has a higher severity of failure rank as it can lead to explosions. It is also hard to use for prognosis because the failure is believed to be a hard failure. Several things might indicate an underlying soft degradation leading to *no cooling*—for instance, the temperature in the outside environment of the flexsibles and temperature inside the flexsibles. Literature on the degradation of cables usually considers thermal load (e.g., Arrhenius law) as the indicator for the life of the equipment. Thus, this might also be the case for the flexsibles. However, temperature readings from the outside environment of the flexsibles are not currently available to the author, but they exist according to Elkem.

The failure mode *loss of cooling* is considered to have degrading flow measurement of the flexsible as a symptom. Less water flow in the flexsible indicates more obstructions in this flexsible, e.g., from particulates in the water. The water is assumed to follow the path of least resistance, which means that if one flexsible is more clogged (more obstructions) than the others, it will carry less water. Hence, the flow can be used directly as a health indicator of this failure mode. This failure mode is considered less severe than the previous ones, but it might eventually lead to *no cooling*. Loss of cooling is considered a lot easier to use for prognosis, as the flow measurements degrade slowly. Hence, this failure mode gets the highest MPN - which should warrant further investigation of the failure mechanisms and the connected sensors to develop a diagnosis and prognosis of the flexsibles.

Correlation techniques, and consequently the correlation MPN, is not included in the FMSA as they are deemed obsolete in this context. Further research should be performed before con-

cluding what type of correlation techniques should be used.

## 5.4 Results of FMSA

After the FMECA and FMSA is done, there is one failure mode that stands out. The largest difference between them is that *loss of cooling* seems easier to use for prognosis due to a soft failure mechanism. For the two others, work should be done to find out if there are indications for soft failure mechanisms. In addition, there is more information available concerning the mechanism of failure for *loss of cooling* than the others, which makes the work for establishing models easier. Clogging can also lead to extreme events such as explosions (same as hose break), which means that there are huge potential benefits of more knowledge surrounding this problem. Naturally, there are three failure mechanisms that should be investigated further: **corrosion**, **erosion** and **heat due to current**.

# Chapter 6

# Failure Mechanisms of the Flexsibles

This Chapter is based on the findings in Chapter 5, where the failure mechanisms thought to cause *loss of cooling* were discussed. The failure mechanisms that were found were: **corrosion**, **erosion** and **heat due to current**. It is a literature review on these failure mechanisms highlighting important findings that are suitable in this context. More elaborate theory on these failure mechanisms can be found in Section 3.9. At the moment there is not found any specific scientific literature on "high current water-cooled flexible cables", thus this literature review is based on similar components. For corrosion, the review is be based on the corrosion of copper pipes normally used in water plumbing. Solid particle erosion is typically found in oil pipes and heat-exchangers, thus the review is gathered from this research area. The overheating is linked to current and conductivity, where the general theories presented in Section 3.9 are used to elaborate on this failure mechanism.

## 6.1 Corrosion

As there are many driving forces for electrochemical corrosion, in the next paragraphs there will be an overview of the driving forces (as presented by Leidheiser jr. [1971]) that would be the most important in the flexsible context. Then, general findings of corrosion in similar environments to the flexsibles are discussed.

### 6.1.1 Metal Properties as Driving Forces for Corrosion

**Differential thermal treatment** - such as different currents going through each flexsible pair (historically) can cause potential differences between the copper wires in each cable.
**Surface roughness** - the copper cable are not smooth on the surface. This is due to the general nature of how the cables are made, they are made up of smaller individual wires that are twisted. This generates a lot of nooks and crannies where typical pitting corrosion of copper can occur.

These nooks and crannies will possibly serve as local anodes.
**Differential strain** - in this case caused by the adjustment of electrodes can cause higher corrosion due to plastic deformation. Passive films might rupture creating local anodes relative to the film-covered areas. This might also indicate that tinned flexsibles may be a bad idea, as cracks in the tin layer would induce an aggressive pitting corrosion. However, this is probably also reliant on the environment: on the degree of plastic deformation, the resistance of tin, temperature etc.
**Differential aeration** - comes from the metal being covered by water only by a portion of its length. This leads to a difference in oxygen concentration above and below the waterline (higher above), which creates a potential difference. Oxygen bubbles, or flexsibles not full of water might experience this type of mechanism.
**Thermo-Galvanic corrosion** - some scientific literature have found that the potential difference increases linearly related to the difference in temperature between two copper electrodes. For the flexsibles this would mean that it might be a thermogalvanic corrosion mechanism happening where the different currents meet in the flexsible pair (at the contact clamp presented in 4.4). This is because the current in a flexsible pair are usually different, thus creating different temperatures on the surface as found in Section **??**.
**Contact with other metals** - as newer flexsibles are tinned, to mitigate the corrosion of copper, environmental stress such as strain (from electrode adjustment) or erosion can cause the two metals to get in electrical contact with each other through the solution. This can cause severe corrosion in a short time at the anode. However, the corrosion potentials of different metals are a function of the environment, so the effects of this is considered to be uncertain.

### 6.1.2 Environmental Driving Forces for Corrosion

There are a large amount of parameters that will affect how corrosion occur. These are deemed interrelated, which make it hard to separate these parameters (Leidheiser jr. [1971]). However, in this section the parameters are separated and discussed independently.
**pH** are experimented with by Tam and Elefsiniotis [2009] who finds that the corrosion where higher at lower pH values. Edwards et al. [1994] finds that copper surfaces becomes passive in the presence of chloride at pH larger or equal to 7. In addition, practical corrosion control in water circulating systems can be obtained pH control (reducing pH) (Leidheiser jr. [1971]). These findings relates to the adjustment of the cathodic reaction as presented in formula 3.21. Lower pH values reduces the concentration of hydroxide ions creating a negative potential. Boulay and Edwards [2001] finds that there are more particulate release in by-product of copper corrosion at pH 9.5 compared to pH 7. This might result in a larger erosion effect at larger pH, because of more robust particles (see Section about erosion).
**Chlorine concentration**, when increased, will reduce corrosion in water with high amounts of

microorganisms, probably by killing them (Boulay and Edwards [2001] ). Robertson et al. [1958] did studies on the corrosion in solutions with high salt amounts (thus high chlorine concentration). They found that when the oxygen concentration is constant, in a solution with chloride, the rate of corrosion follow an exponential path dependent on the temperature of the cooling water. The equation of the rate of corrosion were presented as:

$$rate = Ae^{-\frac{9000}{RT}} \tag{6.1}$$

Where $A$ is a constant, R is the gas constant and T is the temperature in the water. In this instance, the corrosion rate of copper where found to be at its maximum at 71-77 °C.

**Oxygen Concentration** in hot water distribution systems, highly influence the corrosion of copper and European practice often involves eliminating dissolved oxygen (Leidheiser jr. [1971]). This is due to reducing the negative potential at the cathodic reaction.

**Temperature** is found to have a profound effect on copper corrosion and its by-product release (Boulay and Edwards [2001]. It was found that in general, higher temperature contributed to a higher copper by-product release. However, at temperatures between 25 and 45 celsius, at maximum bacterial activity, a higher temperature resulted in decreased copper by-products due to killing of microorganisms. Boulay and Edwards [2001] also mention several studies (by Obrecht and Quill, 1960), where they did testing of copper pipes lasting up to 3 years in duration. They concluded that soft waters at pH 7.0 and above, contribute to erosion–corrosion of copper when the temperature of the water is above 45 °C, and that corrosion was worst near 77 °C. This mechanism may be evident in the flexsibles as the operating temperature of the cooling water is around 50 °C. Leidheiser jr. [1971] refers to studies in which highly localized corrosion occurs in condenser tubes. It is associated to hot spots and the attack appears to be a consequence of the high temperature, but thermogalvanic effects (temperature differences) are deemed very important.

**AC** is found to increase corrosion rate in copper exposed to conducting solutions (Leidheiser jr. [1971]). The rate was associated with dissolution occurring at the anodic reaction. This comes from water pipes that have flowing water, and the AC might increase the temperature on the surface - increasing the anodic reaction.

**Flow rate** are found to have an effect on corrosion of copper. At solutions saturated with air, the rate of corrosion of copper in flowing 3 % NaCl increases with the rate of flow Leidheiser jr. [1971]. This amount of salt creates a chlorine concentration that is a lot higher than what is normally observed in regular tap water. However, Ross and Hitchen [1951] finds that the corrosion of copper decreases with increasing flow. In these studies the water used were soft water, with less concentrations of chlorine ions. The mechanism behind this was believed to be the depolarisation of cathodic processes as function of water velocity. Depolarisation of the cathodic processes means that the driving force of the cathodic reaction is reduced, by reducing the neg-

ative potential. Higher water flow velocity then reduces the rate of corrosion. These results are somewhat ambivalent, as there might be contradictory mechanisms at the anode and cathode reaction, in conjunction with the flow rate.

Higher flow rate is then probably increasing the anodic reaction because of the increased availability of reactant (chlorine). The reaction happen on the surface of the copper, which is stationary, while the flow of water continuously supply the anodic reaction with new chlorine ions (Kuźnicka [2009]). While the cathodic reaction, which is dependent on reduction of oxygen will be reduced because the cathodic reaction is happening in the medium that are constantly being transferred away by the water flow.

#### Elkem's theory

At Elkem, corrosion are believed to come from high amounts of chlorine and oxygen in the water. Temperature is believed to increase the rate of the reaction, thus creating more by-product that clogs the flexsibles. This is deemed as the main failure mechanisms, which is evident in their implementation of tinned flexsibles (mentioned in Chapter 4). In addition, they regulate the pH level of the water by adding components to the water to increase its alkalinity, which will decrease the cathodic reaction. Thus, they have put in place measures to mitigate for both the anodic and cathodic reaction. However, Furnace 2 does not experience this type of clogging, but uses the same cooling water. This leads to believing that this might not be the case. Corrosion is probably a part of the degradation process, but might not be as crucial as earlier believed.

## 6.2 Solid Particle Erosion

Erosion increases by increased hardness and size of particles - which is evident in water solutions at high pH. Higher velocity of particles, by for instance increased water flow, increases the erosion. The impact angle of solid erosion particles also affect the amount of erosion, and are assumed to be low, causing erosion in ductile materials such as copper. Lastly, erosion and corrosion can combine, causing impingement which is presented next.

### 6.2.1 Erosion-Corrosion

Kuźnicka [2009] looks at erosion-corrosion mechanisms in heat exchanger tubes made of copper. Only one type of corrosion is observed, which is called repassivating pitting. It means that chloride-rich water induces pitting but inhibits pit penetration. Due to this the passive film layer on top of the pits, is loosely bonded with the substrate (copper). This means that the

repassivated pits become potential places of erosion–corrosion initiation, which is called impingement. Impingement involves removing loosely adhered, corroded surface layers from the metallic surface by high shear stress in the tube wall created by the flowing liquid. When the metal is not covered by any passive film (e.g. by impingement), inflow of fresh reagent (chloride ions) can cause quick deepening of the pits by dissolution of the uncovered metal (Kuźnicka [2009]).

This is a mechanism that is deemed likely in the flexsibles because corrosion seems likely and the flexsibles experience a high water flow.

## 6.3 Overheating by Current

There is assumed that most of the heat caused by the current in the copper cable are assumed to be transferred to the surrounding water by convection and radiation. Heat transfer usually happen in either of three ways: radiation, conduction and convection (Incropera et al. [2013]). Thus, due to the skin effect, conduction properties are negligible in this case. In addition, in this context radiation causes little heat transfer compared to convection (Incropera et al. [2013]). Hence, the heat is assumed to be dissipated to the water by the equation 3.23. In the next section, the heat dissipation within flexsibles at both furnaces are compared, to give an indication on the difference in heat dissipation.

### 6.3.1 Heat Dissipation by Flexsibles on each furnace

The temperature coefficient of copper, $\alpha$, is 0.00393 while the $\rho_0$ is $1.72 \times 10^-8$ (Young and Freedman [2016]). However, the resistivity on the surface of the copper will behave differently with AC and Harold [1942] operates with a resistivity of $\rho_0 = 1.1 \times 10^-6$ ohms at room temperature(20 °C), with a frequency of 50 $Hz$. Notice that this is larger than than the regular resistivity for copper. The parameters are shown in Table 6.1, and are used in equations found in Section 3.9.3 to obtain the relationship of heat dissipation between the flexsibles at each Furnace.

Combining the aforementioned equations, it is easy to see that the flexsibles at each furnace will have a difference in heat dissipation based on their respective cross-sectional area and length. In fact, the resistance on the flexsibles at Furnace 1 are always 1.34 times larger than those at Furnace 2. This means that for the same amount of current, the flexsibles at Furnace 1 dissipates 1.34 more heat as per Equation 3.23.

Another difference between the furnaces is that the depth of penetration at the flexsible at Furnace 2, constitutes a more surface phenomenon than the flexsible of Furnace 1. It is also possible to calculate the temperature of the copper wire surface specifically, based on the current measurements of each flexsible. This is a heat and mass transfer calculation, which can be

*Table 6.1: Flexible parameters for Furnace 1 and 2.*

| **Flexsible parameters** | | |
|---|---|---|
| **Parameter** | **Furnace 1** | **Furnace 2** |
| Skin effect depth, $d$ | 8.89 $mm$ | 8.89 $mm$ |
| Temperature coefficient copper, $\alpha$ | 0.00393 (ř$C$)$^-$1 | 0.00393 (ř$C$)$^-$1 |
| Resistivity of surface at 20 °C, $\rho_0$ | $1.1 \times 10^-6\ \Omega m$ | $1.1 \times 10^-6\ \Omega m$ |
| Length of flexsible in contact with water, $L$ | 2310 $mm$ | 2579 $mm$ |
| Area of cross-section, $A$ | 1000 $mm^2$ | 1500 $mm^2$ |
| Radius of cross-section, $r$ | 17.84 $mm$ | 21.85 $mm$ |

made simpler by some assumptions. A thorough walk-through of such a situation is explained in Incropera et al. [2013], pages 20 and 21.

## 6.4 Combining the Failure Mechanisms

The failure mechanisms presented are probably not independent, but interrelate in some way. In addition, it was not found and causal-based first principle models that are believed to be dominant in the degradation of the flexsibles. Hence, the failure mechanisms are combined in this section, forming a hypothesis on how the flexsibles might fail and degrade. Firstly, the findings in the literature review on failure mechanisms that are found to solidify theories already proposed by Elkem are presented. Then, tentative relationships between the physics of the failure mechanisms that causes clogging phenomena of flexsibles are presented.

#### Findings that solidify Elkem theories

- Low pH increase corrosion.
- High temperatures increase corrosion.
- High chlorine concentrations increase corrosion.
- High oxygen concentrations increase corrosion.
- R-flexsible is probably experiencing more load than the T-flexsible.

#### Flow Chart of Clogging phenomena

A flowchart showing how failure mechanisms might work together to cause degradation of the flexsibles is shown in Figure 6.1. The key takeaway are how all these mechanism come together

forming several **reinforcing effects**. The system is considered to be the surface of the copper cable.

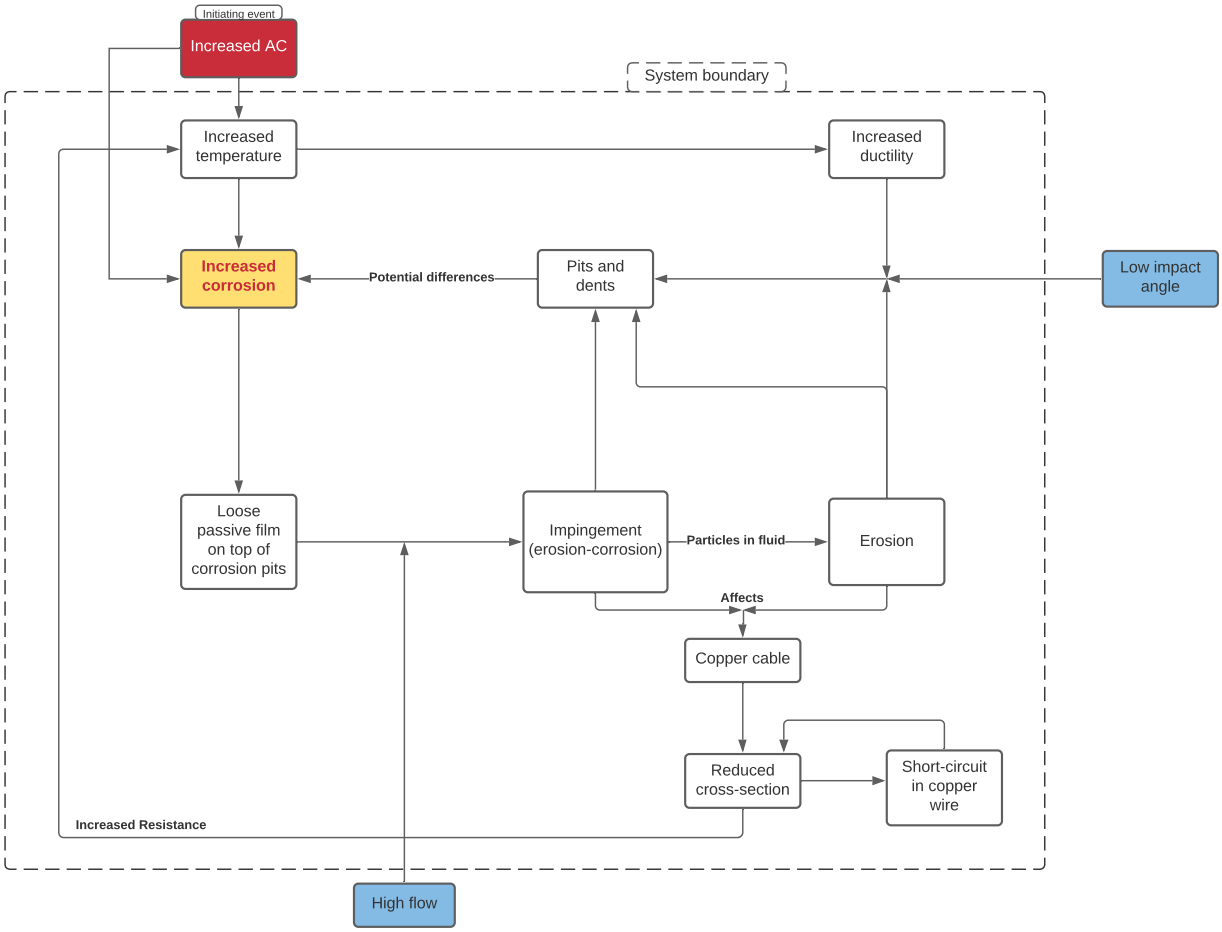


*Figure 6.1: Flowchart of the hypothesized mechanism behind degrading flow.*

In Figure 6.1, the degradation is assumed to start with increasing AC, both increasing the anodic reaction and temperature. This initiates a corrosion mechanism, leading to loose passive film forming at the surface of the copper wire. When there is high flow, this will cause impingement. This leads to particles in the water, causing erosion. Increased temperature causes a more ductile material, which is more prone to erosion at flow with particles hitting the surface at low impact angles. Impingement, erosion and erosion in conjunction with low impact angles and increased ductility all causes more pits and dents in the copper cable surface. This leads to potential differences - leading to more corrosion. The erosion and corrosion mechanisms affects the copper cable, by reducing its cross-section. This leads to increased resistance - thus higher temperature at the surface. The copper cable is built up of smaller copper wires, which can experience short-circuits when the resistance becomes too large. This also aids in the reduction of the cross-section. Increased temperature also leads to higher resistance in the material - which

means that higher temperature causes reinforcing effects.

After the initiation phase, the flow degrades which will decrease impingement (reliant on high flow), but then the erosion mechanism is believed to be more dominant because the flow slow down. The initiation of degradation is here assumed to come from increased AC, but it might also be random. This is due to the initiation mechanisms behind corrosion - which are highly dependent on environmental factors (which can be different from flexsible to flexsible). If there is found no evidence for degrading flow in connection with increased current, the rest of the flow chart is still probably a reasonable approximation of the cause-effect relationships causing degrading flow. The initiation would then be deemed more random, either completely random or correlated to a degree with the increased AC (increased chances of degradation with increased current). This results in the fact that even if the diagnosis is hard to do with other parameters than the flow - the prognosis could incorporate other measurements in conjunction with the flow.

This hypothesis is developed on the basis that the furnaces uses the same water for cooling, but only Furnace 1 experience degrading flow. Hence, water quality might not be the dominant factor leading to the degradation. In addition, the furnaces uses different flexsibles. This might indicate that the type of flexsible in conjunction with the operational load might be important when it comes to mitigating this failure mode.

# Chapter 7

# Results

This chapter is mostly dedicated to the findings obtained from the analysis of data retrieved from Elkem. It is mainly divided into three parts: Data pre-processing, event data, and CM data. First, the initial data preprocessing results are presented, both from the event data and the CM data in Section 7.1. Then, the event data, specifically, with results from a non-parametric life data analysis, is presented in Section 7.2. The analysis will indicate the lifetime of the flexsibles as well as some differences between the furnaces. Next, the CM data will be explored based on the findings in Chapter 6. The HI for the failure mode *loss of cooling* is considered in Section 7.3. Some degradation paths of the HI are then chosen for further investigation in Section 7.4. Further, the findings regarding the HSs are discussed in Section 7.5. Lastly, the RUL prediction is presented in Section 7.6. All figures are generated with Python libraries, and a selection of figures is added in Appendix B. Access to the code for data processing and generation of figures can be provided at request.

## 7.1 Data Cleaning

The first step in processing and analyzing data is data cleaning (Jardine et al. [2006]). Both event and CM data usually contain errors. Event data is usually entered manually and contains human errors like wrong formatting, lack of information, or simply wrong input. For CM data, the errors may be caused by sensor faults, or noise can be created by different operational modes. It is important to clean the data to mitigate the "garbage in garbage out" situation (Jardine et al. [2006]).

### 7.1.1 CM Data

When obtaining the CM data, there was a substantial amount of noise in almost all the data, some more than others. This was found, after some trial and error, to come from stops in the

production. Types of stops and how they affect the data are discussed in Section 4.6. The temperature, current, and flow data will be presented to exemplify this noise. The flow was found to be the least affected (out of the three) by stops, probably because at shorter stops, the water flow goes on as normal. This is also true for the pressure measurements.

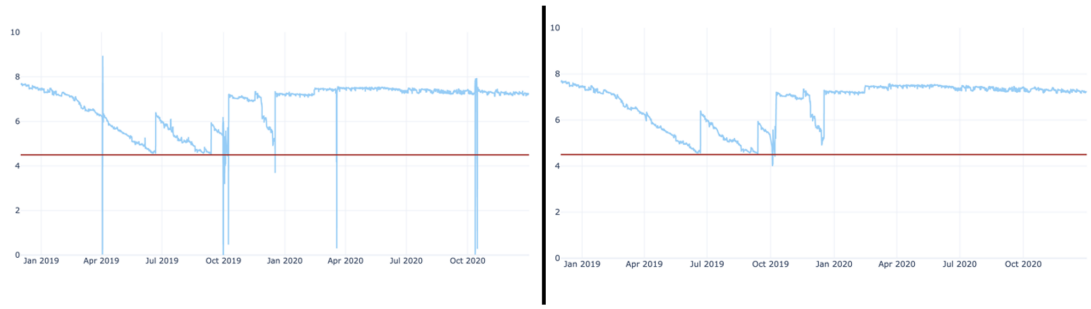


*Figure 7.1: Flow is depicted in blue, while the red line indicates the failure threshold used at Elkem Thamshavn. Left: without filtering of the stops. Right: with filtering of the stops.*

In Figure 7.1, the difference in filtered and unfiltered flow data is clearly evident. The flow data is filtered by the furnace switch. The flow data, in this case, is from the 204T flexsible. The data on flow used is only for those in the TUR flexsible, as the flow is usually very similar (a difference would indicate a water leak). The furnace switch is either on or off, which determines if the furnace is loaded with current or not. The flow data is only filtered exactly when the furnace is switched off, which is usually one hour, sometimes two (corresponds to one or two data points). When filtering, one would get holes in the data, which is filled in by linear interpolation. However, when doing the same for the current and temperature data, it did not filter out the noise. The idea was then to filter out the data for longer periods of time after the furnace stops. After some trial and error, 24 hours seemed to eliminate most of the noise without removing unnecessary amounts of data. In Figure 7.2 there is clearly a difference in filtered and unfiltered current.

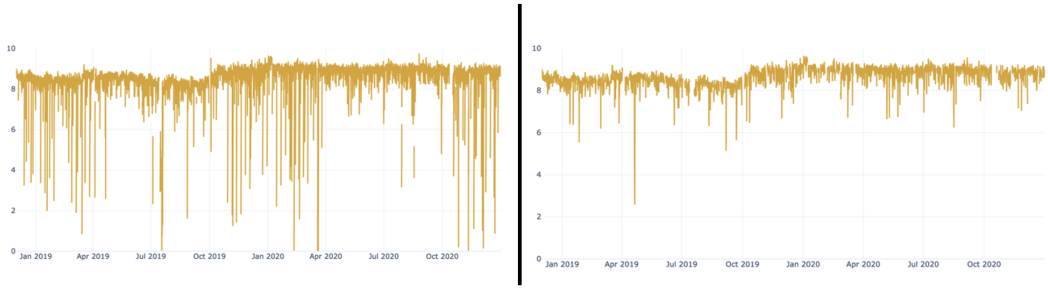


*Figure 7.2: Current in yellow. Left: without filtering of the stops. Right: with filtering of the stops and 24 hours after.*

When it comes to the temperature measurements, the same is found as for the current. This is seen in Figure 7.3. There is a difference in how the temperature measurements in and out are affected by the filtering. It seems that the temperature out of the flexsible (dark blue) is more affected by the filtering than the temperature into the flexsible (light blue). This makes sense as the amount of current is believed to correlate with how much the water is heated, as presented in Chapter 6.

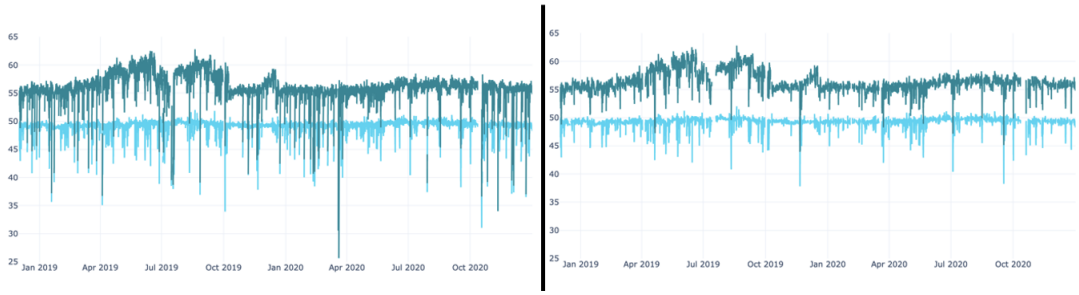


*Figure 7.3: Temperature out of the flexsible in dark blue, temperature into the flexsible in light blue. Left: without filtering of the stops. Right: with filtering of the stops and 24 hours after.*

One more thing to notice is that drops in the right side of Figure 7.3seem to be the same for both temperatures in and out. This makes sense as the temperature into the flexsible will affect the temperature of the water coming out. The flexsible will only give a temperature increase, which is relative to the temperature of the water flowing into it. As the filtering of the data also affects the temperature into the flexsible, this can indicate that the operation of the furnace also will affect the temperature of the water in the general water operation. The noise in the data on the right side of Figure 7.3 is attributed to deviations in the temperature coming into the flexsible. This is clearly seen in Figure 7.4, where the temperature difference between the water in and out is plotted over the time period. In this graph, there are much fewer hard drops in temperature, as the drops that are evident in both temperature readings cancel each other out.

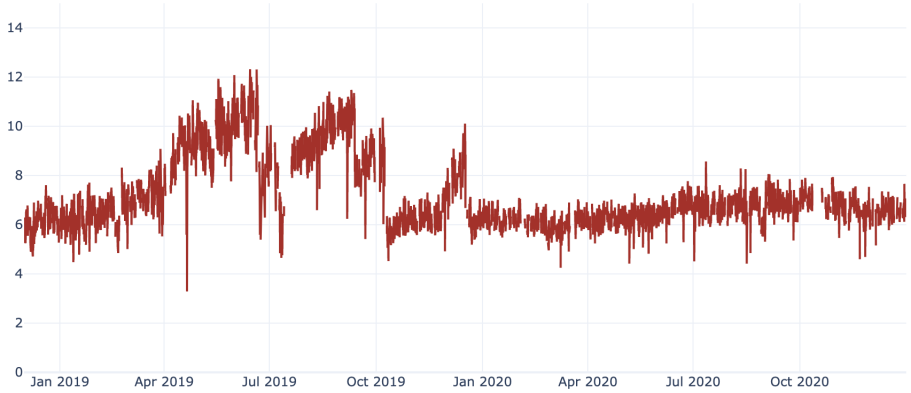


*Figure 7.4: Temperature difference between the water in and out of the flexsible 204T.*

### 7.1.2 Event Data

The event data (the replacements of flexsibles) needed reformatting because the inputs were logged differently over time. This makes it hard to use the data for processing. Hence, some manual labor needed to be done to make the data suitable for analysis. It was mostly reformatting columns of dates and the flexsible columns (locating which flexsible that was replaced). After the data were cleaned, it was used in a Non-Parametric Life Data Analysis.

When working with data sets of repairable items, there are cases where we do not know when the item was put into operation or the observation of the item's lifetime is terminated before the item fails. These cases are called left and right **censoring**, respectively (Rausand and Høyland [2004]). The data set is **complete**, when it is possible to observe the real times of failure for all items that are studied. The data set obtained from Elkem are both left and right-censored, which is called **double censored** (Rausand and Høyland [2004]).

There are different kinds of censoring based on the nature of the censored lifetimes. It is left-censored because the logging of failures started in 2013, and information before that is unavailable. It is right-censored in the way that the time for censoring is stochastic.

## 7.2 Non-Parametric Life Data Analysis

In this section, the focus has been on Nelson-Aalen plots, Kaplan-Meier plots, and TTT plots. The Nelson-Aalen plots indicate whether there is any global trend in the data. The Kaplan-Meier estimator gives an indication of the survivor probability of the flexsibles over their lifetime. The TTT plot (based on Kaplan-Meier) can further be used to establish an optimal age-based maintenance policy, but it is out of the scope of this work. It is assumed that the reader knows about these concepts beforehand, and the plots presented here are developed according to what is described in (Rausand and Høyland [2004]).

### 7.2.1 Nelson-Aalen plot

Figure 7.5 shows the Nelson-Aalen plots for both furnaces. If the Nelson-Aalen plot is linear, it indicates that the items are independent and identically distributed (Rausand and Høyland [2004]). For Furnace 1, the $R^2$ statistic for the linear regression is 0.90. Thus it is assumed to be linear. The regression is affected by a large number of replacements at the start of the data. At Furnace 2, the $R^2$ statistic for linear regression is 0.79, which is because of the large number of replacements in the middle of the graph. The linearity needs to be assessed by other measurements than the $R^2$ to ensure the plot is linear as outlined in (Rausand and Høyland [2004]). However, for simplicity and further calculation, the Nelson-Aalen plots are assumed to be linear. The Nelson-Aalen plot does not separate between failure modes, which can skew the results.

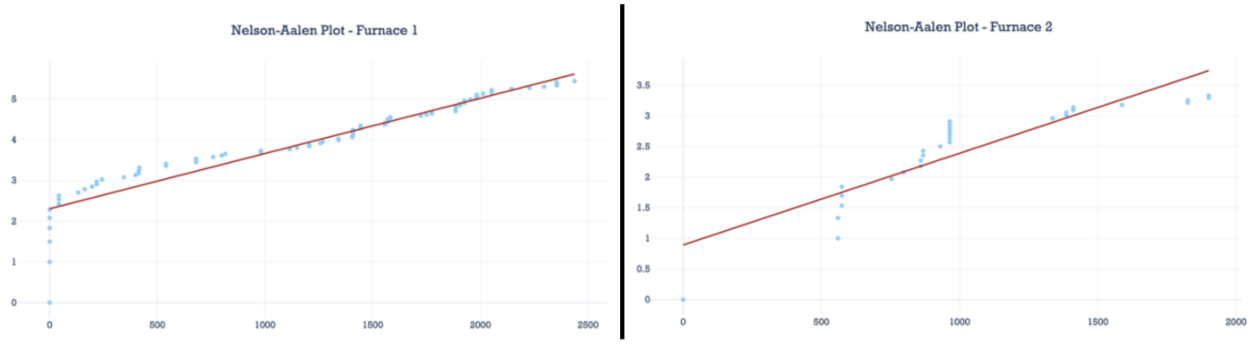


*Figure 7.5: Nelson-Aalen plot of Furnace 1 and 2.*

One failure mode could not have either independent or identically distributed properties while another one has.

### 7.2.2 Kaplan-Meier plot

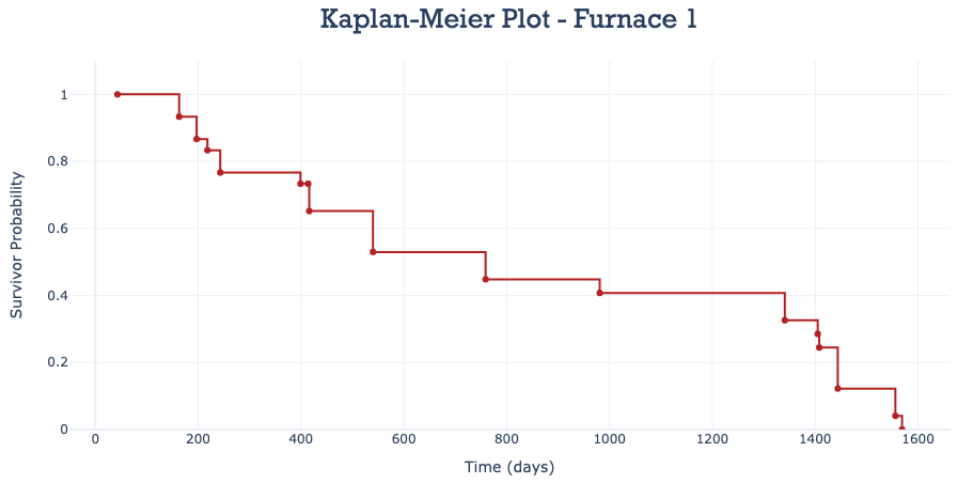


*Figure 7.6: Kaplan-Meier plot of Furnace 1.*

In Figure 7.6 and 7.7 there are Kaplan-Meier plots of Furnaces 1 and 2, respectively. The plots give an estimation of the survivor function for the flexsibles. The data used in the plots are left-censored from the first date of logging the replacements: 05.05.2014. The Kaplan-Meier estimator calculation demands that every item starts at the same time in t =0 (Rausand and Høyland [2004]). Some of the data used are also right-censored. Most of the faults at Furnace 1 come from failure mode loss of cooling, and most of the faults at Furnace 2 come from no current. The data used are thus censored for failures caused by water leaks or darkening (which is assumed to lead to water leaks). After this censoring, it is assumed that all the failures at

Furnace 1 can be linked to the failure mode *loss of cooling*, while all the failures at Furnace 2 can be linked to *no current*. This results in the plots' estimation of the survivor function for one failure mode at each furnace, *loss of cooling*, and *no current*, respectively. Because of this, the estimated $M\hat{T}TF$ for each failure mode can be calculated by integrating the survivor function from zero to infinity (Rausand and Høyland [2004]). The $M\hat{T}TF$ was estimated to be 854 days for Furnace 1 and 1483 days for Furnace 2. This corresponds to roughly 2 years and 4 months, and 4 years respectively. There is not found literature that explicitly states that estimating $M\hat{T}TF$ based on an estimated survivor function gives a sufficient statistic. However, in this case, these estimates are used to give an indication of the flexsibles lifetimes. In addition, the estimates for $M\hat{T}TF$ are close to the mean of the lifetime of all flexsibles and the mean of the chosen degradation paths in Section 7.4.

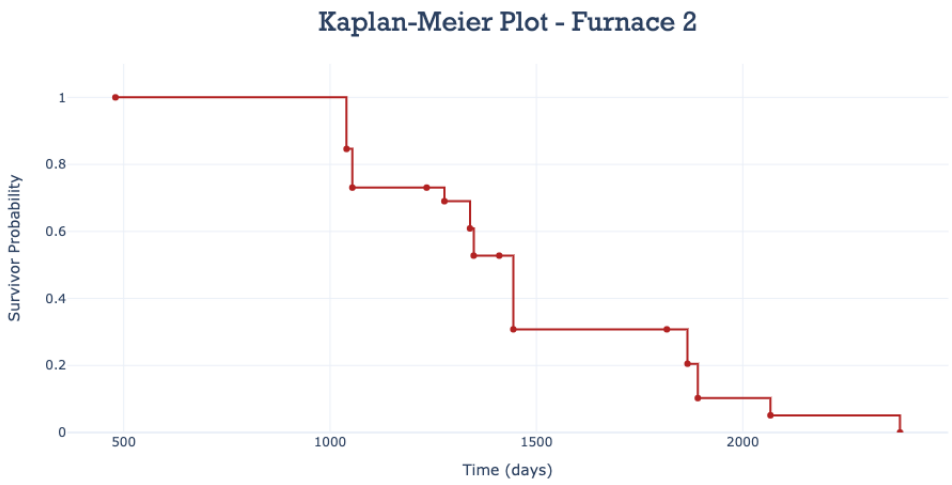


*Figure 7.7: Kaplan-Meier plot of Furnace 2.*

### 7.2.3 TTT-plot

The TTT plot of Furnace 1 is based on the Kaplan-Meier estimator in the last section. It shows that the flexsibles' failure rate increases as the plot is found above the line indicating a constant failure rate (the black line in Figure 7.8). A Weibull transform is fitted to see if the failure times of flexsibles could be Weibull distributed, but the fit is not deemed sufficient enough to conclude with this.

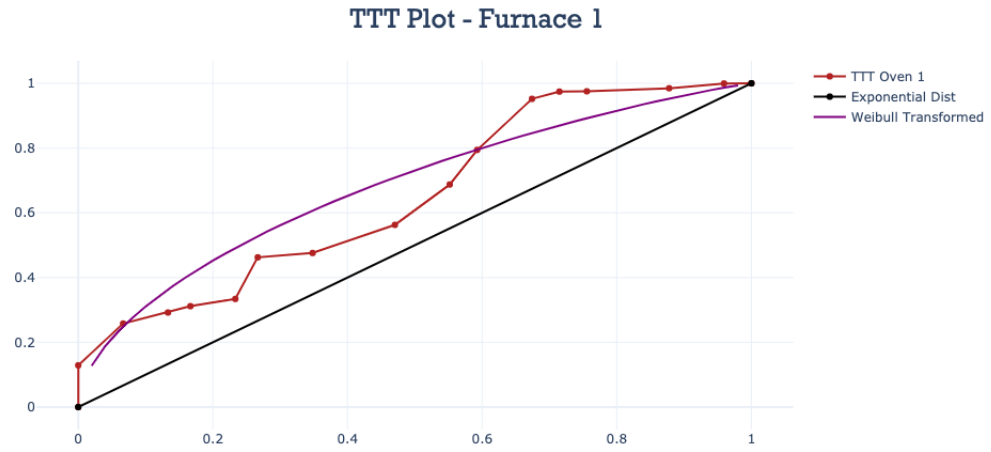


*Figure 7.8: TTT plot of Furnace 1.*

## 7.3 Health Indicator Analysis

The development of a HI is one of the most important parts of any prognosis. It sets the stage for what kind of health states could be used and the accuracy of the forthcoming RUL prediction. The goal in this thesis is to find a physics-based model that is believed to model the degradation of the flexsibles to a sufficient degree (with a large amount of confidence). Hence, the findings in Chapter 6 are combined with the available sensor data to see if any relationships can be implemented into a HI. As there were found no causal-based first-principle model of the degradation of flexsibles in the literature review on failure mechanisms, relationships in the data will build upon the hypothesized degradation model in Section 6.4. If relationships are found, it is possible to build a rules-based first-principle model, combining the knowledge obtained in Chapter 6, and the sensor measurements, ultimately developing a physics-based model that models the degradation of flexsibles.

When modeling the behavior of real systems, the HI does not need to have a root in physical first principles. As long as the HI correlates with the real systems' health and is consistent over time, it would do the job. For instance, if one knew that the health of the flexsibles declined in direct proportion (one-to-one) to the number of bathroom breaks for the mechanics at Elkem Thamshavn, and it was found to give consistent results over time, this *could* be used as a HI of the flexsibles (without the mechanics' knowledge of course). However, in this context, unfortunately, this information is not available, and such a correlation would probably not be consistent over time. This is where physical first principles are a better fit, as they are based on empirical experiments and are assumed to be consistent over indefinite amounts of time. Thus, the HI has a higher probability of being usable in the long term if it is based on physics.

In the next sections, the sensor measurements are visually inspected one by one to elaborate on what information they can provide. In addition, their respective suitability as a HI of the flexsibles is assessed. All the flexsibles were assessed, and they are all cross-examined with each other and the age of the flexsibles to look for patterns that might emerge. These patterns could then be used in either the development of HI, HSs or in the development of the RUL estimate.

### 7.3.1 Current Measurements

The current measurements are assessed as they are believed to be an important part of the initiating of degradation in the flexsibles (see Figure 6.1). They are assessed in three ways. First, by simply looking at the two current measurements for each flexsible pair. Second, by looking at the total current that goes through a flexsible pair indicating the total load a flexsible pair experiences (addition of the two currents). Third, by looking at the current difference, which might indicate a thermogalvanic corrosion mechanism (as described in Section 6.1.1).

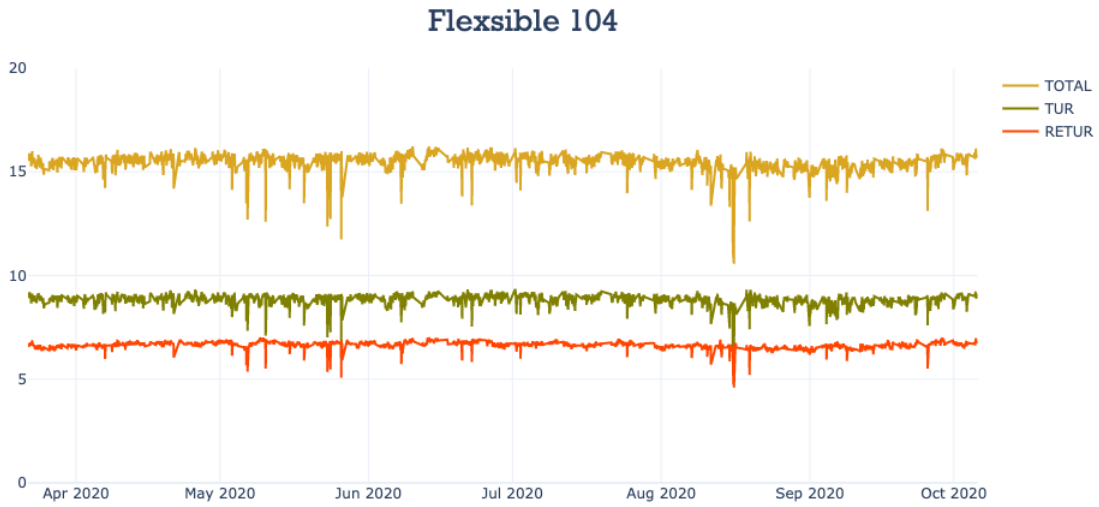


*Figure 7.9: The total current graph, with corresponding current for both flexsibles in the flexsible pair. Flexsible 104 is used as an example.*

The main finding is that the current seems to be very stable across time. Most flexsibles have the same total current, current difference, and respective current for each flexsible in the period of the available data.

However, the most interesting thing was found when inspecting the chosen degradation paths that went from a seemingly healthy state to an unhealthy one, all the way down to the failure threshold. In two of the thirteen cases at Furnace 1, a large jump in the current of the RETUR flexsible seemed to initiate a degrading flow pattern. In accordance, this resulted in a

larger total current and current difference. Thus, it is immediately hard to say if this initiation was caused by a larger load or a larger current difference between the flexsibles in the flexsible pair (and thus temperature difference). The latter could indicate a thermogalvanic corrosion mechanism. However, as each flexsibles' copper cable in one flexsible pair actually is a long distance apart (on an atomic scale), thermogalvanic corrosion is deemed unlikely. The temperature difference in the flexsible pair also increased when the sudden jump in current happened, which can indicate the relationship between current and dissipated heat formulated in Section 3.9.3.

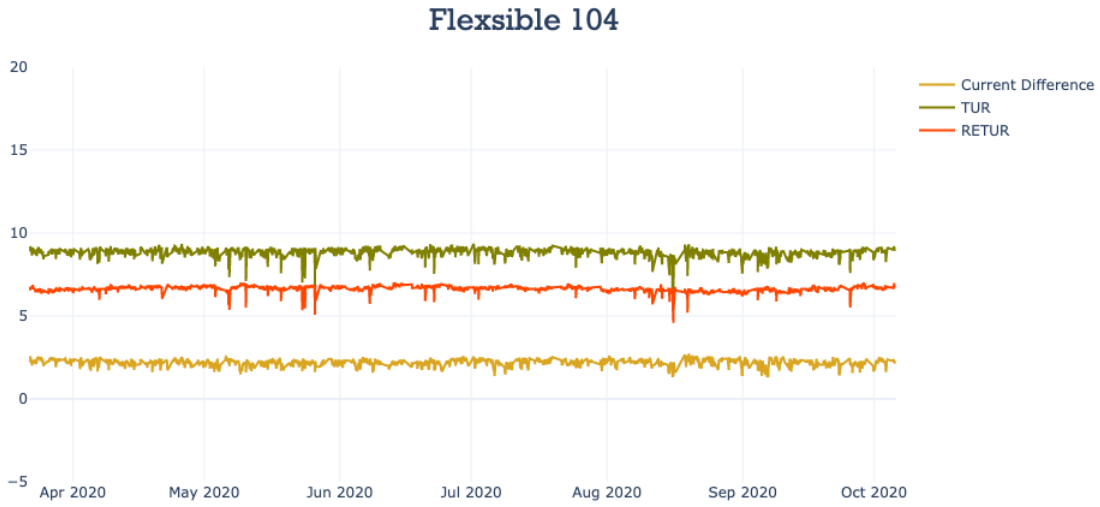


*Figure 7.10: The graph showing difference in current, with corresponding current for both flexsibles in the flexsible pair. Flexsible 104 is used as an example.*

As the current is rather stable and does not gradually change, the current measurements are deemed a poor candidate for a HI. There are not found any indications of what spikes in current can cause either.

### 7.3.2 Temperature Measurements

The temperature measurements are assessed as they are believed to indicate how much each flexsible pair heats the cooling water. This can give additional information on the health of the flexsible pair. Naturally, the temperature difference between what comes into the flexsible pair and what comes out indicates how much the water is heated.

The graphs of temperature differences in the flexsibles were assessed as shown in the example given in Figure 7.11. The main finding is that it follows the degrading flow rather linearly (one-to-one). This means that because the current in each flexsible pair is stable over time, the

temperature difference is assumed only to reflect the information the flow gives. Since the current is stable over time and the temperature difference increases with the flow, it can indicate that when the flow measurements degrade, the increased heat can result from increased resistance in the flexsible as presented in equation 3.23. In this case, the temperature difference can be a candidate to be used as a HI because it supplies some additional information on the resistance in the flexsible's copper cable. However, it could also mean that it is only the degrading flow that *causes* the temperature difference (particles clogging the flexsible pair).


*Figure 7.11: The graph showing difference in temperature, where the exponentially weighted average (EWA) is also shown. Flexsible 104 is used as an example.*

The temperature measurement could be used as a HI as it seems to have good trendability, identifiability, and monotonicity (from Section 3.7.1). Although, the temperature difference is not consistent across flexsibles. This means that some flexsibles operate normally at a temperature difference of 8 °C, while some at 4 °C. In addition, some cross the failure threshold (4.5 $m^3/h$ flow) at 12 °C and others at 6 °C. There is no direct relationship between the level of flow and the level of temperature difference. Hence, by using the temperature difference, one might reduce the epistemic uncertainty but increase the aleatoric uncertainty.

The temperature difference might give a better indication of when a flexsible should be changed because the flow only indicates its cooling capacity. While the temperature difference actually tells you the load a flexsible is under. The flow can be low, but due to other circumstances, the temperature difference is still low. Thus the flexsible is thought to not be under a lot of stress. In the assessment of the temperature difference, there are not found any flexsibles in normal operation that experience a temperature difference above 8 °C. Thus, this could

be a threshold indicating a healthy or unhealthy operation. However, the threshold of when to replace a flexsible is harder to determine. Especially since the degradation paths looked at in this thesis do not give any conclusive answers. The temperature difference could be used in conjunction with the flow measurement to determine when a flexsible should be replaced, thus giving a better indication of the flexsibles' condition. For instance, statistical analysis could be performed to develop an extension to a linear model combining flow and temperature differences.

### 7.3.3 Pressure Measurements

The pressure measurements are assessed as they are believed to indicate how much flow there is in a flexsible pair. The pressure is believed to give additional information on to subjects. Firstly, it could be used in conjunction with the flow measurements in a causal-based first-principle model (e.g., based on Bernoulli's Principle) to develop a HI based on the deviations in this model. In this case, the particles that develop and clog the flexsibles are thought to cause the deviations to the model (which is stable in normal operation) to increase.

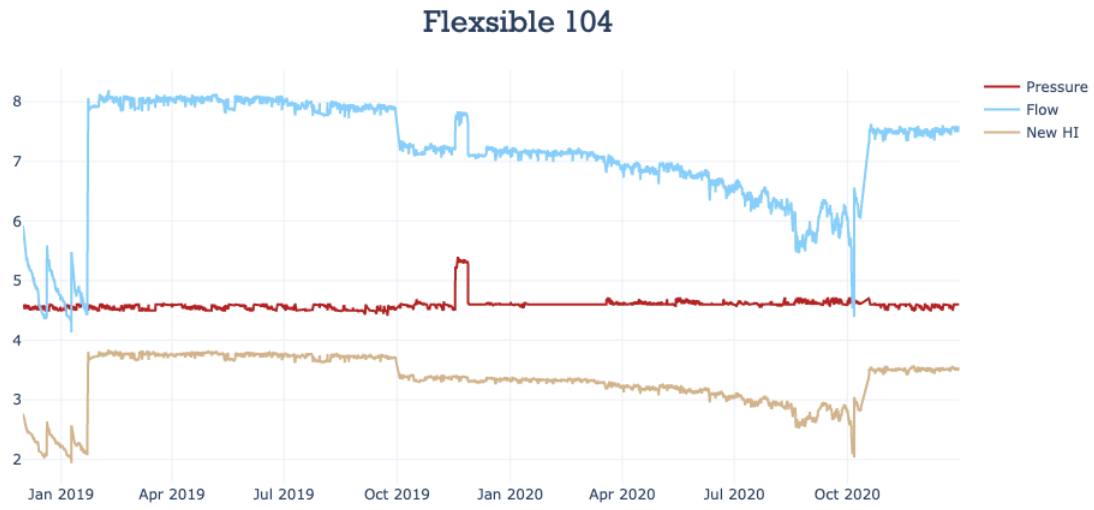


*Figure 7.12: The graph showing flow, pressure, and the combined new HI of both measurements (by equation 7.1). Flexsible 104 is used as an example.*

The problem with this type of model is linked to the nature of the water operation. As the pressure created in the LT-tank is divided on all the flexsibles, thus creating the flow that goes through them, it cannot be used to predict the flow. This is because the water follows the path of least resistance resulting in the flow in each flexsible is an indication of how the pressure dis-

tributes over the flexsible pairs. If the pressure in each flexsible were independently controlled, such a model would make much more sense.

Secondly, pressure measurements can, in conjunction with the flow measurements, create a better HI as they can get rid of the noise associated with pressure. Starting with Bernoulli's principle for incompressible flow and rearranging terms etc. it is possible to get a new HI that looks like this:

$$HI = \frac{flow}{\sqrt{pressure}} \tag{7.1}$$

This could give a better HI as it increases its robustness (signal-to-noise ratio). The flow, pressure, and the new combined HI is shown in Figure 7.12, where it is clear that it will get rid of large jumps in pressure, but the robustness of the HI is not found to improve. Combining this with the results in the last section about temperature difference, a new HI combining flow, pressure, and temperature could be obtained by an extension to the linear model on the following form:

$$HI = \frac{\beta_1 X_1}{\sqrt{\beta_2 X_2}} + \beta_3 X_3 \tag{7.2}$$

$X_1$ denotes the flow, $X_2$ is the pressure, and $X_3$ is the temperature difference. The $\beta$ term is their respective constant. From this equation, there is great potential to create a better HI. However, when developing a new HI like this, there are challenges connected to calculating the corresponding failure threshold. In addition, the optimal relationship (for the optimal HI) between the flow and the temperature difference might not be simply adding them together. The HI in equation 7.1 is also found not to improve the signal-to-noise ratio consistently when used instead of the flow as a HI. This is probably since the pressure measurement deviates to a minimal degree (as seen in Figure 7.12) and that the pressure splits on all the flexsibles. If the pressure rises, it is not necessarily true that it split evenly on all flexsibles. As the water follows the path of least resistance, it will probably be split according to each flexsible's health.

### 7.3.4 Flow Measurements

The flow measurements are assessed as they are believed to indicate the cooling capacity of a flexsible directly. These measurements are currently used as an HI for the flexsibles. Because of the difficulties presented with the other measurements available, the flow will be used as an HI for the development of health states and RUL prediction of the flexsibles.

The flow measurements are not monotonous but usually have a clear degrading trend. Its robustness is similar to the HI that incorporates pressure. The identifiability is deemed poor (as shown in Section 7.5), but none of the other measurements seems to do better. Where the flow

measurements seem to do better than the other measurements is their consistency, as the flow measurements and their corresponding failure seem to be consistent across different flexsibles.

## 7.4 Chosen Degradation Paths

Because of the difficulties in separating all the different degradation paths automatically, only the degradation paths considered to go from a healthy state to an unhealthy state were considered. Those paths that followed after flushing were not considered. It was found that 13 of the 18 flexsible pairs at Furnace 1 had these degradation paths, where it is possible to observe the degradation path from healthy to failure. Figure 7.13 shows the degradation paths that were picked. As the flow between T and R flexsibles in each pair are basically the same (a deviation would indicate a leak), only the flow of the T flexsible is used in the further analysis of the flow.

To assess these degradation paths and what type of degradation modeling should be used, regression is performed on these paths to see if there are any reoccurring trends in the flow data. Specifically, an exponential degradation pattern proposed in Equation 6.1 was considered. This is because it can describe the rate of corrosion in copper in an aqueous solution of high salt amounts. In addition, linearity was also looked for as this can give reasons to use a stochastic Wiener process instead, as presented in Section 3.8.4. Especially since the degradation path seems to both have negative and positive increments.

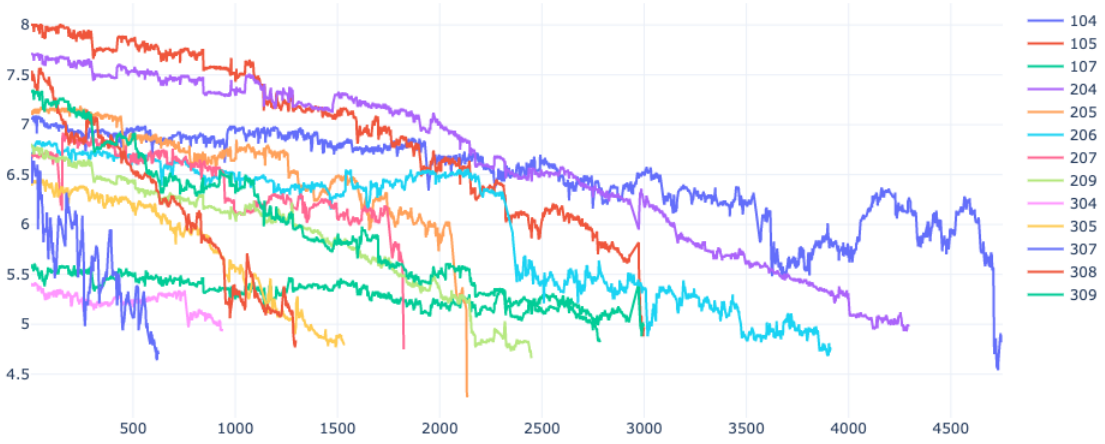


*Figure 7.13: The graph shows all the degradation paths that were considered when developing a prognosis model.*

The chosen degradation paths were all assessed by regression of certain functions. The paths

were chosen to be fitted with linear, polynomial, exponential ($ae^{bx}$), and power-law ($ax^b$) functions. Their respective $R^2$ statistic were obtained to assess their quality of fit. All except for the polynomial are functions with just one term because the more terms you add to a function, the more flexible the regression becomes. Hence, this was done to mitigate for over-fitting of models, increasing the chances of a generalized model. The polynomial function was included to compare with the linear regression to see how much better a more flexible regression would do. If the exponential, power-law, or polynomial did better than the linear regression, it would indicate that the flow degradation probably increases over time. The function used and its corresponding output for one of the flexsible's degradation paths are shown in Figure 7.14.

| 0 | 105 |
|---|---|
| Linear | 0.969296 |
| Polynomial | 0.983869 |
| Exponential | 0.956813 |
| Power law | 0.592932 |
| Linear coeff | -0.0008706 |
| eSTD | 0.127078 |
| eMEAN | -0.0008706 |
| Days from healthy to failure | 118.375 |

*Figure 7.14: The table shows the output that were used to assess each degradation path. Flexsible 105 is used as an example, indicated in the top right.*

In general, the linear regression was the best fit in all of the paths, while the polynomial was only slightly better. It was one path that had a poor $R^2$ statistic on all the fits (flexsible 304), probably because it was rather stable over a long period of time before it had a sudden drop in flow measurement. The exponential function was usually slightly worse than the linear regression, probably because the flow deviates in both directions.

### From Regression to Stochastic Modelling

The physical relationships found in Chapter 6 are hard to describe with the available sensor measurements - as presented in Section 7.3. When conducting a regression (e.g., linear), such as described in Section 3.6, one assumes that the noise $\epsilon$ is independent and identically distributed. The error term (from the regression line) can then be tested to be, e.g., normally distributed. However, the error term can be considered not to be independent and identically distributed, which in practical situations can be more logical (Barros [2019]). In these situations, the process is deemed stochastic, and the process can be modeled by a stochastic degradation model. When stochastic processes are used instead, one thus considers more of the uncertainty in the process. When obtaining RUL predictions, the variance in the answer would be greater than that of a simple regression, but the chance of the prediction being completely wrong is smaller. Thus, the model could give more consistent predictions of the actual degradation by

incorporating these uncertainties.

In addition, the degradation paths seem to be rather linear, and the trend can move up and down. Hence a Wiener process with linear drift might be suitable to model the degradation trend of *loss of cooling*. For the Wiener process to be suitable, the increments of the trend need to be normally distributed. Thus the increments are discussed next.

### 7.4.1 Increment Analysis

To gain more knowledge on how the flow changes based on its flow condition, an increment analysis is performed. Firstly, looking at how the flow increments change based on the flow condition. Secondly, showing the distributions of the increments with histograms.

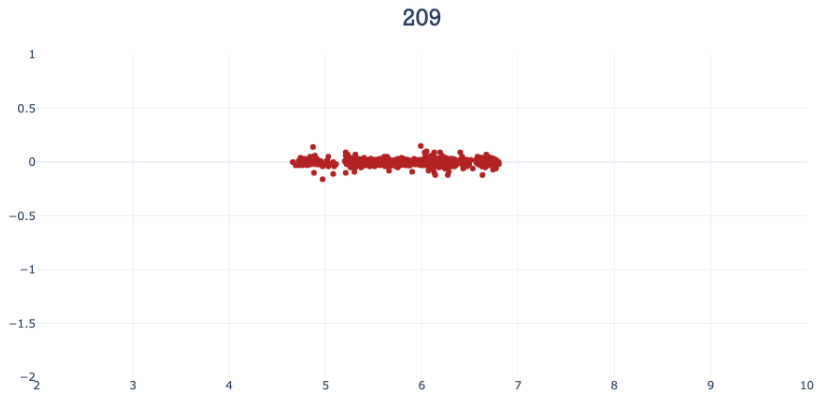


*Figure 7.15: The graph shows the flow (x-axis) plotted in relation to the flow increments (y-axis).*

Figure 7.15 show a plot of flexsible 209 at Furnace 1. It is hard to see how all these data points are distributed (they lay on top of each other) just by looking. Therefore, these plots were fitted with the same functions as in Figure 7.14 and the results can be found by the corresponding $R^2$ statistic in Figure 7.16. From these results, there seems to be little evidence that there is a relationship between the flow increments and the flow condition. However, as the linear coefficients seem to be negative in most cases (10 out 13), the increments actually tend to **decrease** slightly by decreasing flow.

Furthermore, to be able to use a wiener process with linear drift possibly, the increments need to be normally distributed. Hence, the histograms of the flexsibles are plotted in Figure 7.17. They have a much higher variance than what is expected when the distribution is normal. However, this can be looked at as a normal distribution and another independent process resulting in shocks (large jumps in flow).

When looking at the distribution this way, the histograms can be simply filtered for shocks

| | 0 | Linear | Polynomial | Exponential | Power law |
|---|---|---|---|---|---|
| 0 | R^2 | 1.998713e-10 | 0.000001 | 2.053250e-10 | 3.897029e-10 |
| 1 | a | -6.668002e-04 | -0.000040 | -6.668496e-04 | -6.607128e-04 |
| 2 | b | 3.139007e-07 | 0.000507 | -4.828122e-04 | 3.215974e-03 |
| 3 | c | 0.000000e+00 | -0.002262 | 0.000000e+00 | 0.000000e+00 |

*Figure 7.16: The matrix shows the $R^2$ statistic for each of the functions fitted on the graph in Figure 7.15. Flexsible 209 is used as an example.*

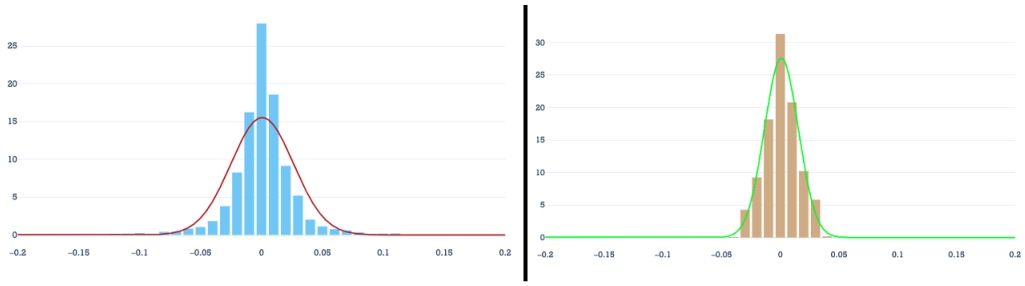

*Figure 7.17: Left: the distribution of increments and corresponding normal distribution fit. Right: the distribution of increments and corresponding normal distribution fit when filtered for shocks. This is an example of flexsible 104.*

above and below certain levels. In this case, filtering based on increments larger than 0.04 and below -0.04 were found to result in the distribution at the right-hand side of Figure 7.17.

The normal distribution of the filtered histogram does not fit perfectly, but this is probably due to the lack of resolution in the measurements. They are averaged over one hour and does only contain two decimals. Now, a normal distribution is obtained, but what is to be done with the remaining shocks that affect the flexsibles? How this can be managed is further discussed in Section 7.6.3.

## 7.5 Health States Analysis

Health states can determine what type of degradation is happening. In this case, there are not found specific trends that happen in certain scenarios or operational conditions, thus the flow measurements are classified into two health states: healthy and unhealthy. This is on the basis that some flexsibles can operate over long periods of time before they degrade. Suddenly the flow can start to drop from its normal flow level, and it is considered to be in an unhealthy state. This is clearly evident in Figure 7.1 between October 2019 and January 2020. However, the flow can stay stable at different levels and does not necessarily start to drop below a certain level. Therefore, the unhealthy state and healthy state is split based on their respective increment.

An unhealthy state is considered to be when the increments have a mean below zero, while

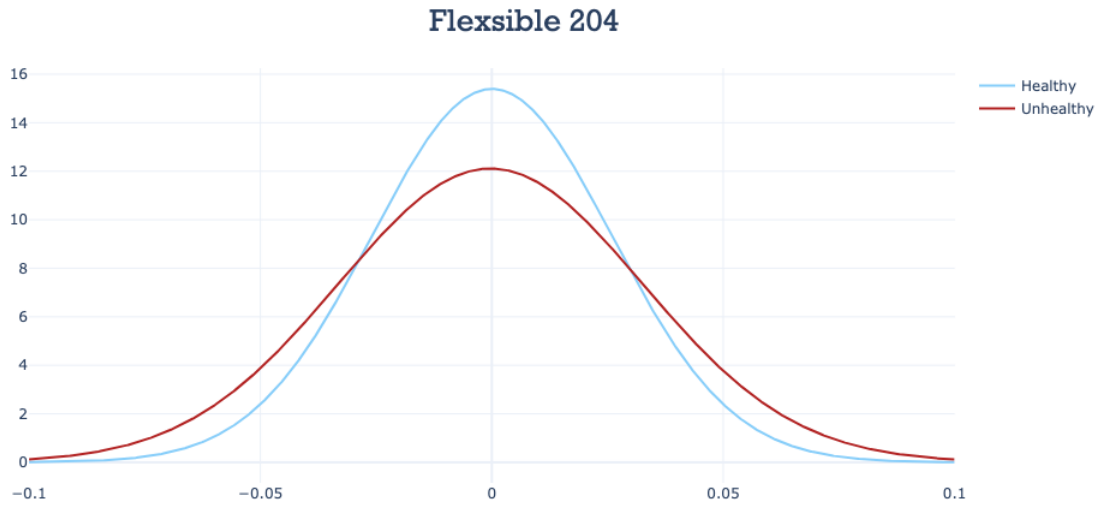


*Figure 7.18: The figure shows the two states in flexsible 204. It is easy to see the large signal-to-noise ratio in the flow measurements.*

a healthy state is considered to be when the increments have a mean above or equal to zero. Hence, to test this out, the flow data were split into their respective health states based on visually inspecting the flow. Within a time period where the flow was degrading slowly, it was considered unhealthy, while a stable flow was considered healthy.

From Figure 7.18, it is obvious that the signal-to-noise ratio of the flow measurements is poor (high variance, compared to the mean). The two distributions are impossible to separate, and a type $\alpha$ error (from Section 3.7.3) - or a false-alarm (also $\beta$ error - non-detection) is almost unavoidable. Thus, a diagnostic test such as Neyman-Pearson's test would not be suitable for this HI. To be clear, these are distributions based on all the flow data for flexsible 204 and are displayed as a smooth normal distribution for easier assessment of the distributions rather than histograms.

## 7.6 RUL Prediction

When conducting the prognosis of the flow measurements, a training set consisting of the thirteen degradation paths was used.

The prognosis is mainly performed by an analytical solution based on the theory presented in Section 3.8.4. This type of solution can continuously obtain a RUL estimate (IG distribution). Thus it is possible to tune the model based on how many days you want to do prognosis for and the probability that it will fail in these number of days. In other words, one chooses the

percentile the stochastic variable (in this case, days) should be at before the Monte-Carlo simulations are initiated (for validation of the analytical approach). The model can then give you an alarm when it obtains an estimate that says it will fail, e.g., with a probability of 10% within the next 14 days. The percentile and the days you want to predict depend on many other variables, such as cost and safety, which are connected to the larger operational context. The Figures 7.19 and 7.22, show Monte-Carlo simulations because it is then easier to visually see where the RUL estimate end up compared to where the prognosis started. The Monte-Carlo simulations in Figure 7.22 are also used to validate the analytical approach. It is easy to see that the RUL estimate by Monte-Carlo simulations (the histogram in dark blue) fits well with the IG distribution in light blue. When using a Wiener process with linear drift for RUL prediction, the parameter estimation is deemed critical, as these determine the level of prediction and accuracy. Hence, different approaches to parameter estimation were tried out, which will be presented next.

### 7.6.1 Parameter Estimation

Firstly, a deterministic approach to parameter estimation was performed. A leave-one-out cross-validation approach, as outlined in Casella et al. [2013] were used to estimate the parameters. Thus when training the data, all the degradation paths that were not used in prognosis were used to find the corresponding mean and variance for the degradation path at hand. The mean and variance for each degradation path were calculated by finding the error terms' mean and variance from the linear regression performed on each path (as presented in Section 3.8.4). When a degradation path experiences shock (larger jumps in flow measurements), this will increase the error terms variance dramatically, thus giving a useless RUL prediction as seen in Figure 7.19. Because of these results, the filtered variance (as depicted in Figure 7.17) was used. The results improve, as seen in Figure 7.22. In this case, the variance used was simply the variance obtained from the histograms that were filtered. The same approach was used in calculating the mean and the variance for each degradation path. This gave better prognosis results, but this model neglect shocks on the system. However, if the prognosis is consistent and works well in practice, it could still be used, even if it does not model the real physics properly.

### 7.6.2 Training the Model

When training the model, early evidence showed that the deterministic parameters based on the linear regressions' error terms were not good enough to give a good RUL prediction, as seen in Figure 7.19. Therefore, the filtered variance was used when optimizing the parameters for the RUL prediction, seen in Figure 7.22.

The parameters that can be tuned for an analytical RUL prediction such as this is the number of days beforehand you want to know that it will fail by a certain probability. Hence, the

prognosis function was tuned on all the 13 degradation paths, obtaining RUL estimates such as in the example Figure 7.22. After some trial and error, it was found that it worked alright at some of the paths when 14 days and a probability of 0.01 was used. All the tuned graphs that were assessed can be found in Appendix B.

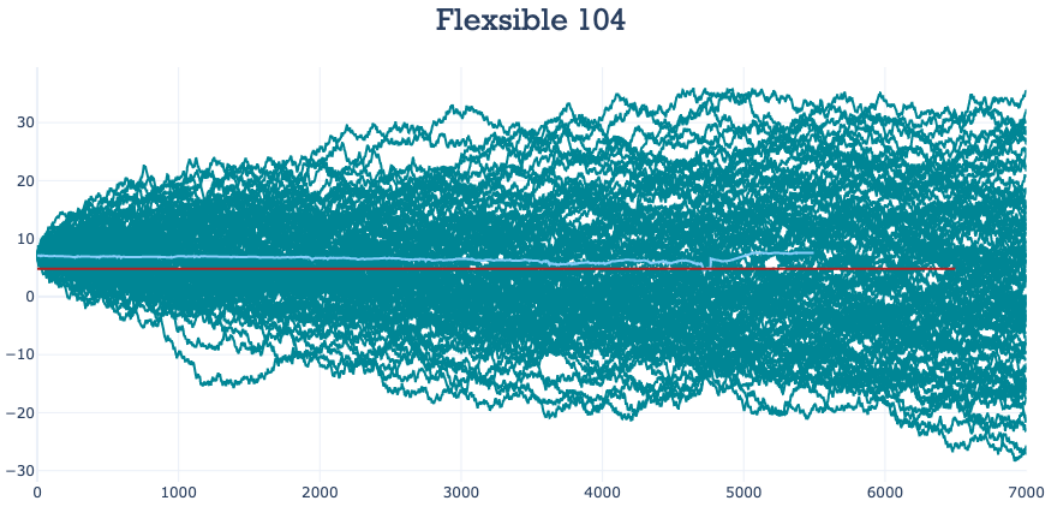


*Figure 7.19: The figure shows the simulations of 100 paths by Monte-Carlo next event simulation. Notice the large amount of variance.*

However, the model met challenges in several of the training sets, mainly because of shocks. If one were to adjust the number of days smaller, the prediction would generally start closer to the failure threshold. This is also true when increasing the probability. However, if one were to do so, the "alarm" usually went off, and an IG distribution was obtained too close to the failure threshold (such as in Figure 7.20). In addition, when many of the flow measurements experience shocks at the end of life, the model will miss by a lot. In general, the variance in the prediction decreases as closer one gets to the failure threshold. But when the drift accuracy is not in tune with the real drift (e.g., shocks), the model will estimate RUL to be much higher than what it really is.

In addition, some of the paths are stable at a low flow level (such as in Figure 7.21), causing the alarm to go off very early in the degradation and thus giving a RUL that is several weeks early. This is because the alarm goes off based on the estimated parameters (from all the other degradation paths) and the failure threshold (based on the equations found in 3.8.4) and then sets a flow threshold where the "alarm" goes off.

Because of these findings, the degradation paths do not seem to be similar, and the consistency of the HI is thus considered worse than what was previously thought. This is probably due

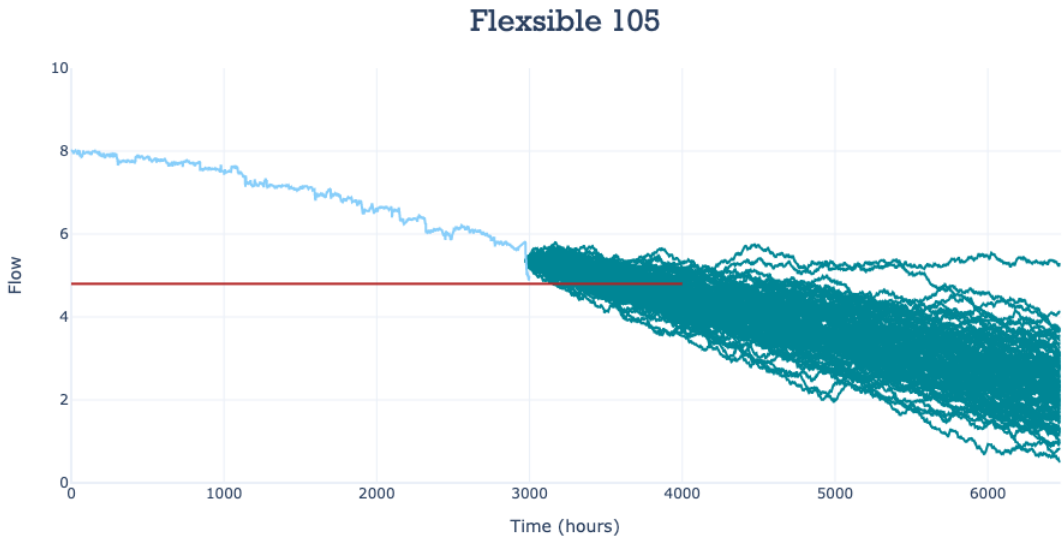


*Figure 7.20: The figure shows the simulations of 100 paths by Monte-Carlo next event simulation. Notice the late initiation of simulation paths.*

to the inherent noise of the flow measurements, which are likely to come from the process itself (i.e., a large aleatoric uncertainty). Hence, the flow measurements can be considered a poor HI because it lacks monotonicity, identifiability (as found in Section 7.5), robustness (signal-to-noise ratio) and consistency.

### 7.6.3 Extensions to the Stochastic Model

After performing the prognosis based on the aforementioned model, several questions still are left unanswered:

1. As shocks are neglected in the current model, how can these be incorporated to gain a better prognosis? Is it possible to explain them by physical properties?
2. How can the parameters be estimated more realistically?
3. How can additional properties be implemented in the model that is found to alter the degradation possibly?
4. How can the inherently bad robustness of the flow measurements be handled? And should another HI possibly be used?
5. Should the model be validated?

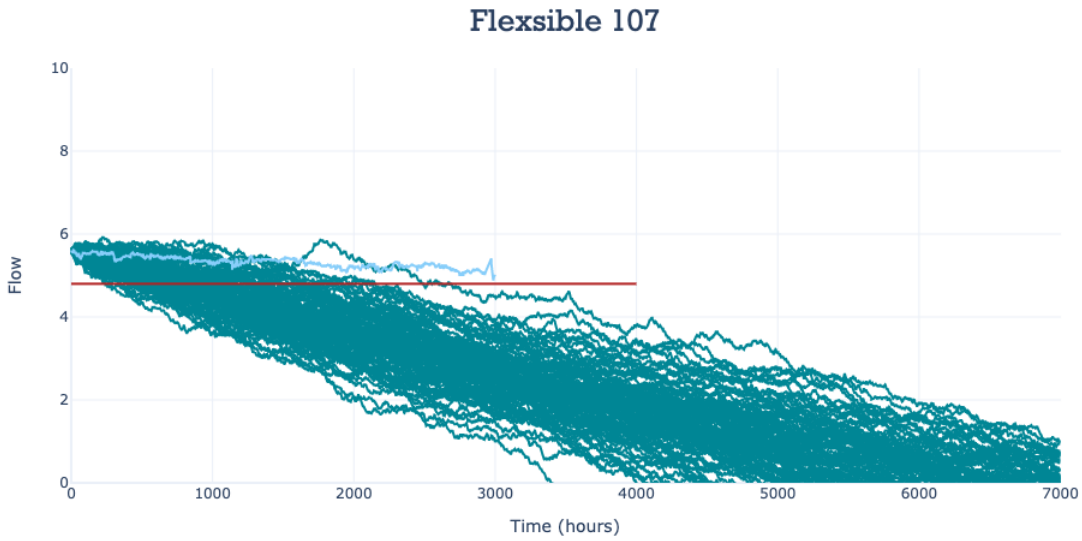


*Figure 7.21: The figure shows the simulations of 100 paths by Monte-Carlo next event simulation. Notice the early initiation of the simulation paths.*

**1. Shocks**

When using the filtered approach to the parameter estimation, one neglects the larger shocks in flow, which can alter the system's health to a large effect. Hence, this should be incorporated into the model. However, there are some challenges with that. What kind of distribution do the shocks have? One could assume a Poisson process that either creates larger shocks or sudden death (crossing of failure threshold). Then, the parameter of this distribution has to be calculated (e.g., by the intensity of shocks compared to normal degradation). Another way of looking at it would be to assume that the increments are distributed by two normal distributions, which could be split up, one for normal degradation (i.e., the filtered distribution) and distribution of the shocks (with large variance). There are coding libraries available in python for these kinds of efforts, such as sci-kit learn. However, the large shocks seem only to be negative, and such an approach would give large shocks both ways. Shocks in a positive direction are exclusively thought to come from flushing. This could be a natural avenue for further work, as Zhang et al. [2018] states that few articles consider Wiener processes with shocks both up and down.

After finding the right distribution (or process) that can model the shocks, one could simply incorporate it into a Monte-Carlo simulation, or one would need to integrate for a computationally faster analytical solution. When solving it analytically (especially with a high amount of variables), it is considered to be a more time-consuming process than solving it numerically.

The shocks could also be modeled by some physical property or measurement if any indication of this was found. However, no specific events or measurements were found to indicate

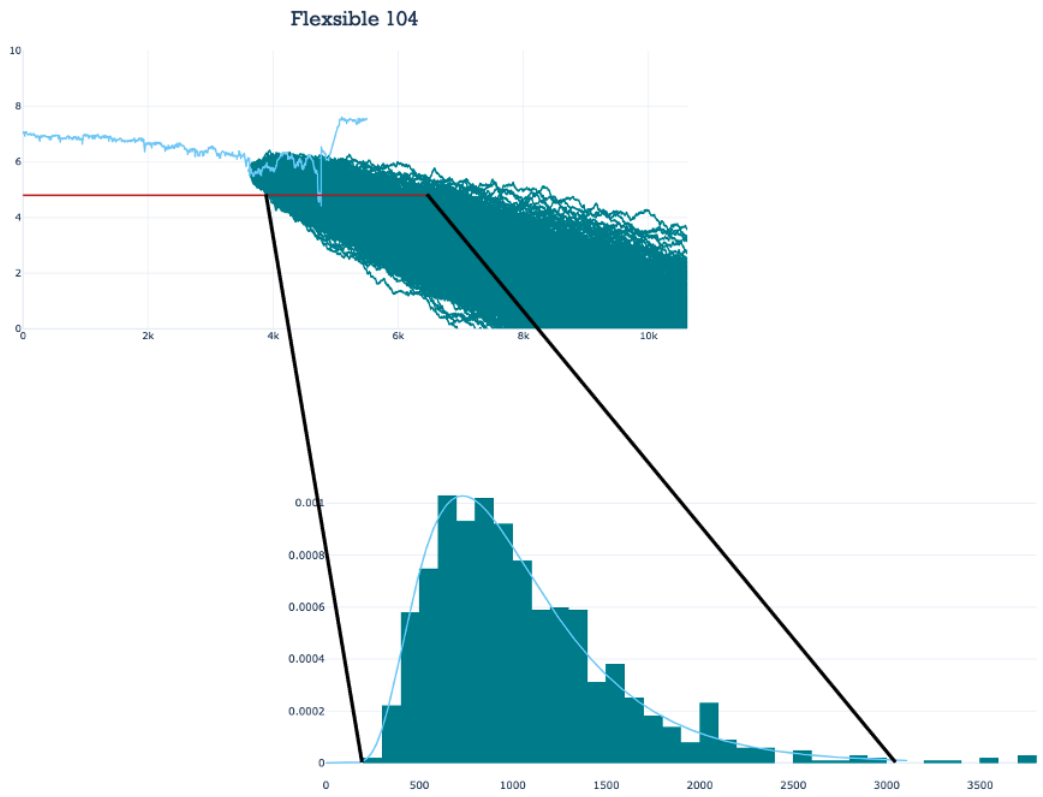


*Figure 7.22: The figure shows the simulation when using the filtered variance from Figure 7.17. The RUL prediction is better but still experiences a large variance. The black lines indicate where the distribution of the failure times corresponds to the simulated path crossing the failure threshold.*

that a typical shock in flow was looming.

### 2. Improved Parameter Estimation

Another way to estimate the parameters is by Bayesian Inference introduced in Section 7.6.1. To simplify the estimation, a fixed variance and an unknown mean can be assumed, and one could obtain the updated drift coefficient by the formula presented in Equation 3.20. The mean could be deemed unknown as it is found to have a higher variance across the degradation paths compared to the variance. This type of Bayesian modeling approach for parameter estimation is believed not to give a better RUL prediction, as the high signal-to-noise ratio is inherent in the flow measurements. It could probably obtain a better drift coefficient for the general flow (filtered increments), but this would not improve the RUL estimate because shocks are still present. Thus, implementing more complex filters based on Bayesian Inference (such as Kalman or Particle Filter) might not be generating better results in this case.

This is because the Bayesian Modelling would lead to less epistemic uncertainty, but the aleatoric uncertainty linked to the HI itself would still be high. To minimize the aleatoric uncer-

tainty, a better HI could be developed.

**3. Additional Properties in the Model**

In addition to shocks, there are some other findings on the properties of the system that could be incorporated into the model. By examining the different sensor measurements of each degradation path, some properties are common on most of them.

1. The degradation tends to decrease by decreasing flow slightly.
2. The probability of shocks increases by decreasing flow.
3. The probability of shocks increases by the mean age of the flexsibles.

When incorporating these findings into an analytical solution to the Wiener process, it becomes rather complex for each new addition, as the integral would increase in complexity. In this case, it might prove more suitable to use a numerical solution such as Monte-Carl simulation. If the degradation trend seems to decrease slightly by decreasing flow, a Geometric Brownian Motion (GBM) could also be used, which incorporates a changing drift by the change in condition.

**4. HI assessment**

As the flow was found to be a rather poor HI because it had worse consistency and robustness than what was initially thought, one should try to find a HI that resolves these problems. It is thought that the pressure could give a better HI, but it seems only to get rid of large deviations such as the one depicted in the middle of the graph in Figure 7.12. Using the temperature difference creates other challenges, but if it is deemed safe to use, it could give a better health indication on *loss of cooling* compared to the flow.

**5. Validation**

Models are usually validated after training them to see how they do against previously unseen data. In this case, when the models are very inconsistent with the training data itself, it seems futile to validate that the models perform poorly. If the model would suddenly perform well on the test set, it would just be by luck.

# Chapter 8

# Discussion

In light of the results in Chapter 7, this chapter will start by providing a deeper understanding of the obstacles in developing a physics-based but also a stochastic model of industrial equipment. The focus is specifically on how to choose the right type of model for the case at hand at the earliest stage possible. While there was no effective way of developing a physics-based model, the focus will be to find out how the development of such models can be improved. Challenges and practical barriers will be discussed in Section 8.1.1. Then, operational applications of the findings are presented in Section 8.2 to evaluate how the results can be used by similar industries in general and Elkem specifically. Lastly, natural avenues for further work are presented in Section 8.3.

## 8.1 Obstacles in the Development of Physics-Based Models

Specifically, there was one question that has been the motivation for this report:

*How is the degradation of physical equipment best modeled?*

To be able to answer this question, several objectives were made in Section 1.1. There was only one objective that was considered not being met. The first objective was accomplished by reviewing related work on similar equipment to the flexsibles. However, few similar cases were found. In addition, Only 10% of degradation modeling literature deals with physics-based models (Lei et al. [2018]). In the works in Chapter 2, it is evident that most of the literature on physics-based models focuses on the same specific physics-based degradation models. Noticing that the literature on physics-based models of machinery referred to by Jardine et al. [2006] and Lei et al. [2018] either is similar or base their research on similar physics-based laws would indicate minimal development in this research area over the years. At the same time, data-driven and stochastic approaches are seen to attract more attention in the field of machinery

prognostics, mainly because of the rise in available data (Lei et al. [2018]).

An important finding is that equipment that seems to have rather explainable physical properties can seem to be a good case for physics-based models, but in reality, they are not. For instance, the flexsible are only made up of three parts. Still, their function relies on a much larger and complex process, which affects the interpretability of the connected sensor measurements. However, both the water operation (4.4) and electric operation (4.5) will heavily affect the flexsibles and are more complicated operations that are not simply explained by the measurements available. Hence, one should be careful to model equipment by physics-based models when their function is not independent of more complex processes.

A strength of this thesis is that it shows how one can structure the development of a prognosis model for physical equipment that serves as bottlenecks in production (such as the flexsibles). The FMSA in Chapter 5, highlights the failure modes of the equipment and finds the failure mode that is deemed most efficient to establish a prognosis for. Then, the failure mechanisms were explored in Chapter 6 to look for physics-based models that could explain the chosen failure mode. While this analysis resulted in a hypothesized flow chart of the degradation phenomena in Figure 6.1, these findings were hard to translate into the available sensor measurements (discussed in Chapter 7). This is a weakness of this thesis, as it was not found any physics-based model that could model the flexsibles to a sufficient degree. Thus, the second objective was not met. However, this resulted in valuable knowledge surrounding the challenges of developing such a model. A crucial part of obtaining a good model of degradation is to obtain the proper HI. This is deemed to mainly be a result of minimizing the aleatoric uncertainty connected to the choice of HI. While Lei et al. [2018] mentions characteristics of a good HI, there are still questions on how an HI would be used when its failure threshold is not intuitively obtained (as discussed in Section 7.3.3). However, it seems that the characteristics of HI proposed by Lei et al. [2018] in general can be used as a framework to assess the performance of an HI.

Objectives 3 and 4 were met, as a stochastic modeling approach was proposed when physics-based models were not available and were implemented on the industrial data (shown in Section 7.6). While modeling the uncertainty in the HI might prove to be the answer to the problems, in this context, it was not. There are several reasons for this, but probably the proper choice of HI is the most prominent one. Hence, several possible HIs were assessed, but the flow was chosen for simplicity to model degradation as it would implicate a simple choice of failure threshold (thus, less epistemic uncertainty). This choice of HI resulted in a substantial aleatoric uncertainty, which was evident in the low consistency of flow measurements. Thus, the RUL predictions based on the flow measurements were inconsistent. This is probably also a result of a deterministic parameter estimation based on leave-one-out cross-validation. The parameter estimation could be improved by estimating Bayesian Inference, and the cross-validation could be performed differently, leading to better estimation results (and lower epistemic uncertainty).

However, the aleatoric uncertainty in the flow measurements is probably so substantial that this would have a minimal effect. Hence, the focus, in this case, should be targeting the development of a proper HI. As choosing the proper HI is deemed very important for proper prognosis, the physical understanding of the system is deemed important for the proper selection of HI. This is shown by equation 7.1 and 7.2 as this would probably not have been found if it was not for the physical understanding of the system obtained in Chapter 5 and 6. Hence, by modeling from a physics-based approach, the chances of implementing an HI that models the real equipment properly increases.

**Proposed Approach to Degradation Modelling**

Based on the strengths and weaknesses in this thesis, the author proposes an approach to degradation modeling when doing so in a practical industrial context. This answers objective number five.

One of the most important obstacles when developing models that explain the behavior of physical systems was to understand the classification of the different model approaches and how they interrelate. Bokrantz et al. [2020] highlights these issues by showing that there is still a high degree of concept proliferation in the smart maintenance literature. This is also evident in the development of degradation models. At the same time, several authors explain the different approaches and exemplify them (e.g., Lei et al. [2018], Jardine et al. [2006] and An et al. [2015]), the different approaches are usually gone through independently. In addition, almost all references refer to hybrid models (a combination of the approaches) as being more proficient than the model approaches used alone, but the literature in this category are found to be minimal (Lei et al. [2018]). However, Liao [2014] reviews different hybrid approaches, but fails to abstract out the relationships between the approaches and is rather more focused on different hybridization examples found in the literature. A problem with this approach is that researchers can tend to start by using a model they know and **then** start looking for practical examples that can fit this model. In practical settings such as in the industry, however, this is not a logical approach. While the industry tends to look for the least complex model that gives the best results (cost and safety efficiency), researchers in Academia usually seek to develop models that can model reality better than before. Thus, the discussion here will revolve around how the model approaches interrelate and how it is possible to use them together effectively (mainly physics-based, stochastic, and data-driven (AI) as presented in Section 3.8.3). This is thought to give future researchers a better understanding of the proper modeling approach for the case at hand and provide a basis for further work. When deciding what type of model to use in modeling degradation in a practical situation, one must decide what type of approach to take before developing a model. In this decision-making process, a natural place to start is with models based on causal-based first principles. For instance, if the degradation (the HI) were found to follow

a linear path completely deterministic (totally consistent), an AI approach would probably find this relationship, and a stochastic process such as the Wiener would reduce to linear regression (the diffusion coefficient would be zero). However, these two approaches would lead to unnecessary work if the degradation could be explained by a known degradation law such as the Paris-Erdogan law of crack propagation in the first place.

In causal-based first principle models (demanding deep knowledge), the HI is considered to be explained by physical law. For instance, one could assume that the flexsibles degradation was directly tied to the Equation 3.23, i.e., the amount of heat it dissipates. If the degradation process would be so easy to predict that deterministic parameters can consistently generate accurate predictions, the degradation pattern would probably be so easy to spot that the development of models is unnecessary. Thus, in most applications in the literature, the physics-based model's parameters are estimated based on Bayesian Inference (An et al. [2015]). This makes sense as degradation patterns will follow the same path, but operational conditions and other properties will alter to what degree they degrade.

In rules-based first principle models (demanding light knowledge), the HI is considered to be explained by an **abstraction** of physical law. For instance, the HI presented in Equation 7.1. Hence, no physical degradation model is available, but one chooses to derive a relationship of degradation from a known physical principle. These types of models are more flexible to the available sensor measurements. For instance, it is impossible to use the corrosion law in Equation 6.1 in this case because the salt concentration in the flexsible case is unknown. Then it could be more natural to use an abstraction of Bernoulli's Principle such as Equation 7.1 to obtain a better HI.

In physics-based models, when used as trend models, their noise (as described in Section 3.6) is assumed to be independent and identically distributed, which will result in a constant variance when using trend models for prognosis (Barros [2019]). When the HI's degradation path (when performed a regression) seems to have deviations from the regression line that is not independent and identically distributed (such as in the flow), a more suitable way of modeling the degradation can be a stochastic degradation model. This approach also Jin et al. [2013], when there are found substantial uncertainties in the HI's degradation path. The results in 7.6 show that simply modeling the degradation by a stochastic process such as Wiener does not solve the problem. This is probably due to the low robustness of the HI chosen. The robustness in the HI can be improved by finding other HIs such as the one found in Equation 7.1. Furthermore, if it was possible to obtain a better HI, possibly the one proposed in equation 7.2 several other properties of the HI could also be improved, such as monotonicity.

If the degradation trend of the chosen HI is still hard to predict by the aforementioned models and there are large amounts of data available, a data-driven (AI) approach might be suitable (An et al. [2015]). This type of approach might be better suited to develop a HI that can predict

the degradation better. For instance, AI approaches can combine the sensor measurements to create a HI that has substantially more robustness because it can find correlations (unknown physics) that are hard to find by humans. However, data-driven models create HI's that are unknown (typically referred to as black boxes (Lei et al. [2018])). But with large amounts of data and when models are thoroughly tested, this type of "black-box" approach is deemed effective. This becomes a discussion on what you are modelling for if it is for inference or prediction (mentioned in Section 3.2). Physics-based approaches are usually better at obtaining inference than data-driven methods. In contrast, data-driven methods can obtain good predictions that, in certain cases, are infeasible to physics-based approaches.

Typical causal-based first-principle (physics-based) models are based on numerous empirical tests and experiments across time that have revealed relationships so consistent that they are considered laws of physics. For instance, equation 3.23 is considered to be such a formula. Similarly, data-driven models have the potential to find relationships between large amounts of data that are currently unavailable to humans and would probably have needed large amounts of creativity even to be conceptualized. Hence, one can say that both physics-based models and data-driven models minimize the uncertainties in their models by utilizing the available data. In circumstances where there are substantial uncertainties involved in the obtained HI, stochastic models can be used to incorporate the uncertainties into the models.

### 8.1.1 Challenges and Practical Barriers

In this context, when large amounts of data are available for processing, data cleaning is deemed very important (Jardine et al. [2006]). A degradation model will be highly affected by the available quality of data.

Thus, this thesis might be an example of the "garbage in - garbage out" situation. Hence, efforts in cleaning data to improve its signal-to-noise ratio (robustness) could be found effective. However, the sensor measurements seem to be inherently little robust, as there was no way of minimizing the signal-to-noise ratio of the available sensor measurements (e.g., by looking for alternative HIs). In addition, when trying to find relationships in the data, it was found hard and time-consuming to do manually by inspecting graphs. While the author recognizes tools that could do this job, such as Principal Component Analysis, it is not conducted because of time constraints. Simpler pair plots of the measurements were conducted but gave inconclusive answers and graphs that were hard to interpret, probably because of the high level of noise. To mitigate this, smoothing techniques were tried out, such as exponentially weighted average (EWA). It was possible to find trends when visually inspecting the graphs but was hard to make sense of when combining the processed data in pair plots.

Furthermore, the data available in this context were not complete as the CM data were not available for a whole lifetime of a flexsible. Thus, it was hard to conclude how a flexsible usually

behaves over its lifetime based on all the measurements. Also, it would be possible to look for other time scales to model the degradation, such as total accumulated current and accumulated temperature difference over a flexsibles lifetime, and look for correlations there.

How the data were processed can be deemed critical to the amount of time used to process this amount of data. Thus, human resources with capabilities in data management are deemed very important. The work in this thesis quickly became a problem where data processing skills are required and not just knowledge about how to code. The code needs to be effective when processing large amounts of data, especially when graphically presenting the data.

## 8.2 Operational Applications

This section aims to answer objective six. The results in this thesis are deemed to give plenty of insights into what can be done in an operational context. The process of developing a physics-based model would give several benefits.

For practical purposes, such a process conducted here and especially a literature review on failure mechanisms as in Chapter 6 is considered to be rather time-consuming. Hence, in such circumstances, one might want to trade off physical knowledge for more uncertainty in the model and go for stochastic modeling approaches. On the other side, this demands more knowledge of the modeling of stochastic processes, which can be more difficult to obtain than simpler regression models physics-based models tend to be based on.

In an operational setting, the Wiener process obtained in Section 7.6 is thought to work as a decision-making tool. For instance, the linear Wiener process' RUL can be predicted analytically. This means that the prognosis could constantly (for every sensor measurement) obtain a RUL prediction. It would not be beneficial to have a human resource manually looking at all these updated RUL predictions in a practical setting, especially if the prediction is found to be long into the future. Hence, one could tune the model to give you an alarm whenever a certain percentile for a RUL prediction is crossed. This is what is done in Section 7.6 where the initiation of Monte-Carlo simulations indicates when such an alarm goes off. Then, this solution could be tuned based on other decision-making constraints and cost functions to give an appropriate amount of time before a failure is imminent. The company can then organize the proper action for this failure. When the alarm goes off, it would also be possible to inspect the RUL prediction manually. Also, the tuned analytical RUL prediction obtained from a Wiener process could be used to initiate a more complex Monte-Carlo Simulation incorporating several of the properties found in Section 7.6. Simulations are usually computationally demanding. Thus it would not be effective to run them constantly. The most efficient way would be to go for an analytical approach, but this approach can be challenging to develop when the degradation modeling is complex.

In the flexsible case, the prognosis could be used to mitigate failures when the plant is not properly manned. Unplanned stops on weekends, at night, and holidays are linked to high costs and could then be mitigated by a proper prognosis. In addition, the planning of maintenance could be improved as there are constraints to how many flexsibles can be replaced at one planned stop each week. Thus, mitigating several preventive replacements that need to be done (because of the high risk of failure until the next planned stop) would be beneficial to increase cost-efficiency. General safety would also be increased at Elkem Thamshavn as water-cooling equipment can cause leaks leading to a large explosion if it finds its way into the furnace.

The TTT plot shown in Figure 7.8 shows that the flexsibles have an increasing failure rate. This indicates that a preventive or even predictive maintenance policy would be effective. If the failure rate was not increasing, a corrective maintenance policy simply replacing when a failure occurs.

A finding that might influence operations at Elkem Thamshavn is that the flexsibles' degradation process is probably not independent of each other. While the Nelson-Aalen plot in Section 7.2 indicates that the flexsibles are independent and identically distributed, this might not be a logical assumption. Firstly, the electric operation at Furnace 1 is connected in parallel, resulting in other flexsibles taking the current-load of one is slightly degraded. The Nelson-Aalen plot results are probably skewed because the flexsibles can be held "artificially" alive after its first passage of the failure threshold by flushing. Thus, the logged replacements of flexsibles used in the life data analysis are based on expert opinions on when to replace because flushing can keep flexsible operational over a long time after their initial crossing of the failure threshold.

For the operational setting at Thamshavn, they should be focusing their efforts on looking into the differences between furnaces, as the electric operation might be affecting the degradation of flexsibles at Furnace 1. This is based on the furnaces sharing the same water operation, which deem the degradation coming from poor water quality unlikely.

## 8.3 Further Work

This thesis demonstrates how a degradation model can be built from a physics-based perspective and can be used in practical modeling cases. However, certain aspects can be improved, and others are not explored yet.

One such aspect is the development of an effective HI, which can reduce the aleatoric uncertainty present in the available sensor measurements, thus creating a better basis for RUL prediction. A new HI could have better properties and avoid occurrences such as the shocks evident in the flow measurements and make the prognosis based on the Wiener process ineffective. A good place to start exploring new HIs would be the equations proposed in Section 7.3.3. Specifically incorporating the temperature difference. This makes sense since the func-

tion of the cooling water is to keep the flexsibles cooled. Thus the temperature difference is a direct indicator for this. However, if one were to establish such a new HI, there are still epistemic uncertainties connected to the choice of failure threshold.

In addition, other approaches to the Wiener process could also be further explored. The parameters are assumed deterministic in this thesis but can be better modeled by a Bayesian Inference approach typically used in the literature (An et al. [2015]). This approach could also determine how large the aleatoric uncertainty is and if lowering the epistemic uncertainty would improve RUL predictions in this case. In addition, to mitigate the shocks present in the flow, one might look to incorporate this into the model either analytically or numerically (e.g., Monte-Carlo simulations). One might find indications based on other measurements on when they occur or model them into the stochastic model by approaches brought up in Section 7.6. While the analytical approach is much more computationally efficient, simulations are easier to use when adding extensions to the model, such as those discussed in Section 7.6.3. When one also considers the decrease in the cost of computational power, simulations might be suitable. This is especially evident when many parameters in the model increase the complexity of integrals in the analytical approach. Further, the flow was found to decrease in degradation by decreasing flow, which might be modeled by a Geometric Brownian Motion (Zhang et al. [2018]).

While a hypothesis on the clogging phenomena is presented in Figure 6.1, the cause and effect relationships in such a complicated process with so many variables are, in reality, hard to determine. Thus, analysis or experiments should be conducted to find out how these failure mechanisms interrelate. In addition, failure modes usually have interrelated effects, while they are deemed independent in this thesis. Thus, further work should elaborate on the failure mechanisms of the other failure modes to see if their interrelation is observable.

Further work should aim at implementing the results in this thesis into a maintenance decision-making context. One could imagine that if the degradation of flexsibles was better modeled, giving better information of their time to failure, optimizing the production process better with maintenance actions. Thus, reducing cost.

In addition, event data should be further explored. The results in the Non-Parametric Life-Data Analysis should quality checked by e.g., proper calculations for assessing the Nelson-Aalen plot.

The scientific literature should be targeting data acquisition and processing to find more effective ways of processing such large amounts of data used in this thesis. Consequently, also look for efficient ways for building proper HIs. Specifically, VHIs (such as the one in equation 7.2) would increase the aleatoric uncertainty as opposed to PHIs, which are more intuitively assessed. Lei et al. [2018] proposes HI assessments, but these are specific to certain circumstances. Thus, the literature should focus on developing quantitative assessment methods for HIs to improve the development of degradation modeling.

Lastly, as this thesis has shown how to go from a physics-based approach to a stochastic, a natural next step would be to assess this problem from a data-driven approach. A data-driven approach might find relationships that manual models and processing of data done here have no chance of doing. However, in this circumstance, data quality and proper validation of the models would be even more important.

# Chapter 9

# Conclusion

The vast amounts of available sensor data in modern production systems present the industry with big opportunities. In conjunction with the emergence of better digital technologies, maintenance has become an essential business function. However, companies seem to be struggling when implementing maintenance policies based on sensor data. A promising way of improving maintenance is by prognosis, obtaining information of when a component will fail in the future. As such, the objective of this study has been to find ways to develop such a physics-based model for prognosis based on real industrial data and show natural ways of approaching the problem when physics-based models are deemed unavailable.

To conclude, it was found that that a physics-based approach might be a suitable place to start any degradation modeling. The results of a better understanding of the equipment's functions and physical properties can have business values on its own. In addition, results in this thesis indicate that physics-based approaches can be very valuable when combined with other approaches for degradation modeling, such as stochastic approaches. This is in somewhat conjunction with the common literature, which deems hybrid approaches as preferable. Still, the results in this thesis argue for physics-based approaches to be the specifically preferred approach to base a hybrid approach upon. Hence, a physics-based approach should be **the starting point** to any process aiming at doing prognosis of an asset's lifetime.

However, when the physical properties of the degradation model do not seem to fit with the sensor measurements available, a stochastic model might be appropriate to incorporate more uncertainties in the model. In general, it was found that the natural path of the modeling approach would be to go from minimal to the maximum amount of stochasticity in the model as the uncertainties (or complexities) in the model increased.

In addition, physics-based models should be carefully chosen when the equipment's function under analysis relies on more complex systems or processes. This is an addition to the current literature on physics-based models, as it is usually specified that only the equipment under analysis needs to be easy to model.

# Bibliography


Aftenposten. Vil ta tid aa finne aarsaken til Elkem-eksplosjonen, 2006. URL https://www.aftenposten.no/norge/i/bGRnl/vil-ta-tid-aa-finne-aarsaken-til-elkem-eksplosjonen.

S. Alaswad and Y. Xiang. A review on condition-based maintenance optimization models for stochastically deteriorating system. *Reliability Engineering and System Safety*, 157:54–63, 2017. doi: 10.1016/j.ress.2016.08.009.

D. An, N.H. Kim, and J.-H. Choi. Practical options for selecting data-driven or physics-based prognostics algorithms with reviews. *Reliability Engineering and System Safety*, 133:223–236, 2015. doi: 10.1016/j.ress.2014.09.014.

P. Baraldi, F. Mangili, and E. Zio. A Kalman filter-based ensemble approach with application to turbine creep prognostics. *IEEE Transactions on Reliability*, 61(4):966–977, 2012. doi: 10.1109/TR.2012.2221037.

P. Baraldi, F. Mangili, and E. Zio. Investigation of uncertainty treatment capability of model-based and data-driven prognostic methods using simulated data. *Reliability Engineering and System Safety*, 112:94–108, 2013. doi: 10.1016/j.ress.2012.12.004.

Anne Barros. No Title. In *Data driven prognostic and Predictive Maintenance*, pages 1–61. 2019.

W. Bartelmus. Diagnostic information on gearbox condition for mechatronic systems. *Transactions of the Institute of Measurement & Control*, 25(5):451–465, 2003. doi: 10.1191/0142331203tm0099oa.

P. Baruah and R.B. Chinnam. HMMs for diagnostics and prognostics in machining processes. *International Journal of Production Research*, 43(6):1275–1293, 2005. doi: 10.1080/00207540412331327727.

STEIN BJØRU. Halv million i bot etter eksplosjon. *Adresseavisen*, 2007.

J. Bokrantz, A. Skoogh, C. Berlin, T. Wuest, and J. Stahre. Smart Maintenance: an empirically grounded conceptualization. *International Journal of Production Economics*, 223, 2020. doi: 10.1016/j.ijpe.2019.107534.

Nicolle Boulay and Marc Edwards. Role of temperature, chlorine, and organic matter in copper corrosion by-product release in soft water. *Water Research*, 35(3):683–690, 2001. ISSN 00431354. doi: 10.1016/S0043-1354(00)00320-1.

C.S. Byington, M.J. Roemer, G.J. Kacprzymki, and T. Galie. Prognostic enhancements to diagnostic systems for improved condition-based maintenance [military aircraft]. In *IEEE Aerospace Conference Proceedings*, volume 6, pages 2815–2824, 2002. ISBN 9780780372313. doi: 10.1109/AERO.2002.1036120.

F. Cadini, E. Zio, and D. Avram. Monte Carlo-based filtering for fatigue crack growth estimation. *Probabilistic Engineering Mechanics*, 24(3):367–373, 2009. doi: 10.1016/j.probengmech.2008.10.002.

George Casella, Stephen Fienberg, and Ingram Olkin. *Springer Texts in Statistics*, volume 102. 2006. ISBN 9780387781884. doi: 10.1016/j.peva.2007.06.006. URL http://books.google.com/books?id=9tv0taI8l6YC.

George Casella, Stephen Fienberg, and Ingram Olkin. *An Introduction to Statistical Learning*. 2013. ISBN 9780387781884. URL http://books.google.com/books?id=9tv0taI8l6YC.

J. Chiachío, M. Chiachío, S. Sankararaman, A. Saxena, and K. Goebel. Condition-based prediction of time-dependent reliability in composites. *Reliability Engineering and System Safety*, 142:134–147, 2015. doi: 10.1016/j.ress.2015.04.018.

G.H. Choi and G.S. Choi. Application of minimum cross entropy to model-based monitoring in diamond turning. *Mechanical Systems and Signal Processing*, 10(5):615–631, 1996. doi: 10.1006/mssp.1996.0042.

B. de Jonge and P.A. Scarf. A review on maintenance optimization. *European Journal of Operational Research*, 285(3):805–824, 2020. doi: 10.1016/j.ejor.2019.09.047.

Marc Edwards, Travis Meyer, and John Rehring. on Copper Corrosion Rates. 86(December): 73–81, 1994.

K. El-Tawil and A.A. Jaoude. Stochastic and nonlinear-based prognostic model. *Systems Science and Control Engineering*, 1(1):66–81, 2013. doi: 10.1080/21642583.2013.850754.

Elkem. UBS - Digital Road Show - 21 September 2020. Technical report, 2020. URL https://www.elkem.com/globalassets/corporate/investor/other-financial-presentations/elkem-asa---ubs---digital-roadshow---21-september-2020.pdf.

Alaa Elwany and Nagi Gebraeel. Real-time estimation of mean remaining life using sensor-based degradation models. *Journal of Manufacturing Science and Engineering, Transactions of the ASME*, 131(5):0510051–0510059, 2009. ISSN 10871357. doi: 10.1115/1.3159045.

Guerin Fabrice, Mihaela Barreau, and Julien Hersant. Mathematical and Statistical Models and Methods in Reliability. *Mathematical and Statistical Models and Methods in Reliability*, (October):0–6, 2010. doi: 10.1007/978-0-8176-4971-5.

FLOHE. FLOHE - High Current Cables. 2021.

A. Fuller, Z. Fan, C. Day, and C. Barlow. Digital Twin: Enabling Technologies, Challenges and Open Research. *IEEE Access*, 8:108952–108971, 2020. doi: 10.1109/ACCESS.2020.2998358.

Z. Gao, C. Cecati, and S.X. Ding. A survey of fault diagnosis and fault-tolerant techniques-part I: Fault diagnosis with model-based and signal-based approaches. *IEEE Transactions on Industrial Electronics*, 62(6):3757–3767, 2015. doi: 10.1109/TIE.2015.2417501.

GE. General Electric Digital Twin, 2020. URL https://www.ge.com/digital/applications/digital-twin.

M.A. Haile, J.C. Riddick, and A.H. Assefa. Robust Particle Filters for Fatigue Crack Growth Estimation in Rotorcraft Structures. *IEEE Transactions on Reliability*, 65(3):1438–1448, 2016. doi: 10.1109/TR.2016.2590258.

Thorsteinn Hanneson. *The Si process*. 2016. URL www.elkem.is.

A Harold. Formulas the Skin Effect *. *proceedings of IRE*, pages 299–311, 1942.

M. Hermann, T. Pentek, and B. Otto. Design principles for industrie 4.0 scenarios. In *Proceedings of the Annual Hawaii International Conference on System Sciences*, volume 2016-March, pages 3928–3937, 2016. ISBN 9780769556703. doi: 10.1109/HICSS.2016.488.

K. E. Heusler. Present state and future problems of corrosion science and engineering. *Corrosion Science*, 31(C):753–761, 1990. ISSN 0010938X. doi: 10.1016/0010-938X(90)90193-9.

I. Howard, S. Jia, and J. Wang. The dynamic modelling of a spur gear in mesh including friction and a crack. *Mechanical Systems and Signal Processing*, 15(5):831–853, 2001. doi: 10.1006/mssp.2001.1414.

Frank P Incropera, Adrienne S Lavine, Theodore L Bergman, and David P DeWitt. *Principles of heat and mass transfer*. Wiley, 2013.

ISO. ISO 13379-1. page 33, 2012.

A.K.S. Jardine, D. Lin, and D. Banjevic. A review on machinery diagnostics and prognostics implementing condition-based maintenance. *Mechanical Systems and Signal Processing*, 20(7): 1483–1510, 2006. doi: 10.1016/j.ymssp.2005.09.012.

G. Jin, D. Matthews, Y. Fan, and Q. Liu. Physics of failure-based degradation modeling and lifetime prediction of the momentum wheel in a dynamic covariate environment. *Engineering Failure Analysis*, 28:222–240, 2013. doi: 10.1016/j.engfailanal.2012.10.027.

G. Kear, B. D. Barker, and F. C. Walsh. Electrochemical corrosion of unalloyed copper in chloride media–a critical review. *Corrosion Science*, 46(1):109–135, 2004. ISSN 0010938X. doi: 10.1016/S0010-938X(02)00257-3.

B. Kuźnicka. Erosion-corrosion of heat exchanger tubes. *Engineering Failure Analysis*, 16(7): 2382–2387, 2009. doi: 10.1016/j.engfailanal.2009.03.026.

H. Lasi, P. Fettke, H.-G. Kemper, T. Feld, and M. Hoffmann. Industry 4.0. *Business and Information Systems Engineering*, 6(4):239–242, 2014. doi: 10.1007/s12599-014-0334-4.

Y. Lei, N. Li, S. Gontarz, J. Lin, S. Radkowski, and J. Dybala. A Model-Based Method for Remaining Useful Life Prediction of Machinery. *IEEE Transactions on Reliability*, 65(3):1314–1326, 2016. doi: 10.1109/TR.2016.2570568.

Y. Lei, N. Li, L. Guo, N. Li, T. Yan, and J. Lin. Machinery health prognostics: A systematic review from data acquisition to RUL prediction. *Mechanical Systems and Signal Processing*, 104:799–834, 2018. doi: 10.1016/j.ymssp.2017.11.016.

Henry Leidheiser jr. *The Corrosion of Copper, Tin and their Alloys*. New York, 1971.

L. Liao. Discovering prognostic features using genetic programming in remaining useful life prediction. *IEEE Transactions on Industrial Electronics*, 61(5):2464–2472, 2014. doi: 10.1109/TIE.2013.2270212.

K.F. Martin. A review by discussion of condition monitoring and fault diagnosis in machine tools. *International Journal of Machine Tools and Manufacture*, 34(4):527–551, 1994. doi: 10.1016/0890-6955(94)90083-3.

C.H. Oppenheimer and K.A. Loparo. Physically based diagnosis and prognosis of cracked rotor shafts. *Proceedings of SPIE - The International Society for Optical Engineering*, 4733:122–132, 2002. doi: 10.1117/12.475502.

M.E. Orchard and G.J. Vachtsevanos. A particle-filtering approach for on-line fault diagnosis and failure prognosis. *Transactions of the Institute of Measurement and Control*, 31(3-4):221–246, 2009. doi: 10.1177/0142331208092026.

S. Pareek, D. Jain, S. Hussain, A. Biswas, R. Shrivastava, S.K. Parida, H.K. Kisan, H. Lgaz, I.-M. Chung, and D. Behera. A new insight into corrosion inhibition mechanism of copper in aerated 3.5 wt.% NaCl solution by eco-friendly Imidazopyrimidine Dye: experimental and theoretical approach. *Chemical Engineering Journal*, 358:725–742, 2019. doi: 10.1016/j.cej.2018.08.079.

Mazdak Parsi, Kamyar Najmi, Fardis Najafifard, Shokrollah Hassani, Brenton S. McLaury, and Siamack A. Shirazi. A comprehensive review of solid particle erosion modeling for oil and gas wells and pipelines applications. *Journal of Natural Gas Science and Engineering*, 21:850–873, 2014. ISSN 18755100. doi: 10.1016/j.jngse.2014.10.001.

Y. Qian, R. Yan, and R.X. Gao. A multi-time scale approach to remaining useful life prediction in rolling bearing. *Mechanical Systems and Signal Processing*, 83:549–567, 2017. doi: 10.1016/j.ymssp.2016.06.031.

Adil Rasheed, Omer San, and Trond Kvamsdal. Digital twin: Values, challenges and enablers from a modeling perspective. *IEEE Access*, 8:21980–22012, 2020. ISSN 21693536. doi: 10.1109/ACCESS.2020.2970143.

Marvin Rausand and Arnljot Høyland. *System Reliability Theory: Models, Statistical Methods, and Applications*. Wiley, Hoboken, NJ, 2nd edition, 2004.

W.D. Robertson, V.F. Nole, W.H. Davenport, and F.P. Talboom. Electro-chemical society. *Electrochemical society*, 105:569, 1958.

T.K. Ross and B.P.L. Hitchen. *Corrosion sci.* 1951.

Anders Schei, Johan Kr Tuset, and Halvard Tveit. *Production of high silicon alloys*. 1998.

X.-S. Si, W. Wang, C.-H. Hu, and D.-H. Zhou. Remaining useful life estimation - A review on the statistical data driven approaches. *European Journal of Operational Research*, 213(1):1–14, 2011. doi: 10.1016/j.ejor.2010.11.018.

J.Z. Sikorska, M. Hodkiewicz, and L. Ma. Prognostic modelling options for remaining useful life estimation by industry. *Mechanical Systems and Signal Processing*, 25(5):1803–1836, 2011. doi: 10.1016/j.ymssp.2010.11.018.

Y. S. Tam and P. Elefsiniotis. Corrosion control in water supply systems: Effect of pH, alkalinity, and orthophosphate on lead and copper leaching from brass plumbing. *Journal of Environmental Science and Health - Part A Toxic/Hazardous Substances and Environmental Engineering*, 44(12):1251–1260, 2009. ISSN 10934529. doi: 10.1080/10934520903140009.

Robert M. Van de Kerkhof, Henk A. Akkermans, and Nils G. Noorderhaven. Knowledge Lost in Data: Organizational Impediments to Condition-Based Maintenance in the Process Industry. 2016.

A. Vania and P. Pennacchi. Experimental and theoretical application of fault identification measures of accuracy in rotating machine diagnostics. *Mechanical Systems and Signal Processing*, 18(2):329–352, 2004. doi: 10.1016/S0888-3270(03)00014-1.

Jasper Veldman, Warse Klingenberg, and Hans Wortmann. Managing condition-based maintenance technology: A multiple case study in the process industry. *Journal of Quality in Maintenance Engineering*, 2011.

W. Wang. Towards dynamic model-based prognostics for transmission gears. In *Proceedings of SPIE - The International Society for Optical Engineering*, volume 4733, pages 157–167, 2002. doi: 10.1117/12.475505.

A. Werner, N. Zimmermann, and J. Lentes. Approach for a holistic predictive maintenance strategy by incorporating a digital twin. In *Procedia Manufacturing*, volume 39, pages 1743–1751, 2019. doi: 10.1016/j.promfg.2020.01.265.

D. Xu, J. Huang, Q. Zhu, X. Chen, Y. Xu, and S. Wang. Residual fatigue life prediction of ball bearings based on Paris law and RMS. *Chinese Journal of Mechanical Engineering (English Edition)*, 25(2):320–327, 2012. doi: 10.3901/CJME.2012.02.320.

Hugh D. Young and Roger A. Freedman. *University Physics with modern physics*. 2016.

V. Zeller, C. Hocken, and V. Stich. *Acatech industrie 4.0 maturity index – a multidimensional maturity model*, volume 536. 2018. ISBN 9783319997063. doi: 10.1007/978-3-319-99707-0{_}14.

Z. Zhang, X. Si, C. Hu, and Y. Lei. Degradation data analysis and remaining useful life estimation: A review on Wiener-process-based methods. *European Journal of Operational Research*, 271 (3):775–796, 2018. doi: 10.1016/j.ejor.2018.02.033.

F. Zhao, Z. Tian, and Y. Zeng. Uncertainty quantification in gear remaining useful life prediction through an integrated prognostics method. *IEEE Transactions on Reliability*, 62(1):146–159, 2013. doi: 10.1109/TR.2013.2241216.

E. Zio and G. Peloni. Particle filtering prognostic estimation of the remaining useful life of nonlinear components. *Reliability Engineering and System Safety*, 96(3):403–409, 2011. doi: 10.1016/j.ress.2010.08.009.

# Appendix A

# Acronyms

**HI** Health Indicator

**HS** Health State

**MTTF** Mean time to failure

**RUL** Remaining Useful Life

**CBM** Condition-Based Maintenance

**PHM** Prognostics and Health Management

**FMSA** Failure Mode Symptoms Analysis

**FMECA** Failure Mode, Effects & Criticality Analysis

**CM** Condition Monitoring

**ML** Machine Learning

**VHI** Virtual Health Indicator

**PHI** Physical Health Indicator

# Appendix B

# Appendix

In this appendix the graphs from the different RUL predictions by the Wiener process with linear drift is presented.

## B.1 Training Models: Wiener Process

In this section, the degradation paths that were used to tune the Wiener process parameters described in Section 7.6 is presented. All simulations are performed with 100 paths, for fast computation. This is evident in the histograms that does not fit the theoretical RUL obtained analytically.

### B.1.1 Flexsible 104

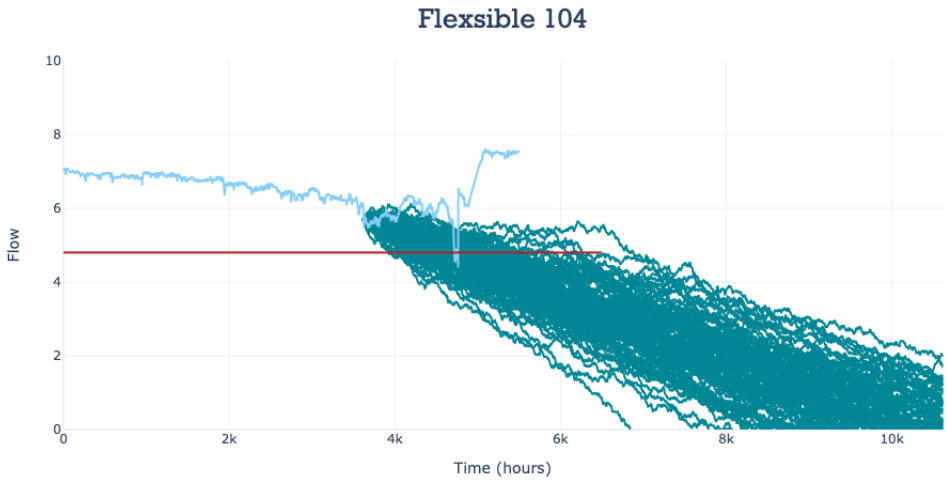


*Figure B.1: The wiener process shown by a Monte-Carlo simulation.*

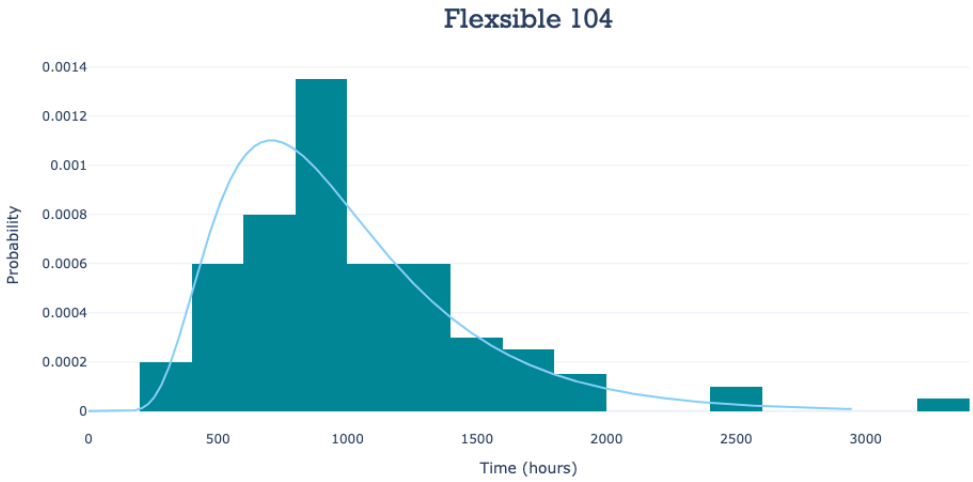


*Figure B.2: Histogram of the RUL prediction for flexsible 104.*

### B.1.2 Flexsible 105

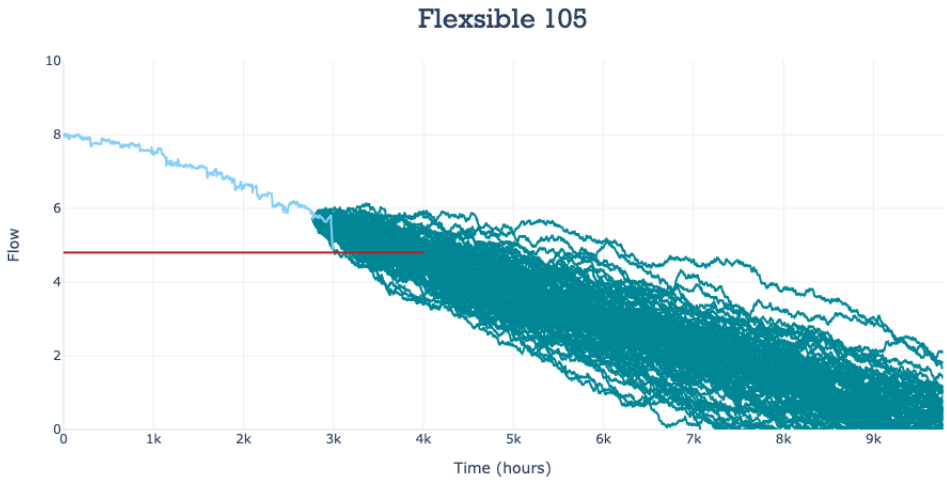


*Figure B.3: The wiener process shown by a Monte-Carlo simulation for flexsible 105.*

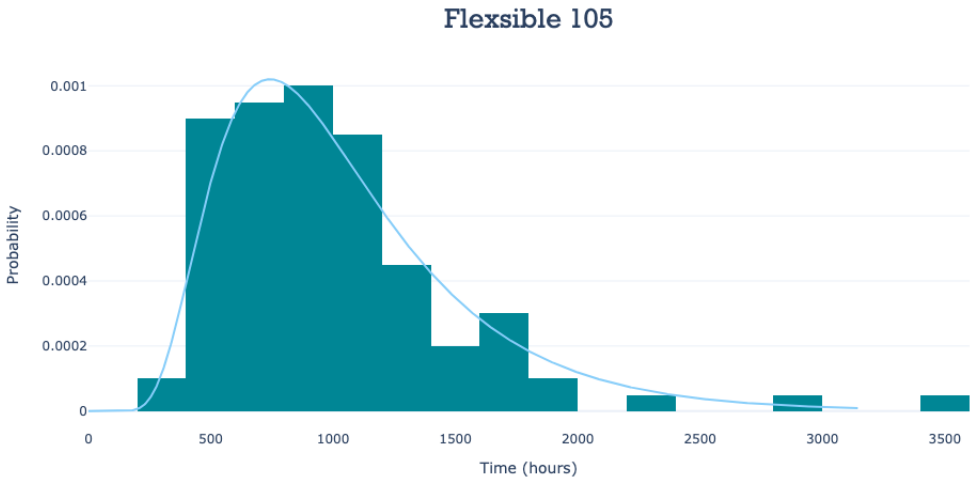


*Figure B.4: Histogram of the RUL prediction for flexsible 104.*

### B.1.3 Flexsible 107

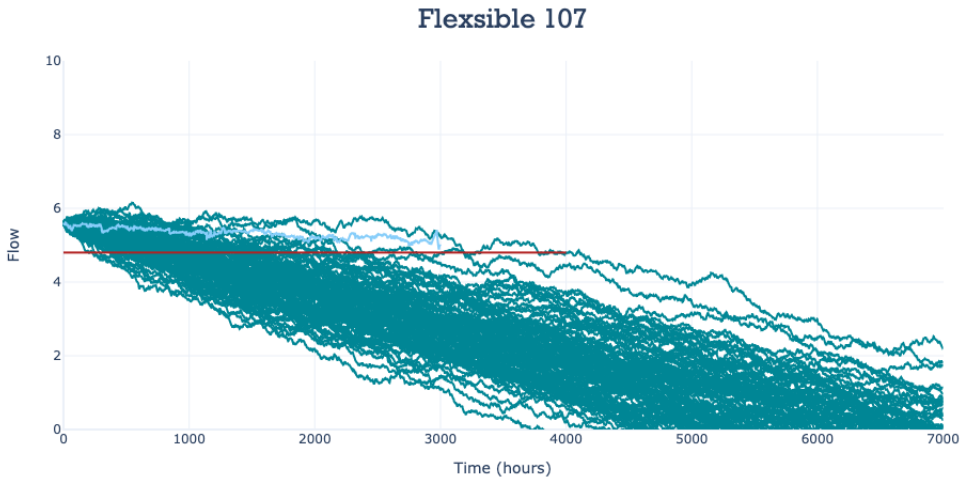


*Figure B.5: The wiener process shown by a Monte-Carlo simulation for flexsible 105.*

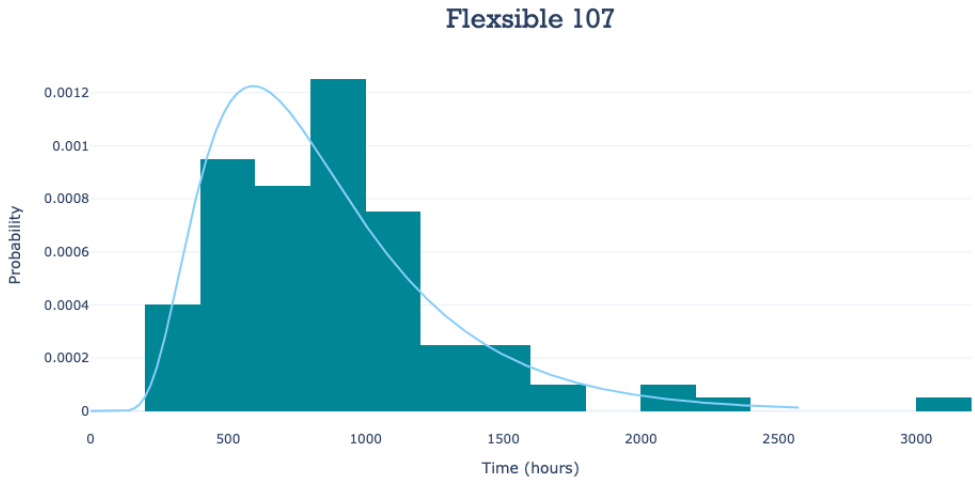


*Figure B.6: Histogram of the RUL prediction for flexsible 104.*

### B.1.4 Flexsible 204

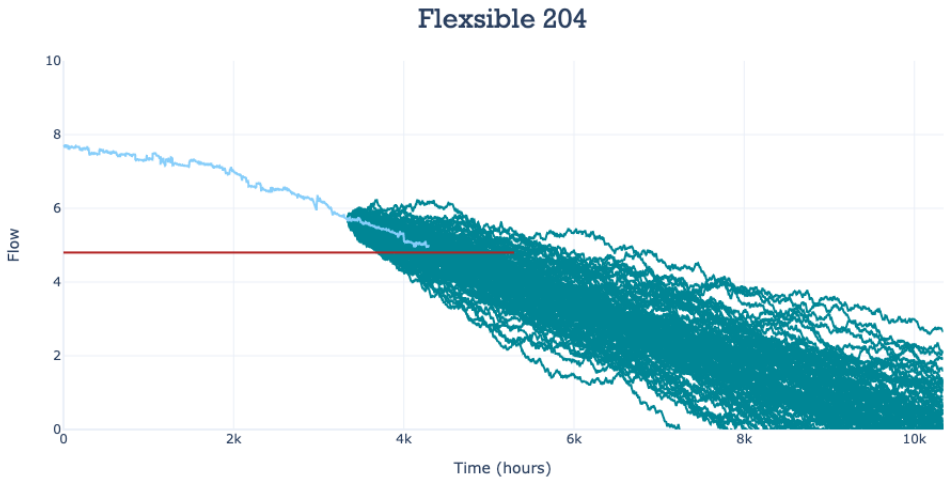


*Figure B.7: The wiener process shown by a Monte-Carlo simulation for flexsible 105.*

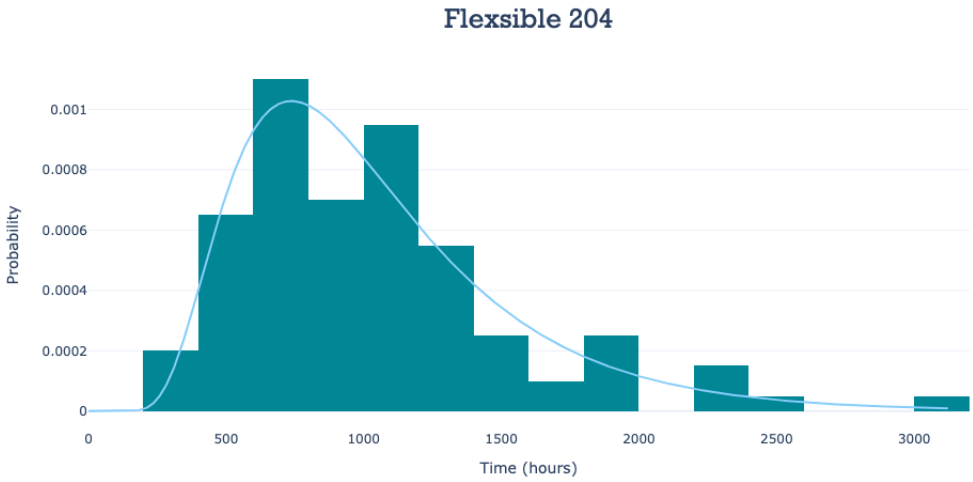


*Figure B.8: Histogram of the RUL prediction for flexsible 104.*

### B.1.5 Flexsible 205

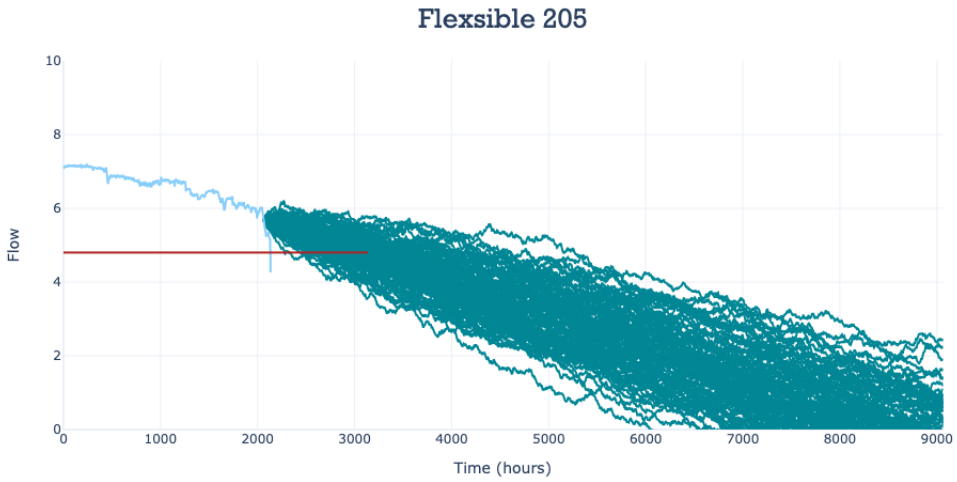


*Figure B.9: The wiener process shown by a Monte-Carlo simulation for flexsible 105.*

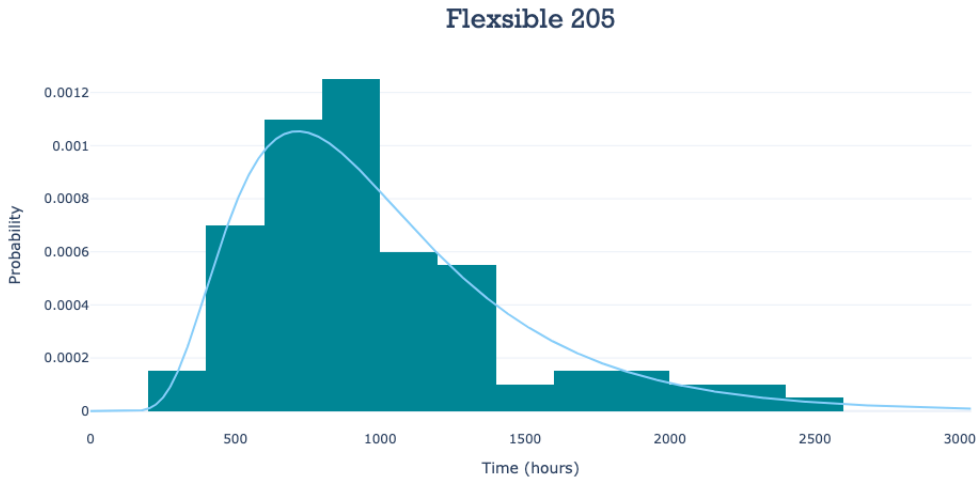


*Figure B.10: Histogram of the RUL prediction for flexsible 104.*

### B.1.6 Flexsible 206

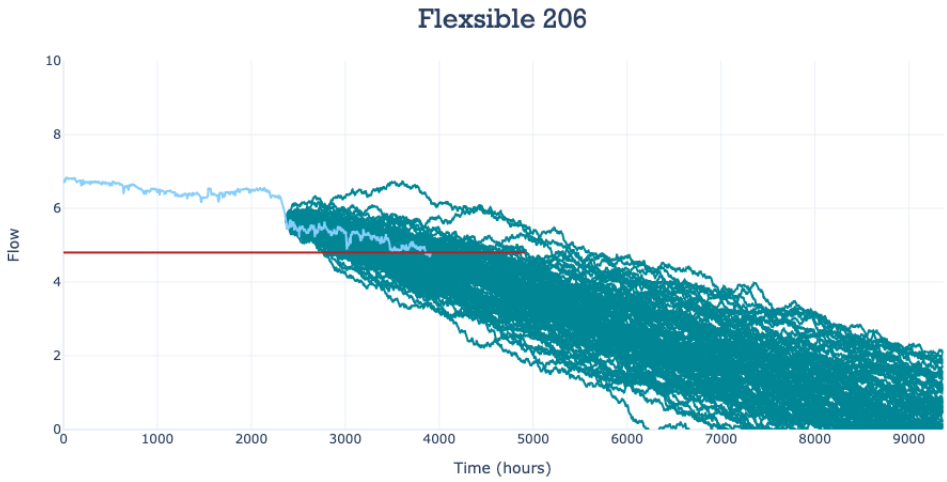


*Figure B.11: The wiener process shown by a Monte-Carlo simulation for flexsible 105.*

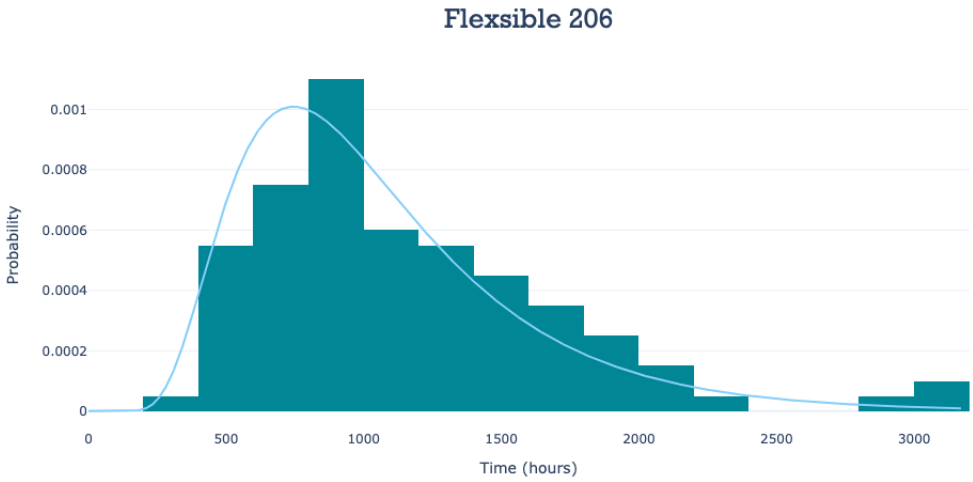


*Figure B.12: Histogram of the RUL prediction for flexsible 104.*

### B.1.7 Flexsible 207

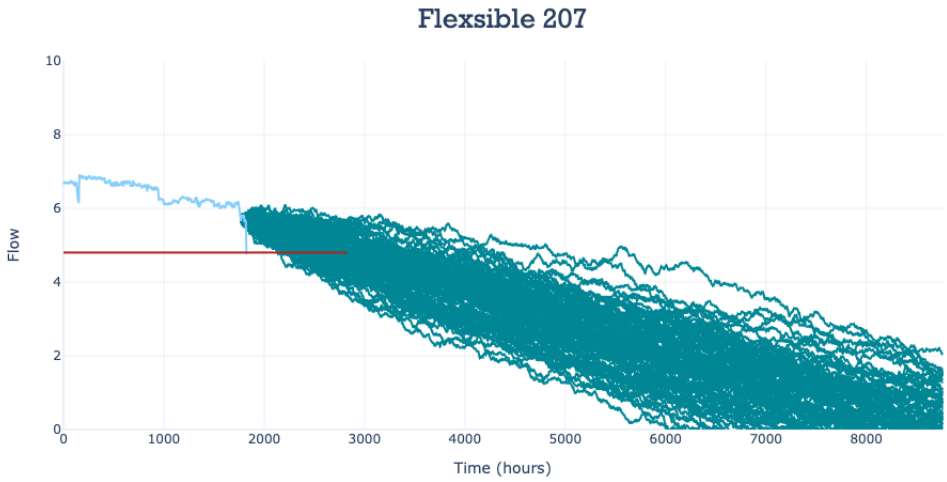


*Figure B.13: The wiener process shown by a Monte-Carlo simulation for flexsible 105.*

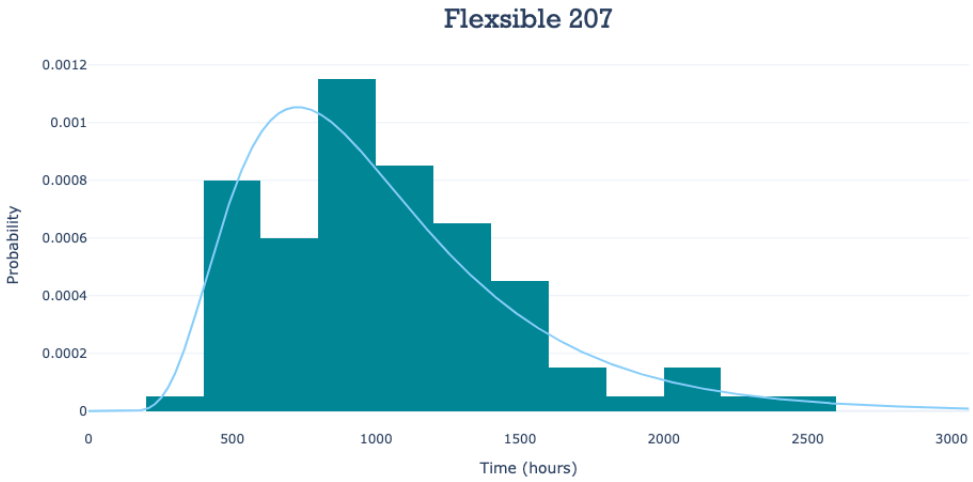


*Figure B.14: Histogram of the RUL prediction for flexsible 104.*

### B.1.8 Flexsible 209

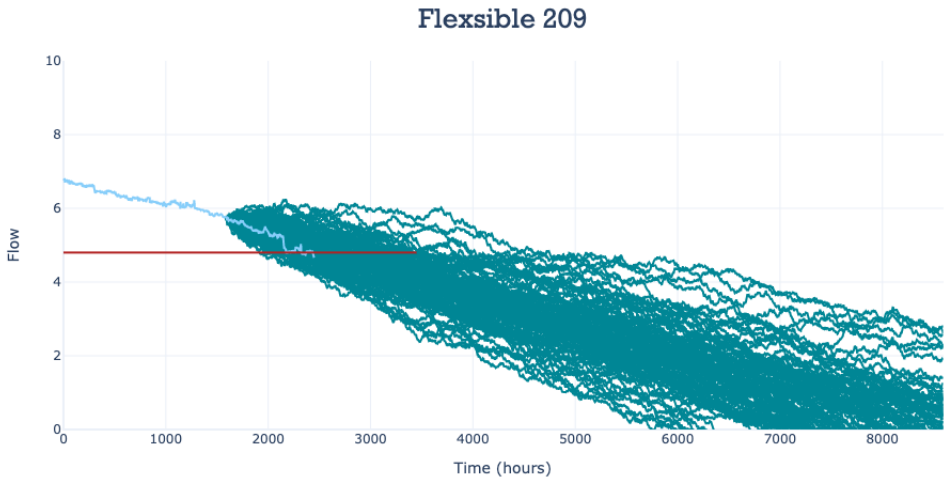


*Figure B.15: The wiener process shown by a Monte-Carlo simulation for flexsible 105.*

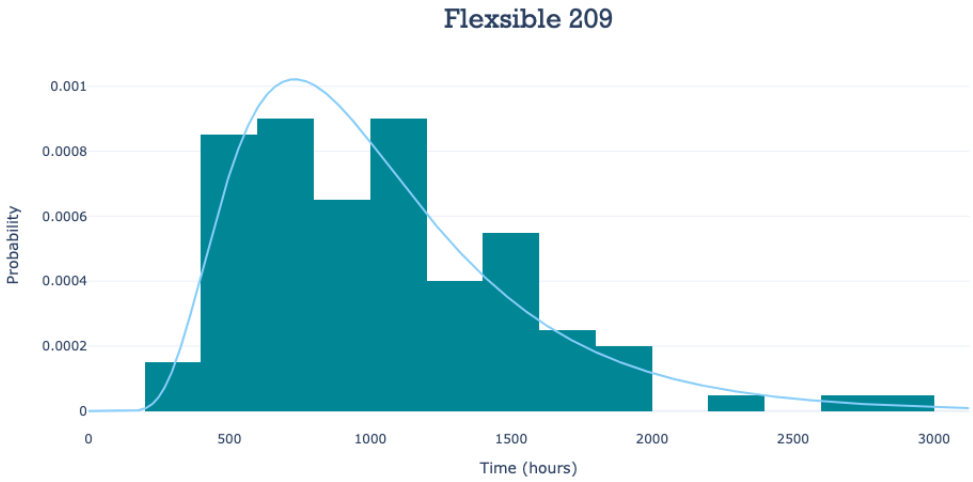


*Figure B.16: Histogram of the RUL prediction for flexsible 104.*

### B.1.9 Flexsible 304

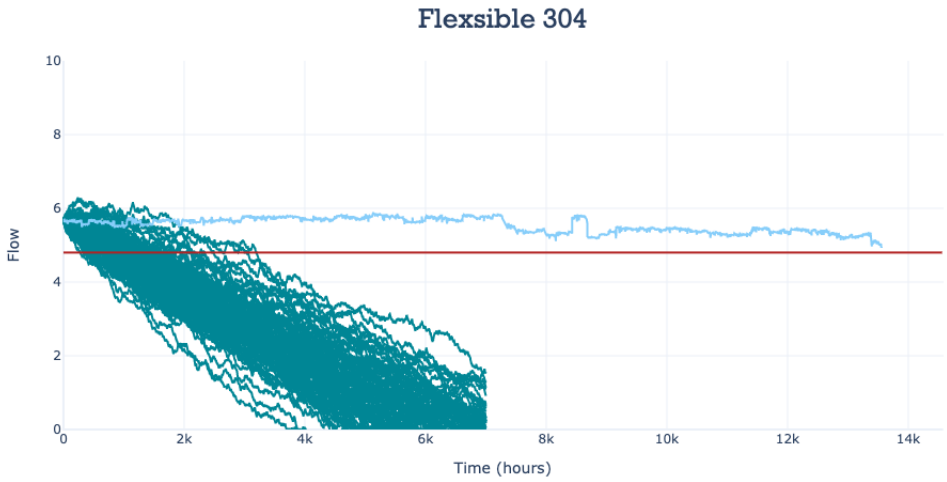


*Figure B.17: The wiener process shown by a Monte-Carlo simulation for flexsible 105.*

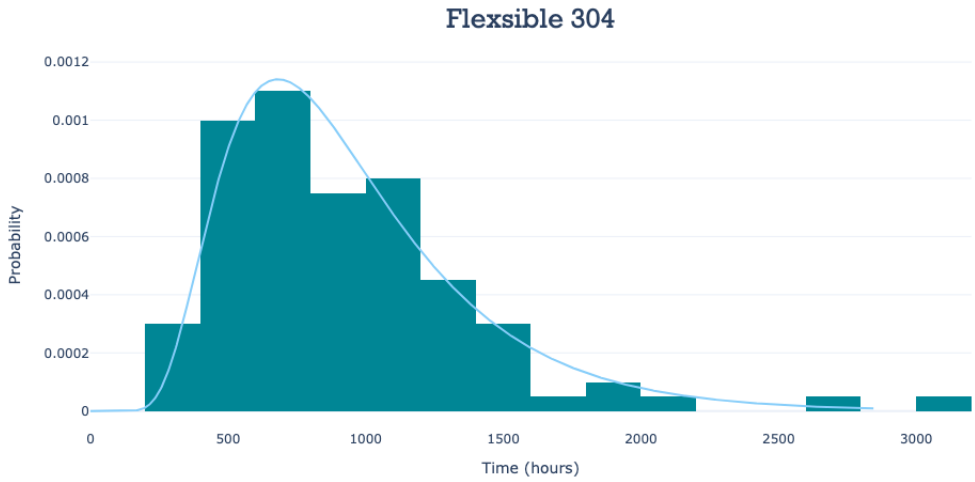


*Figure B.18: Histogram of the RUL prediction for flexsible 104.*

### B.1.10 Flexsible 305

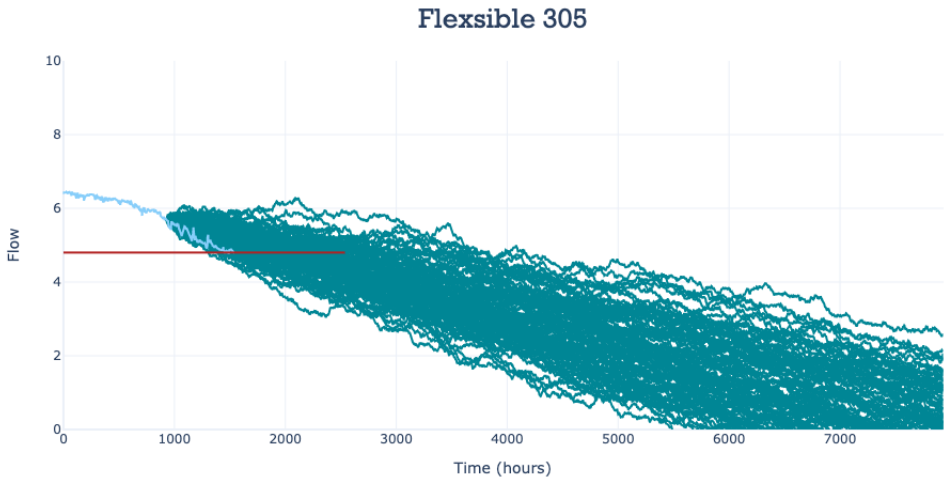


*Figure B.19: The wiener process shown by a Monte-Carlo simulation for flexsible 105.*

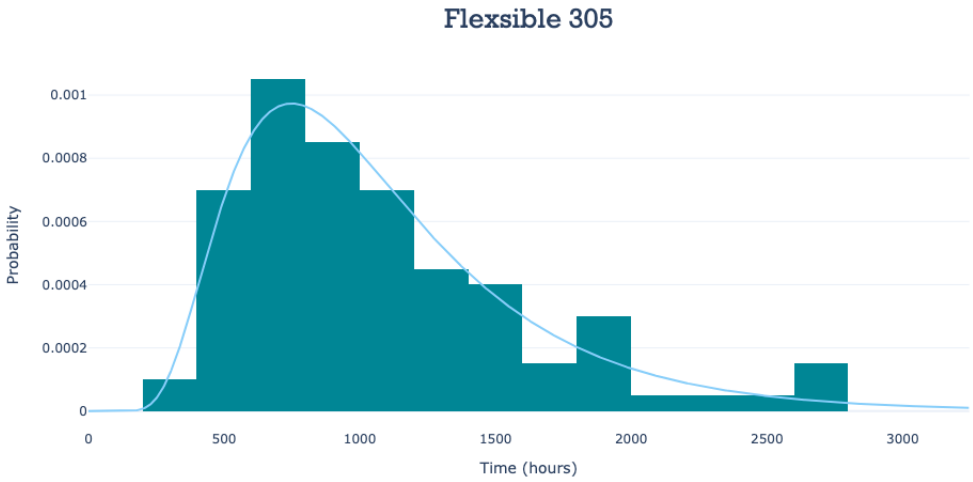


*Figure B.20: Histogram of the RUL prediction for flexsible 104.*

### B.1.11 Flexsible 307

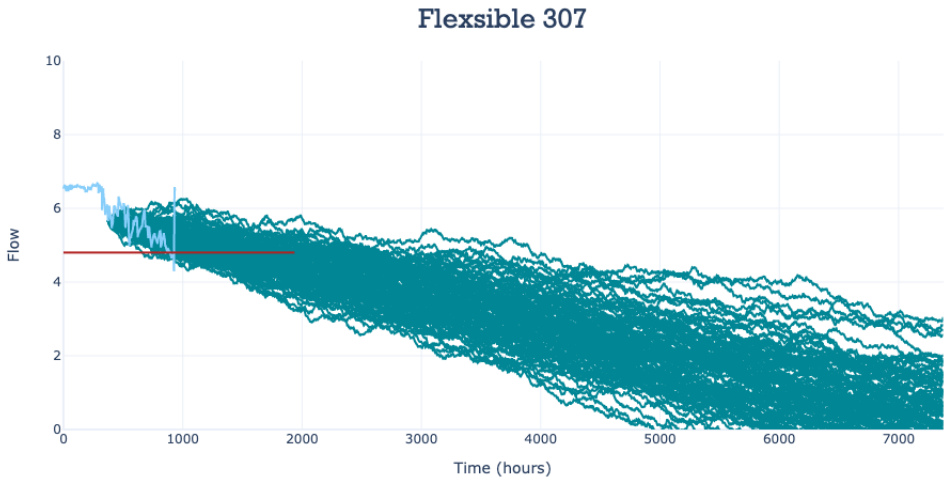


*Figure B.21: The wiener process shown by a Monte-Carlo simulation for flexsible 105.*

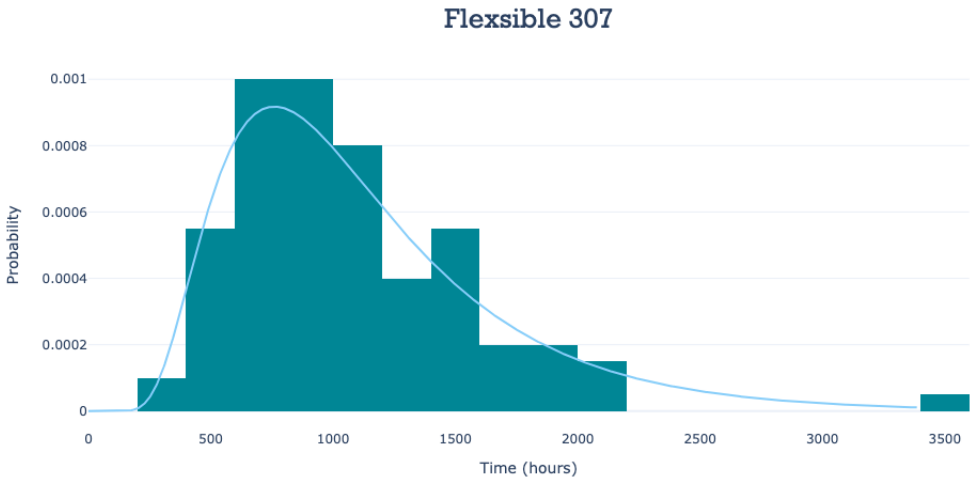


*Figure B.22: Histogram of the RUL prediction for flexsible 104.*

### B.1.12 Flexsible 308

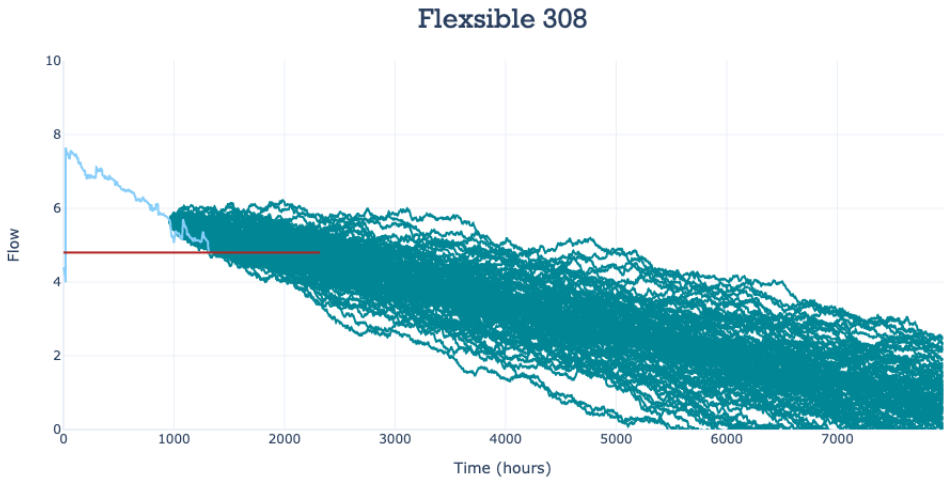


*Figure B.23: The wiener process shown by a Monte-Carlo simulation for flexsible 105.*

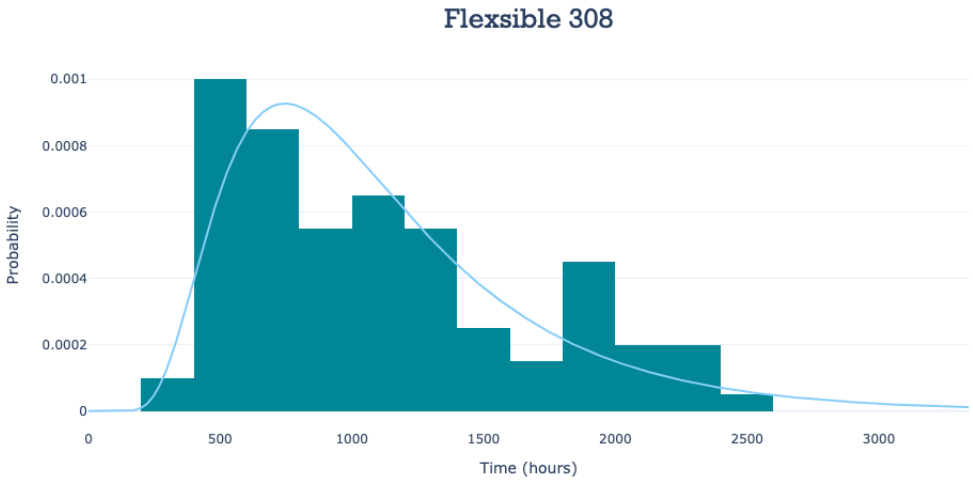


*Figure B.24: Histogram of the RUL prediction for flexsible 104.*

### B.1.13 Flexsible 309

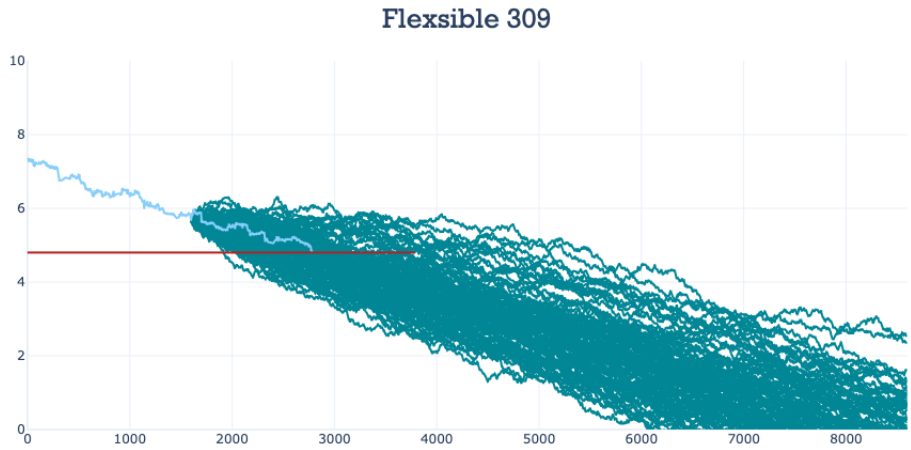


*Figure B.25: The wiener process shown by a Monte-Carlo simulation for flexsible 105.*

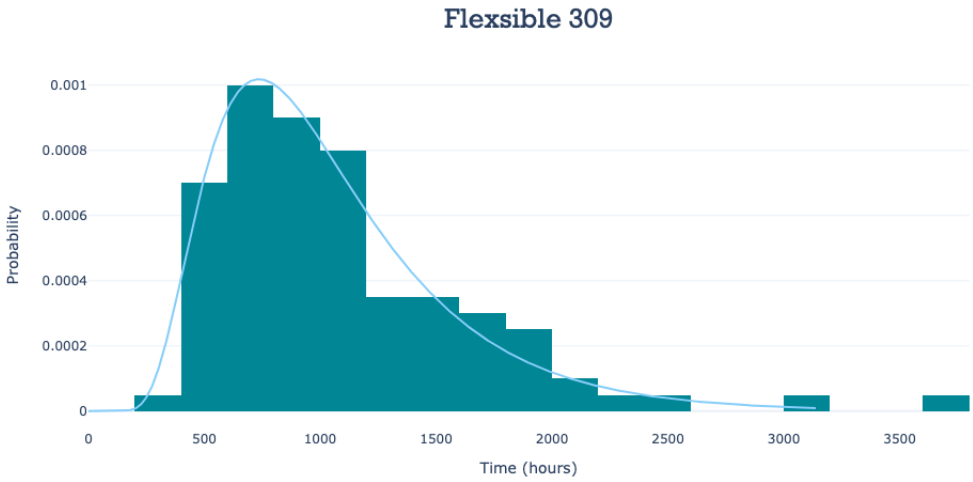


*Figure B.26: Histogram of the RUL prediction for flexsible 104.*

Håvard Holm Bjørnebekk

# Modeling Degradation for Prognosis in a Complex Environment - From a Physics-Based Perspective

NTNU
Norwegian University of
Science and Technology